General Disclaimer

One or more of the Following Statements may affect this Document

- This document has been reproduced from the best copy furnished by the organizational source. It is being released in the interest of making available as much information as possible.

- This document may contain data, which exceeds the sheet parameters. It was furnished in this condition by the organizational source and is the best copy available.

- This document may contain tone-on-tone or color graphs, charts and/or pictures, which have been reproduced in black and white.

- This document is paginated as submitted by the original source.

- Portions of this document are not fully legible due to the historical nature of some of the material. However, it is the best reproduction available from the original submission.

SATELLITE GEOLOGICAL AND GEOPHYSICAL REMOTE SENSING OF ICELAND (SR 9651)

Type III Final Report

Richard S. Williams, Jr.
U.S. Geological Survey
Reston, Virginia 22092

(E78-10096) SATELLITE GEOLOGICAL AND GEOPHYSICAL REMOTE SENSING OF ICELAND Final Report, 15 Jan. 1973 - 15 Aug. 1974 (Geological Survey, Reston, Va.) 109 p
HC A06/MF A01 CSCL 08F G3/43

N78-19574
Unclas
00096

SATELLITE GEOLOGICAL AND GEOPHYSICAL REMOTE SENSING OF ICELAND

Richard S. Williams, Jr.
U.S. Geological Survey
Reston, Virginia 22092

1 January 1978

Type III Final Report for Period 15 January 1973-15 August 1974

Prepared for:

Goddard Space Flight Center
Greenbelt, Maryland 20771

Publication authorized by the Director, U.S. Geological Survey

Satellite Geological and Geophysical
Remote Sensing of Iceland (SR 9651)

Sections of the Final Report

Appendices

Addenda

TECHNICAL REPORT STANDARD TITLE PAGE

1. Report No.	2. Government Accession No.	3. Recipient's Catalog No.

4. Title and Subtitle	5. Report Date
SATELLITE GEOLOGICAL AND GEOPHYSICAL REMOTE SENSING OF ICELAND (SR 9651)	1 January 1978
	6. Performing Organization Code

7. Author(s)	8. Performing Organization Report No.
Richard S. Williams, Jr. and Icelandic co-investigators (IN 079)	

9. Performing Organization Name and Address	10. Work Unit No.
U.S. Geological Survey EROS Program (LIA)- MS 730 Reston, Virginia 22092	Task No. 4-3
	11. Contract or Grant No. S-70243-AG
	13. Type of Report and Period Covered Type III Progress Rpt. 15 Jan 73 - 15 Aug 74
12. Sponsoring Agency Name and Address Frederick Gordon, Jr. ATTN: Code 902 Goddard Space Flight Center (NASA) Greenbelt, Maryland 20771	14. Sponsoring Agency Code

15. Supplementary Notes

16. Abstract The following are the principal results of the Landsat research project in Iceland: 1, delineation of part of a geothermal area by snowmelt pattern (Námafjall) and of geothermally altered ground in 3 geothermal areas (Námafjall, Torfajökull, and Reykjanes); 2, delineation of new basaltic lava flows in 3 areas, tephra fallout pattern in one area, and an image of an effusive volcanic eruption (Heimaey); 3, mapping of many new structural geologic and volcanic features, particularly within icecaps, and on snow-covered terrain at low solar elevation angle (<10°); 4, planimetric revision of small scale maps (1:100,000) of Surtsey (erosion) and Heimaey (volcanic eruption) feasible; 5, delineation of 90% of the area of Iceland covered by icecaps, mapping of changes in proglacial lakes, mapping of nunataks and some depositional glacial features, and mapping of a surging glacier (1.8km advance) and speed of flow of another glacier (600m/11 mos.); 6, mapping of changes in distributaries from glaciers and of changes in a lake and outwash plain caused by a jökulhlaup; and compilation of an uncontrolled orthoimage mosaic of Iceland (false-color-composite) at 1:1,000,000-scale, publication of two 1:500,000-scale (fall and winter) and preparation of two 1:250,000-scale Landsat image maps of Vatnajökull, Iceland.

17. Key Words Suggested by Author	18. Distribution Statement
Geomorphology Volcanology Glaciology Iceland Landsat image maps Geothermal	

19. Security Classif. (of this report)	20. Security Classif. (of this page)	21. No. of Pages	22. Price
Irrelevant	Irrelevant	64	

Figure 2A. Technical Report Standard Title Page. This page provides the data elements required by DoD Form DD-1473, HEW Form OE-6000 (ERIC), and similar forms.

Satellite Geological and Geophysical
Remote Sensing of Iceland (SR 9 651)

Summary of Research Results

Analysis of Landsat imagery of Iceland acquired during different seasons and intervals of time produced a number of research findings in several disciplines of geology and related sciences which undoubtedly have applications to other regions of the planet. A brief summary of the most important findings is as follows:

Geothermal - ERTS imagery has sufficient resolution to map, from MSS color composites, areas of altered ground caused by high-temperature geothermal activity at the Námafjall, Torfajökull, and Reykjanes geothermal areas. A small area of intense thermal emission on the east side of the Námafjall geothermal area could also be mapped because of the snowmelt pattern.

Volcanology - The major axes of the fallout pattern of tephra from the May-July 1970 volcanic eruption from Hekla Volcano can be mapped where sufficient depth of deposition was present to seriously affect the normal vegetation. Lava flows from the 1961 volcanic eruption at Askja; some of the lava flows from the 1947-48 eruption, and all of the lava flows from the 1970 eruption at Hekla; and the areas covered by tephra and lava from the 1973 eruption on Heimaey could be delineated.

Structural Geology and Geomorphology - Low sun angle imagery ($<10°$) of snow-covered terrain has been particularly valuable in mapping structural and volcanic features concealed beneath glacial ice in the active volcanic zones of Iceland. Such imagery has also shown the very marked differences in volcanic geomorphology from a regional standpoint within the active zones.

Marine Geology - Enlargements from standard (3d generation) negatives enabled planimetric revisions to be made to the 1:100,000-scale maps of the islands of Surtsey and Heimaey; a change in the former is the result of erosion, and a change in the latter is the result of new land created by the 1973 volcanic eruption.

Hydrometeorology - Changes in extent of snow cover with time can be monitored on successive images.

Glaciology - The change in size of sediment plumes from the many glacial rivers which discharge into the sea along the south coast can be monitored and give a qualitative indication of seasonal changes in melting rates of glaciers. Changes in area of lakes, particularly glacier-margin lakes because of their powder-blue color, can be mapped most easily on MSS false-color composites. The increase in surface area of an ice-dammed lake was monitored until the occurrence of a jökulhlaup, after which the surface area of the lake was reduced considerably. ERTS imagery is especially amenable to showing the entire areal extent of Iceland's glaciers and icecaps at a point in time. Recently deglaciated terrain can be distinguished on MSS false-color composites because of the absence of vegetation when compared with older deglaciated terrain. ERTS imagery, acquired about 1 year apart, shows that the Eyjabakkajökull glacier, an outlet glacier on the northeast part of Vatnajökull, has surged nearly 2 km. Some of the effects of subglacial geothermal and volcanic activity under Vatnajökull can be seen in the form of collapse features on the surface of the icecap, after the occurrence of two jökulhlaups.

Vegetation - MSS false-color composites permit the mapping of at least five distinct vegetation types (forested areas, cultivated areas, grasslands, reclaimed areas, and lichen-covered bedrock) and barren areas (absence of color).

Cartography - New planimetric Landsat image maps are under preparation at 1:250,000-scale which will accurately show some of the areas of Iceland covered by glacial ice.* The high latitude of Iceland permits considerable stereoscopic coverage on side-lapping ERTS imagery. Features with relief as little as 100 m can be discerned stereoscopically. This method of studying landforms, vegetation distribution, occurrence of snow cover, glaciers, and geologic structure stereoscopically generally permits a more precise analysis to be made of these phenomena.

*Two (fall and winter) 1:500,000-scale Landsat image maps of Vatnajökull, Iceland, were subsequently published by the U.S. Geological Survey in 1976 and 1977, respectively.

SUMMARY OF STUDIES IN ICELAND WITH ERTS-1 IMAGERY

Discipline	Experiments	Research Objectives	Research Results
GEOLOGY	Geothermal	Delineation of geothermal areas by extent of snow-melt pattern	Delineation of part of geothermal area by snowmelt pattern. Delineation of geothermally altered ground in 3 geothermal areas (Námafjall, Torfajökull, and Reykjanes).
GEOLOGY	Volcanic Eruption	Delineation of areas of new basalt flows and tephra falls	Delineation of new basalt flows in 3 areas and tephra fallout pattern in 1 area. Image of effusive volcanic eruption.
GEOLOGY	Geologic Structure	Mapping, on a regional basis, of faults, fissures, lineaments, and other structural features in the neovolcanic zone	Mapping of many new structural geologic and volcanic features, particularly within icecaps, and on snow-covered terrain at low sun angle ($<10^{\circ}$).
GEOLOGY	Volcanic Geomorphology	Mapping of the regional aspect of volcanic landforms	Regional distribution of different volcanic landforms mappable, particularly unique landforms.
GEOLOGY	Marine Geology	Mapping of any changes in the coastline of Iceland and any submarine features visible	Planimetric revisions of maps (to 1:100,000 scale) of Surtsey (erosion) and Heimaey (volcanic eruption) feasible. Mapping of seasonal change of sediment plumes from glacial rivers.
HYDROLOGY	Ephemeral Snow and Ice	Mapping of changes in snow cover over time; mapping of surface water distribution, and mapping of ice freeze-ups and thaws on major lakes	Mapping of surface water distribution can be achieved. Some mapping (lack of seasonal imagery) of changes in snow cover and thaw of lake ice.

TABLE 3 - CONTINUED

Discipline	Experiments	Research Objectives	Research Results
HYDROLOGY	Glaciological Features	Delineation of areas covered by glaciers; mapping of changes in ice-margin lakes; mapping of nunataks; and mapping of depositional glacial features	Delineation of 90% of the area covered by icecaps; mapping of changes in glacier-margin lakes; mapping of some nunataks and some depositional glacial features. Mapping of surging glacier (1.8km movement) and flow of another glacier (600m/11 mos.).
HYDROLOGY	River Flooding	Mapping of spring runoff, floods along river valleys, and changes in distributaries from glaciers	Mapping of changes in distributaries from glaciers. Mapping of changes in lake and outwash plain caused by a jökulhlaup.
OCEANOGRAPHY	Sea Ice	Mapping of changes in ice flow concentrations with time off northern and eastern coasts	No usable imagery.
AGRICULTURE/ FORESTRY	Grasslands and Forest	Delineation of grasslands and particularly change in vigor with time	Mapping of 5 classes of vegetation; grasslands, cultivated areas, reclaimed land, forested areas, lichen-covered lava flows, and barren areas on false-color composites.
CARTOGRAPHY	-		Compilation of an orthoimage mosaic of Iceland at 1:1,000,000 (false-color composite) and planned 1:250,000-scale orthoimage maps of Vatnajökull, Iceland. Study of landforms with stereoscopic images. Measurement of 100m elevation difference. Planimetric revisions on existing maps. Publication of two 1:500,000-scale Landsat image maps of Vatnajökull, Iceland (Fall and Winter scenes). [Editor's note: Both Vatnajökull maps were published in 1977]

107000-1-X

Reprinted From

PROCEEDINGS of the NINTH INTERNATIONAL SYMPOSIUM ON REMOTE SENSING OF ENVIRONMENT

15 - 19 April 1974

Sponsored by

Center for Remote Sensing Information and Analysis
Environmental Research Institute of Michigan

Institute of Science and Technology
The University of Michigan

Office of Applications
National Aeronautics and Space Administration

Office of Research and Development
and Office of Water Program Operations

Federal Highway Administration
U.S. Department of Transportation

U.S. Geological Survey
U.S. Department of the Interior

U.S. Department of Agriculture

U.S. Air Force Office of Scientific Research

U.S. Coast Guard
U.S. Department of Transportation

National Oceanic and Atmospheric Administration
U.S. Department of Commerce

Division of Water Control Planning
Tennessee Valley Authority

NAC Incorporated
Tokyo, Japan

Willow Run Laboratories

ENVIRONMENTAL
RESEARCH INSTITUTE
OF MICHIGAN
Ann Arbor, Michigan

ENVIRONMENTAL STUDIES OF ICELAND WITH ERTS-1 IMAGERY*

Richard S. Williams, Jr., U. S. Geological Survey,
EROS Program Office, Reston, Virginia 22090
Ágúst Böðvarsson, Icelandic Surveying Department;
Sturla Friðriksson, Agricultural Research Institute;
Guðmundur Pálmason, National Energy Authority;
Sigurjón Rist, National Energy Authority;
Hlynur Sigtryggsson, Icelandic Meteorological Service;
Kristján Sæmundsson, National Energy Authority;
Sigurður Thorarinsson, University of Iceland;
Ingvi Thorsteinsson, Agricultural Research Institute;
Reykjavík, Iceland

ABSTRACT

ERTS imagery has sufficient resolution to map, from MSS color composites, areas of altered ground caused by high-temperature geothermal activity at the Námafjall, Torfajökull, and Reykjanes geothermal areas. A small area of intense thermal emission on the east side of the Námafjall geothermal area could also be mapped because of the snowmelt pattern. The major axes of the fallout pattern of tephra from the May-July 1970 volcanic eruption from Hekla Volcano can be mapped where sufficient depth of deposition was sufficient to seriously affect the normal vegetation. Lava flows from the 1961 volcanic eruption at Askja; some of the lava flows from the 1947-48 eruption, and all of the lava flows from the 1970 eruption at Hekla; and the areas covered by tephra and lava from the 1973 eruption on Heimaey could be delineated. Low sun angle imagery (<10°) of snow-covered terrain has been particularly valuable in mapping structural and volcanic features concealed beneath glacial ice in the active volcanic zones of Iceland. Such imagery has also shown the very marked differences in volcanic geomorphology from a regional standpoint within the active zones. Enlargements from standard (3d generation) negatives enabled planimetric revisions to be made to the 1:100,000-scale maps of the islands of Surtsey and Heimaey; a change in the former is the result of erosion, and a change in the latter is the result of new land created by the 1973 volcanic eruption. Changes in extent of snow cover with time can be monitored on successive images. The change in size of sediment plumes from the many glacial rivers which discharge into the sea along the south coast can be monitored and give a qualitative indication of seasonal changes in melting rates of glaciers. Changes in area of lakes, particularly glacier-margin lakes because of their powder-blue color, can be mapped most easily on MSS false-color composites. The increase in surface area of an ice-dammed lake was monitored until the occurrence of a jökulhlaup, after which the surface area of the lake was reduced considerably. ERTS imagery is especially amenable to showing the entire areal extent of Iceland's glaciers and icecaps at a point in time. New planimetric maps are under preparation at 1:500,000- and 1:250,000-scales which will accurately show the area of Iceland covered by glacial ice. Recently deglaciated terrain can be distinguished on MSS false-color composites because of the absence of vegetation when compared with older deglaciated terrain. ERTS imagery, acquired about 1 year apart, shows that the Eyjabakkajökull glacier, an outlet glacier on the northeast part of Vatnajökull, has surged nearly 2 km. Some of the effects of subglacial geothermal and volcanic activity under Vatnajökull can be seen in the form of collapse features in the surface of the icecap, after the occurrence of two jökulhlaups. MSS false-color composites permit the mapping of at least five distinct

*Publication authorized by the Director, U. S. Geological Survey.

vegetation types (forested areas, cultivated areas, grasslands, reclaimed areas, and lichen-covered bedrock) and barren areas (absence of color). The high latitude of Iceland permits considerable stereoscopic coverage on side-lapping ERTS imagery. Features with relief as little as 100 m can be discerned stereoscopically. This method of studying landforms, vegetation distribution, occurrence of snow cover, glaciers, and geologic structure stereoscopically generally permits a more precise analysis to be made of these phenomena.

INTRODUCTION

During the Eighth International Symposium on Remote Sensing of Environment, not long after the delayed launch of ERTS-1 spacecraft, a binational, multi-disciplinary, ERTS-1 experiment in Iceland was described (Williams, 1972). The objective of the experiment was to study the varied dynamic environmental phenomena of Iceland, with particular relevance to the disciplines of geology, hydrology, oceanography, and agriculture. Ten experiments were outlined: five in geology, three in hydrology, and one each in oceanography and agriculture. Since then another one has been added, in cartography. It is directed at the study of some of the photogrammetric aspects of ERTS, such as stereoscopy with side-lapping images, but more importantly to bridging the gap between results from the 10 primary experiments by integration of new data into updated maps and the preparation of new types of maps of Iceland.

There are three special characteristics of ERTS MSS imagery, not currently available from any other satellite, military or civilian, that make such imagery unique to the mapping of environmental phenomena. One, it can be related to the figure of the earth (Colvocoresses, 1973a, 1973c, and 1974); two, it has close to radiometric fidelity of spectral reflectance of the earth within a single image recorded on videotape rather than film; and three, it provides systematic, routine, repetitive coverage of an area. In particular, it is this last characteristic which is being heavily exploited in the Iceland experiment and which offers such promise in the mapping of dynamic phenomena in Iceland. Of course, the study and delineation of dynamic phenomena, to be useful to resource managers and other decision makers, must be depicted on graphs or maps. This requires the preparation of timely maps of dynamic phenomena - still only a promise, not yet a reality from the total ERTS system, although this potential is embodied in current ERTS technology (Colvocoresses, 1972; Colvocoresses and McEwen, 1973).

As was noted by the authors (Williams and others, 1973b), imagery from ERTS-1 is providing scientists with the first feasible means to measure and map certain types of environmental phenomena on a regional and global basis. ERTS-1 MSS imagery provides a completely new source of data on dynamic environmental phenomena which was previously unavailable, except of limited areas, to cartographers and resource managers. From an ecological viewpoint, the availability of ERTS imagery could not have come at a more propitious time in human history, coming as it has at the time of increased environmental awareness by scientists and laymen alike. It gives environmental scientists not only a global view of the dynamic environment of our planet but also of man's impact upon it.

Although the full ramifications of open access to ERTS imagery by scientists and resource managers will take many years, if not decades, to be completely established, several organizations and countries have quickly recognized the significance of such environmental data to their own problems. One of these countries is Iceland, an island republic with a relatively small, but rapidly growing population of 213,070 (1 Dec 1973) in an area of 103,000 km^2 (population density of about 2 persons per km^2). Iceland, because of its cool climate, low population density, and paucity of natural resources has early recognized the

Note: The Icelandic alphabet has 33 letters, including 3 letters no longer used in English: ð, þ, and æ. In English printing these letters are usually transliterated to d, th, and e, respectively, to avoid confusion. In this paper, however, all Icelandic place names and journal names are retained with their Icelandic spelling. Icelandic spelling is also retained in all personal names and patronymic surnames, except where the surname begins with Þ. In the latter case Þ has been transliterated to Th.

potential value of ERTS imagery and the data collection system to provide, at low cost and in near real time, certain types of dynamic environmental data. Because the Icelanders depend on the surrounding seas for fish and crustaceans and on the limited area of arable land for agricultural products, their economic well-being is heavily dictated by their natural environment. Understanding and recognizing changes in, and redirecting human and capital resources in response to, the often capricious nature of the natural environment of Iceland has decidedly important economic and social implications.

The study of Iceland with ERTS imagery is still far from finished, and many of the findings in this paper are, for that reason, qualitative rather than quantitative. With several months of research activity now completed, however, the Ninth International Symposium on Remote Sensing of Environment provides an excellent forum to present our initial results. Some of the findings are of scientific value, but others have important consequences of practical use to Iceland in the wisest possible management of its limited natural resources. Let us first examine the results of the geological experiments.

GEOLOGICAL STUDIES

Geothermal Experiment

Iceland has a number of high-temperature geothermal areas of which 17 have been recognized to date (Figure 1). These high-temperature geothermal areas range in size from 1.0 km^2 (Reykjanes) and Námafjall (~6 km^2) to the large Torfajökull area (~100 km^2) and have natural heat outputs which range from 4×10^6 cal/s (Reykjanes) (Björnsson, and others, 1972) to over 500×10^6 cal/s (Torfajökull) (Böðvarsson, 1960). The basic objective of the geothermal experiment was to determine the minimum size and heat discharge from a geothermal area which could be delineated on MSS imagery due to snowmelt. Snowmelt in geothermal areas had been observed by the authors, other scientists, and White and Miller (1968) who had endeavored to use the phenomenon as a basis for heat flow measurements in Yellowstone National Park in what they termed "snow-fall calorimetry." It should also be noted that three of the 17 high-temperature geothermal areas are partly or mainly subglacial, leading to the possibility that such activity might be detectable because of snow and ice melting over such geothermal areas.

The results of this experiment are as follows: Only part of the Námafjall geothermal area could definitely be delineated on the basis of a snowmelt pattern on a winter-time image of the area (Mývatn, C6, 9 Mar. 73, 1229-12142-7)[2/] (Figure 2). It would appear, therefore, that under optimum snow-cover conditions the ground resolution capability of the ERTS-1 MSS sensor can distinguish by an anomalous snowmelt pattern at least part of a small geothermal area (~6 km^2), with a heat dissipation of $100\text{-}200 \times 10^6$ cal/s, partly natural and partly from drill holes. Another interesting aspect of this particular ERTS-1 image, however, is the open water on the eastern shore of lake Mývatn caused by outflow of thermal water near Vogar (Rist, 1969, p. 121-127; Barth, 1950, p. 18). Also on Figure 2 can be seen other small open water areas caused by a high volume of spring discharge, at the main river outlet of the lake, and a complex pattern of open water in lake Grænavatn, just south of Mývatn.

Figure 3, a summertime image of the adjacent area (Akureyri, C5, 19 Aug. 73, 1392-12185-5) shows the areal extent of altered ground in the Námafjall geothermal area. The altered area appears as a light greenish hue on MSS false-color composites (bands 4, 5, 7). Geothermally altered ground can also be seen at the Torfajökull and Reykjanes geothermal areas.

2/ The convention used in this paper in referring to specific ERTS-1, MSS images of Iceland is to give the geographic name of the image, alphanumeric matrix designator, date, image ID number, and MSS band. For the first two refer to Figure 31 in this paper. Individual images may be purchased from the EROS Data Center, Sioux Falls, South Dakota 57198, or from Landmælingar Íslands, Laugavegi 178, Reykjavík, Iceland.

These two findings with respect to Icelandic geothermal areas support the use of ERTS imagery as a global reconnaissance tool in searching for geothermal activity in remote areas on the basis of either an anomalous snowmelt pattern, open water in an otherwise frozen and snow-covered terrain, or altered ground. The sensors on ERTS are the first satellite sensors available to the international scientific community to have sufficient resolution and enough spectral bands to detect phenomena resulting from geothermal activity. The capability to delineate geothermally altered ground is perhaps the most valuable from a reconnaissance exploration viewpoint, in that such high-temperature activity would destroy any vegetation present, thus producing a vegetation anomaly (if vegetation were normally present) and a marked color change (alteration of bedrock or soil).

Iceland is primarily a land of basaltic bedrock, more or less covered by glacial deposits (including loess) derived from such bedrock. However, some andesitic and rhyolitic rocks are present, generally in association with Tertiary and Quaternary central volcanoes, and also in the case of Late Pleistocene and Holocene central volcanoes usually juxtaposed to the high-temperature geothermal areas (Figure 1). Rhyolitic rocks in the Torfajökull geothermal area are particularly well delineated on MSS false-color composites of the area (See Figures 8, 21, and 23).

Finally, several collapse features in the Vatnajökull icecap, resulting from subglacial volcanic (?) and geothermal activity could be delineated on ERTS imagery. These features will be discussed more fully under the Glaciological Features and River Flooding Experiments.

Volcanic Eruptive Products Experiment

Within the last 12 years Iceland has had four volcanic eruptions: Askja in 1961, Surtsey in 1963-1967, Hekla in 1970, and Heimaey in 1973. The eruption of Askja in 1961 produced a lava flow which was approximately 9.5 km long and covered an area about 11 km^2 (Thorarinsson, 1963; Thorarinsson and Sigvaldason, 1962). Most of the eruptive products were lava flows. Figure 4 is a 1:100,000-scale topographic map of the new lava flows at Askja. Aerial photographs (Figure 5) and terrestrial photographs show a sharp contrast of new flows (dark) over the older pumiceous sheet (light). Figure 6 is a part of a mostly cloudy ERTS-1 image of this area (Ódáðahraun, C7, 30 July 73, 1372-12074-5) but with fortuitous breaks in the clouds over the crater lake, Öskjuvatn, and most of the 1961 lava flows. Sufficient detail of this new flow is preserved to permit enlargement to scales of 1:250,000 and even to 1:100,000, thereby permitting the ERTS imagery to be used to directly map the areal extent of such lava flows.

Hekla erupted in May 1970 after one of the shortest inter-eruptive periods in its history during the last millenium (or since the beginning of the settlement of Iceland) (Thorarinsson, 1970). The initial stages of the eruption were primarily tephra-producing. The tephra deposits covered a large area downwind (to the NNW) and were reputed to have darkened part of the Greenland Icecap (Anonymous, 1970a) (Figure 7). According to Thorarinsson (1970, p. 46), the tephra fallout covered an area in Iceland of about 22,000 km^2 or 20 percent of the island. Within the 1 cm isopach contour the area was approximately 2,000 km^2. The 1970 tephra was very rich in fluorine ultimately the cause of the death, by fluorosis poisoning, of 7,500 sheep. If an ERTS-type satellite had been functioning during the tephra fall, it would have been possible to map the fallout pattern, thus circumscribing the fluorine-affected areas and permitting faster, more accurate warnings to the affected districts.

On an ERTS-1 image of the area, taken 4 years after the eruption (Hekla, D5, 19 Aug. 73, 1392-12191-5), only the areas of heavy deposition (4 cm or more), where the suffocated vegetation has not yet recovered, can still be delineated (Figure 8). Although more visible on the band 4 image, the three areas of new lava flows can also be delineated. Figure 9 is a geologic map of the Hekla area.

Surtsey is a small (2.5 km^2) volcanic island in the Vestmannaeyjar archipelago. The volcano had an eruptive history which lasted from 1963-1968, with the last surficial lava flow occurring in early June 1967 (Thorarinsson, 1968). The island is composed of tephra on the northern part of the island and as intercalations and surficial deposits elsewhere on the island with basalt flows to the south. The most recent flows are very dark in color, but tephra deposition, eolian

redeposition, and other weathering processes tend to lighten the surface coloration in a short time. For that reason it is impossible to delineate between tephra deposits and lava flows on Surtsey on ERTS-1 images (Figures 8 and 14). One unexpected finding did result, however. Where steam emanates through the tephra pile due to boiling off from sea water in contact with cooling magma at depth, such as on the northern rim of Surtur I [easternmost of the two initial craters and the site of the development of a crater row in August 1968 (Williams and others, 1968)], palagonitization of the tephra is taking place (Jakobsson, 1972a). The palagonitized area appears on ERTS images as an area of higher reflectivity in all bands, but is most pronounced in band 5 (0.6-0.7μm) and band 6 (0.7-0.8μm) (Figures 8 and 14).

The volcanic eruption on Heimaey, also in the Vestmannaeyjar archipelago, added about 2.5 km^2 of new land to the eastern side of the island (Williams and Moore, 1973). This increase in land area can be delineated on ERTS-1 imagery (Figures 8 and 17). The initial stages of the eruption were dominated by heavy deposition of tephra which completely buried parts of the town of Vestmannaeyjar as well as vegetation in the northern half of the island and on some of the surrounding islets. On a false-color composite (bands 4, 5, 7) version of Figure 8, the areas of new lava, the areas covered by tephra, and the areas where the vegetation was destroyed or seriously affected can all be delineated.

The island of Heimaey was fortuitously imaged by ERTS-1 prior to the eruption in November 1972 (Þórisvatn, D6, 21 Nov. 72, 1121-12143), only once during the eruption (Vestmannaeyjar, E6, 9 Mar. 73, 1229-12151) (because of cloud cover) and several times after the eruption had ceased (e.g., Hekla, D5, 19 Aug. 73, 1392-12191). The first two images were published in Williams and others, 1973b, and are included in this paper as Figure 10. The latter image also appears as Figure 8 and Figure 17. Cloud cover was a serious problem in imagery acquisition during the eruption. NASA made a valiant effort to obtain imagery of the eruption (23 January - 3 July 1973) with nine different ERTS-1 images during the period between and including 1 February - 27 March 1973, but only the 9 March 1973 image was relatively cloud free. All the other images were cloudy over the island with the exception of the 3 February 1973 image (Þingvallavatn, D4, 3 Feb. 73, 1195-12260), where there was insufficient illumination, and the island was at the extreme edge of the image - with the eruption plume outside the field of view to the east.

It is obvious that although ERTS imagery has sufficient resolution to map new lava flows and tephra falls on a global basis, it does so on a change detection basis. That is, it provides a "time-lapse" look at an area, generally separated by at least 18 days or even perhaps by many cycles. The exception, of course, is that at higher latitudes such as Iceland (65°N.) the separation of orbits may permit images of dynamic phenomena, weather permitting, to be acquired 3 days in a row (separation of 48 h) before the next 18-day cycle begins. For some types of dynamic phenomena the repetition cycle for ERTS is too long, such as with volcanic activity. Fortunately, there is available another environmental satellite, the NOAA satellite series, with an order of magnitude less resolution [800 m for NOAA-2's VHRR (Very High Resolution Radiometer) scanner versus 80 m for ERTS-1's MSS instrument]. This satellite can image every spot on the globe at least twice each day (daytime and nighttime) with both visible (0.6-0.7μm) and thermal sensors (10.5-12.5μm). Unfortunately for areas outside North America, there is a severe tape recorder time limitation for data acquisition. NOAA-2 VHRR imagery, however, has the potential for providing coverage of large scale dynamic phenomena, such as volcanic eruption plumes, thermal emission from volcanic eruptions, sea and lake ice concentration and movement, and large floods, on a 12 h basis. Therefore, NOAA-2 imagery could provide 36 times more imagery of dynamic phenomena in the same time interval as ERTS imagery. As such, it offers an excellent complement to many ERTS studies.

As an example of this, Figure 11 is a NOAA-2 thermograph (Iceland, 25 Jan 73, 1040 UT, VHRR/IR [10.5-12.5μm]) of the volcanic eruption on Heimaey which was acquired only 33 hours after the eruption began. On the thermograph the lava flows appear as a series of eight black (hot) pixels at the base or western end of a white (cold) eruption cloud which extends 60 km to the east. At its widest extent the eruption cloud is 12 km as viewed from above. North of the eruption plume is the south coast of Iceland. On the companion VHRR/VIS (0.6-0.7μm) image the eruption cloud is shown but faintly. At this time of day, at this time of year, and at this northern latitude (63°26'N.) the Earth's surface is still in darkness,

but the eruption cloud and clouds swirling around a cyclone in the southeast are high enough to catch the grazing rays of the sun.

The first usable ERTS-1 imagery of the volcanic eruption was not acquired until 9 March 1973 or 45 days after the eruption began (Figure 10). Therefore, ERTS can provide imagery of an area before an event starts, possibly during an event, and after an event has ceased. For certain types of environmental phenomena the NOAA-2 satellite helps bridge the information gap at this stage in the development of earth resources satellite technology.

It is evident from the results of this experiment in Iceland, therefore, that ERTS imagery offers the geologist the opportunity to map tephra falls throughout the world and also the areal extent of new lava flows, of particular importance in remote areas. Tephra falls, which can be surprisingly large in extent, often have a devastating impact on agricultural lands. Accurate and timely mapping of areas of tephra deposition would be important in disaster relief efforts and in recovery plans.

Geologic Structure Experiment

Figure 1 shows many of the large-scale structural features which dominate the landforms in the active zone of rifting and volcanism of Iceland. The active volcanic zones of Iceland have probably seen about 200 volcanic eruptions during the last millenium (Thorarinsson, 1960), including about 30 different volcanoes (Thorarinsson, 1966). Within these active zones are various types of volcanoes, non-eruptive fissures (Icel., gjár), fault zones (particularly grabens), and various rift systems. As the largest supramarine segment of the Mid-Atlantic Ridge, the active zones of Iceland hold great interest to geologists and geophysicists (Björnsson, 1967). Of particular interest to the understanding of the structure and geotectonics of Iceland are the changes in direction of the active zones as they cross Iceland. For instance, from the Reykjanes peninsula to the western margin of Vatnajökull the trend of the zones is NE-SW; north of Vatnajökull the trend is more N-S. How Iceland fits into modern concepts of sea-floor spreading and transform fault hypotheses (Ward, 1971; Sæmundsson, 1974) and its relationship to the Mid-Atlantic Ridge (Pálmason and Sæmundsson, 1974) are also important geological questions.

It was expected that ERTS imagery would permit the neovolcanic zone of Iceland to be studied from a small-scale, regional vantage point, and that the low sun angle of the imagery could markedly enhance the structural "grain" of the island. It was anticipated that such imagery would allow the mapping - on a regional basis - of faults, fissure swarms, lineaments and other structural features within the active zones as well as structural features outside the zone. Most of the expectations turned out to be true but with some unexpected results. Low sun angle by itself certainly helped to accentuate relief and structural features, but only to a point, because too low a sun angle provides insufficient illumination of the terrain, thus causing detail to be lost. The low level of illumination could, however, be offset by the increased reflectivity of snow-covered terrain. In Iceland, the combination of low sun angle and snow-covered terrain provided some unusual imagery of the structure and morphology within the active zones and particularly within the margins of the five large icecaps which sit astride these zones: Vatnajökull, Hofsjökull, Langjökull, Mýrdalsjökull, and Eyjafjallajökull (Figures 1 and 20).

Figure 12 is a remarkable ERTS image of the Vatnajökull icecap and surroundings which was acquired at a sun angle of only 7° (Vatnajökull, D7, 31 Jan. 73, 1192-12084-5). Most of the area is snow covered, except for the coastal plain nearest the ocean and the ablating snout of Skeiðarárjökull, thus providing sufficient reflectivity to permit the image to be recorded at such low illumination. The grazing angle of illumination produced elongated shadows of even the most subtle features. Of particular importance to knowledge of the structural geology of that part of the active zone covered by Vatnajökull is the fine detail shown in the surface of the icecap. Many of these features which are partly or wholly buried under Vatnajökull were previously unknown or only suspected (Thorarinsson and others, 1973; Williams and others, 1973c). The morphology of Bárðarbunga (3) an area east of Hamarinn (4), and Esjufjöll (5) suggest buried central volcanoes. Two elliptical features, one at Kverkfjöll (1) and another at Esjufjöll are recognized as probable subglacial calderas.

Two prominent volcano-tectonic lineaments can be traced across the image. The first strikes N.45°E. for at least 80 km along a line of nunataks and subglacial volcanoes, calderas, and geothermal areas between the two subglacial calderas at Kverkfjöll (1 and 2), through the eastern side of Grímsvötn (6), to the southwestern edge of Vatnajökull. Except for historical volcanic activity at the Öræfajökull central volcano, 50 km southeast of this lineament (just north of the North arrow), this volcano-tectonic line sharply divides areas of active volcanism (to the northwest) from areas of older volcanism (to the southeast). The second lineament strikes N.35°W. along Vatnajökull's southern margin, cutting across the first volcano-tectonic lineament, and separating two markedly different tectonic regimes: fissure eruptions to the southwest, central volcano complexes to the northeast.

Several other low sun angle, snow-covered terrain images of Iceland also show new features beneath other icecaps. A large domal feature, very similar to the Bárðarbunga area in Vatnajökull, can be delineated on the northwestern part of Hofsjökull. Linear features and a possible caldera within Langjökull also appear on low sun angle imagery of this icecap. Low sun angle imagery of Mýrdalsjökull shows subtle depressions within a poorly delineated calderalike feature on the southeast part of the icecap.

Preliminary results from computer enhancement of the Vatnajökull image (Figure 12) by scientists at the Jet Propulsion Laboratory (F. C. Billingsley, A. F. Goetz, and A. George Lauer, personal communication) has shown the potential of such enhancement to studies of low relief features and geologic structure in snow-covered areas. Not only is the full range of reflectance variation retained on the computer compatible tapes and better resolution achieved (first generation rather than the usual third), but manipulation of image contrast and gray-scale variation through specially written contrast-stretching and ratioing computer programs enables much improved, custom imagery to be made available to the scientist (Billingsley and Goetz, 1973). In polar regions, and even in non-polar, snow-covered regions, such computer-assisted analysis is important to deriving maximum information from the ERTS images.

Outside the active zone of rifting and faulting, in the areas of Tertiary and Quaternary flood basalts, ERTS imagery has recorded several probable central volcano complexes because of their distinctive circularity and size (Williams and others, 1973a). These areas of circular structure will eventually be studied in the field, but the ERTS imagery has assisted in locating areas for specific field investigations. The reason some of these areas were not identified as such before is due to the remoteness of such areas and the fact that a number of aerial photographs, mosaicked together, would be necessary to see the entire structural pattern, a pattern easily missed on a single aerial photograph.

Volcanic Geomorphology Experiment

The active zone of rifting and volcanism of Iceland, which is highly generalized in Figure 1, is actually quite complex from a structural and volcanic viewpoint. The active volcanic zone, Pleistocene to Holocene in age, is 60 km wide in the north, but bifurcates in the south with a western limb about 40 km in width and an eastern one about 70 km wide. Jakobsson (1972b) has recently proposed calling the petrographically similar northern and western zones collectively the Median Zone, in a restricted sense. The active zone has two "outliers" to the northwest and southeast, Snæfellsnes and Öræfajökull, respectively. Both of these large and beautiful stratovolcanoes, as well as numerous other volcanoes, have been active in postglacial time. There is no question that the active volcanic zones, one fourth of Iceland or about 25,000 km^2, have been a prolific producer of lava. Approximately 12,000 km^2 are covered with post-glacial lavas, which have erupted from 150-200 Holocene volcanoes (Thorarinsson and others, 1959). On the basis of earlier estimates summarized by Karl Sapper, Rittman (1962) estimated that 24 percent of the total outflow of lava from the Earth's land surface, between A. D. 1500 and 1914, has been from volcanoes and fissure eruptions in the neovolcanic zone of Iceland.

The magnitude of volcanic activity has created a number of volcanic landforms. Thorarinsson (1960) has placed most of the basaltic volcanic landforms in Iceland into a logical classification system (Table 1). Iceland's cool windy climate severely limits the growth of vegetation in many parts of the country. Most of the soils are either wholly or in part of transported origin (eolian, glacial or fluvial).

Chemical weathering proceeds but very slowly. Except for lichen growth and eolian deposits on lava flows, most postglacial volcanic lanforms appear little changed from their origin morphology. It was expected, therefore, that Iceland would afford an excellent opportunity to observe the regional aspects of volcanism with ERTS imagery, and that the regional view of volcanic landforms in relation to the volcanic structure of Iceland would be of value to geological studies in Iceland. It was also anticipated that such imagery would give volcanic geomorphologists their first real look at a small-scale view of regional volcanism, important by itself, but also of immense value to extraterrestrial studies, particularly of possible volcanic landforms on the lunar surface and probable volcanic landforms on the lunar surface and probable landforms on the Martian surface.

The results from this experiment are that ERTS provides the first satellite imagery with sufficient resolution to systematically map many of the Earth's volcanic landforms. Of the volcanic types classified by Thorarinsson (Table 1), representative examples of each could be identified on ERTS-1, MSS imagery. However, only 6 of the 13 types could be definitely recognized without additional information. They are: shield volcano (Figure 23), stratovolcano (Figure 12), tephra ring (Figures 2 and 3), maar (Figure 8), spatter cone row (Figure 12), and stratified ridge (Figure 8). These landforms are in addition to the delineation of lava flows, tephra falls, and calderas which were discussed in the Geologic Structure Experiment. It was also possible to delineate some of the larger tectonic fissures, grabens, a rhyolitic coulee in the Torfajökull which was very distinctive on the false-color composites, and two types of volcanic landforms which were formed and are probably forming today under the Vatnajökull icecap: hyaloclastite ridges and table mountains, composed primarily of hyaloclastite breccia and pillow lavas.

The volcanic landforms and geologic structure of the area to the southwest of Vatnajökull are striking. The shadows cast by the serrated crest of the hyaloclastite ridges, the craters of the crater rows, and grabens cause these landforms to stand out sharply at the low sun angle. The image also shows very clearly how extremely straight lined some of the serrated ridges are, and how for long stretches they show no tendency to the en échelon pattern so characteristic of many fissure systems in southwest and north Iceland. There is little question that a study of the regional topography of this area could have a strong bearing on the understanding of the submarine topography of the Mid-Atlantic Ridge as shown on Heezen's maps (Heezen and others, 1959).

North of Vatnajökull, and in other places in the active zone of Iceland as well, are some classic examples of table mountains (Figure 2) (Kjartansson, 1960; van Bemmelen and Rutten, 1955). These volcanic edifices, several beautiful examples of which are shown in Figure 2, are basically a type of shield volcano, but which have a unique geomorphology. Beginning as subglacial eruptions, they built up as a confined pedestal of hyaloclastite breccias and pillow lavas before perforating the overlying icecap. After perforation, a supraglacial lake formed, and the resulting rock morphology was primarily that of pillow lavas. As soon as the lava became subaerial, a normal shield volcano formed, often with a large central or pit crater. The table mountains and hyaloclastite ridges are distinctive features of the Icelandic landscape, even more so when viewed stereoscopically on side-lapping ERTS images. This is true in the study of most of the landforms of Iceland. In many cases features are overlooked on the two-dimensional image which are immediately evident in the stereoscopic view. For many types of geomorphic and structural geologic studies the ability to analyze the image in a stereoscopic manner is mandatory. The two-dimensional limitation of most ERTS imagery is a distinct handicap in geomorphic studies in particular.

It is suggested that the study of the volcanic landforms of Iceland on ERTS imagery may be of particular importance to the continuing studies of the geomorphology of the Martian surface and perhaps even to the lunar surface as well. There are some striking analoges between the volcanic landforms of Iceland and the Martian surface features recorded on Mariner 9 imagery. If, as some scientists now suggest, different climatic variations existed in the Martian past, many of the aspects of the present geomorphological environment of Iceland may have been present - including the juxtaposition of volcanism and glaciation. As one example, Nix Olympica's morphology, as depicted on Mariner 9 imagery, may be the result of subglacial volcanism, the steep sides (2 km high) having formed subglacially in an icecap environment. As can be seen on Figure 2, similar yet smaller volcanic

edifices are called table mountains in Iceland. A number of other analogies are also quite striking but are beyond the scope of this paper.

Marine Geology and Coastal Geomorphology Experiment

The marine geology and coastal geomorphology studies were directed at mapping coastline changes, shoal areas, and any areas of kelp. Only the first objective has been reached so far. Little time has been devoted to searching for areas of shoaling, and the few images of the most promising kelp areas, in the vicinity of Breiðafjörður (the bay north of Snæfellsjökull in Figure 1), have been mostly cloudy. Good imagery of the Breiðafjörður area would be most useful, because Iceland is about to embark on a sustained harvest of kelp beds in the area as the basis for a new industry. It is probable that ERTS could give an estimate of the exploitable area of kelp beds and also monitor the area of annual harvest and subsequent regeneration. This experiment must await usable imagery, however.

One aspect of the coastal marine environment which was not considered at first, is the littoral drift of sediment-laden marine waters and the dispersal pattern of sediment-laden fresh water into marine waters. Sediment plumes from the many glacial rivers are very prominent on the ERTS-1 imagery, especially on MSS band 4. All of the major rivers of Iceland, but particularly those which include glaciers in their watersheds exhibit marked seasonal variation in the size of sediment plumes. This is particularly true of the glacial rivers which discharge their sediment-laden waters along the southern coast of Iceland (Figures 8, 21, and 22). Not only is it possible to measure qualitative changes in the size of such plumes on a seasonal basis, but dispersal of sediment-laden fresh-water plumes in a marine environment may have an influence on optimum locations for fishing. Research will be initiated on this possible correlation. An effort will also be made to determine whether or not the size of a sediment plume from a particular river can be correlated with river discharge and perhaps even with variations in melting rates of glaciers.

The most important findings from this experiment relate to the islands of Surtsey and Heimaey, islands of volcanic origin in the Vestmannaeyjar archipelago off the south coast of Iceland (Figure 1). Careful enlargements were made from 3d generation, 70 mm negatives to scales of 1:1,000,000; 1:500,000; 1:336,900; 1:250,000; 1:168,450; and 1:84,225, for all four MSS bands, for comparison with existing maps.

Surtsey is a small volcanic island (about 2.5 km^2) which appeared above the ocean's surface on 15 November 1963 and was in discontinuous eruption between that date and early June 1967. Surtsey had complex eruptive history, but the final increase in size of the island due to eruptive activity was in late August and early September 1966, when it increased to 2.8 km^2 in area (Thorarinsson, 1968). Ever since it appeared above the ocean's surface, wave action has reshaped its coastline, thereby posing a problem for cartographers trying to accurately portray the island on topographic maps. Figure 13 is a 1966 map of Surtsey which is based on 24 August 1965 aerial photography. A special Surtsey map (Surtsey, Landmælingar Íslands, 23 Oct. 1964, 1:10,000 scale) was also published at an earlier date. The more recent 1969 map (Aðalkort Blað 6, Miðsuðurland, Landmælingar Íslands, 1:250,000 scale) shows Surtsey as it appeared on 17 July 1967 aerial photography. Both the 1:100,000- and 1:250,000-scale maps are revisions of previous map editions which were published by the Geodætisk Institut of Copenhagen, Denmark. It is interesting to note that the most recent official map of Surtsey, the U. S. Department of Defense's Joint Operations Graphic (Ground) (Series 1501, Sheet NP 27, 28-2, Edition 1, Vestmannaeyjar, Iceland, 1:250,000 scale), which was published in January 1969, "from best available source," claims that Surtsey is based on 1968 data, when in fact it shows the island as it existed in 1965.

A number of maps of Surtsey have been drafted for scientific papers (Thorarinsson, 1968; Norrman, 1970, 1972a, and 1972b). Landmælingar Íslands has also acquired frequent aerial photography, more during the period of volcanic activity and less since that time. Since September 1966, when changes in the coastline of Surtsey caused by volcanic activity ceased, the change has been due to erosional forces: recession of the windward southwest-facing lava cliffs and progradation of the wide beach on the leeward northeast shore now dominated by a prominent bulbous ness. This prominent ness, as well as the present coastline of

Surtsey, can be seen on Figure 14, an enlargement of an ERTS-1 MSS image (Surtsey, E5, 19 Aug. 73, 1392-12194-6). At map scales of 1:100,000, or smaller, ERTS imagery could be used to revise planimetric maps of volcanic islands.

Figure 15 is a recently revised map of Heimaey which is based on 1965 data, published in 1966, and revised, by red overprint, on 23 January 1973, within a week after the volcanic eruption began. Figure 16 is an enlargement of an ERTS image of Heimaey prior to the volcanic eruption (Þórisvatn, D6, 21 Nov. 72, 1121-12143-6). The west side of the island is partially obscured by a lenticular cloud; however, the eastern half is cloud free. Figure 17 is an enlargement of an ERTS image of Heimaey after the eruption had ceased (Hekla, D5, 19 Aug. 73, 1392-12191-6). The increase in land area, due to lava flows, on the east side of Heimaey can be clearly seen. Again, these images point out the fact that, at least to map scales of 1:100,000 or smaller, ERTS imagery may be directly used to effect planimetric revisions of existing maps, or in the absence of existing maps, show changes caused by volcanism by comparison of "before" and "after" images. In remote areas, ERTS imagery offers volcanologists a powerful new tool in the study of changes on volcanic islands and perhaps even produce a "time-lapse" record of an eruption in progress.

HYDROLOGICAL STUDIES

Ephemeral Snow and Ice Experiment

It was expected that ERTS imagery would permit the mapping of variations in snow cover in Iceland over time, mapping of surface water distribution, and mapping of ice freezeups and thaws on major lakes. Both snow cover changes and freezing and thawing of lakes are very dynamic phenomena, particularly the former. The paucity of fall, spring and early summer imagery of Iceland, the former because of darkness and the latter two seasons because of tape recorder malfunction, severely limited periodic coverage of these two aspects of the experiment. On ERTS images, lakes were either snow covered and frozen on wintertime images or ice free on summertime images. In no case was any freezeup recorded on imagery; in only one case was an ice breakup observed, on a mostly cloudy image of lake Apavatn in southwestern Iceland (Þórisvatn, D6, 27 Mar. 73, 1247-12145). About a month earlier the mostly cloud-covered image showed the partially frozen lake Þingvallavatn (Þingvallavatn, D4, 21 Feb. 73, 1213-12261).

Of particular importance to Iceland is the persistence of snow cover into the summer months, particularly in the rangelands of the interior, which are used for grazing by sheep when the snow has melted. Persistence of snow is related to the amount of snowfall during the previous winter and to the coolness of the summer months. There has been some deterioration of climate in Iceland since the early 1960's. The persistence of snow in the interior and of concentrations of sea ice on the north and east coasts, particularly in the late 1960's, serve as indicators of a colder climate in Iceland. Snow cover and its persistence is of particular importance in the polar regions because, "Areas of prolonged coverage are potential sources of glaciation" (Anon., 1970b, p. 88).

Although snow cover has, of course, been successfully mapped from satellite imagery of the TIROS, ESSA, and Nimbus series, as well as from photography from Apollo 9 (Barnes and Bowley, 1966, 1968a, 1968b, 1969a, 1969b, 1970, and 1972; Fritz, 1962; Tarble, 1963; Popham and Samuelson, 1964; and Popham and others, 1966), the resolution characteristics of the ERTS-1 MSS instrument provide far more accurate snow cover information, in most cases approaching high-altitude aerial photography in detail, but offering a much greater area of simultaneous coverage (Barnes and others, 1972 and 1974; Barnes and Bowley, 1973b; Meier, 1973; Wiesnet, 1972; and Wiesnet and McGinnis, 1974).

The Nimbus and NOAA series of weather satellites have not yet been displaced by ERTS, because they provide much more coverage of an area at least twice daily with their highest resolution sensors (North America only; tape recorder limited outside North America), and multiple daily coverage with lower resolution sensors. Snow cover can change very rapidly, particularly in the springtime. Therefore the weather satellites retain their preeminence over ERTS in snow-cover mapping because of their greater frequency of coverage (Wiesnet and McGinnis, 1974). Figure 18 shows some of the detail of snow cover available from NOAA-2 imagery of Iceland. Between late March and early July 1973, no ERTS imagery exists of Iceland.

This NOAA-2 image shows that much of the snow cover of Iceland has melted by 22 May 1973, except in the highlands. For snow cover mapping, ERTS imagery can only be considered to be complementary to weather satellite imagery.

Nearly every ERTS image of Iceland shows some change in previous distribution of snow cover. Great detail is evident in many of the images. In midsummer images, areas of snowpack can be seen, including long, linear white strips, where the previous winter's snow has drifted against linear volcanic and structural landforms. Even in mid- and late-summer, ERTS imagery has often recorded fresh snowfalls, particularly in the higher elevations. Where the air temperature is above 0°C, fresh snowfalls often appear white on bands 4 and 5, and black on bands 6 and 7 (Williams and others, 1973a). Thus areas of melting snow, either on the terrain or glaciers, can be mapped.

The most important application of ERTS imagery, resulting from this experiment, was in the delineation of surface water distribution in Iceland, particularly in the mapping of lakes. Of particular interest were the changes in lakes fed by glaciers when compared with existing maps and the effect engineering activities are having on Þórisvatn, a large V-shaped lake north of Torfajökull in central Iceland. Flow in its northern outlet, Þórisós, to the Kaldakvísl river has been reversed. Sediment-laden (glacial rock flour) water from Kaldakvísl, which drains the northwestern edge of Vatnajökull, is now entering the lake via Þórisós. On band 4 imagery (Vatnajökull, D7, 9 Sept. 72, 1048-12080-4), a distinct sediment plume can be seen extending into most of the western arm of the lake, although becoming less distinct with increasing distance from its former outlet. It is still distinguishable for a distance of 10 km, however. This sediment should have an impact on the natural ecology of the lake, originally a ground-water table lake with no incoming streams and but one outlet (Sigbjarnason, 1972).

Numerous smaller lakes around the country have different shapes and areas than their representation on maps. It is the glacier-margin lakes, however, which have exhibited the greatest change from existing maps. Some have even changed in area during the course of a year of ERTS imagery. These lakes will be discussed more fully under the Glaciological Features and River Flooding Experiments.

Glaciological Features Experiment

Of all the ERTS experiments in Iceland the glaciological features experiment has yielded the greatest amount of new scientific data. This is due to the dynamical aspects of glaciers and related features in Iceland, the very great size of some of Iceland's icecaps and glaciers, the logistical difficulty in studying these icecaps, and the obvious change in so many types of glaciological features when compared with existing topographic maps. ERTS imagery, because of its repetitive, high resolution, synoptic coverage of glaciers, provides glaciologists with an important new tool in monitoring changes in glaciological features as well as delineating features on the surface of glaciers which have hitherto gone unobserved. In particular many new features have been revealed on the four largest icecaps of Iceland, Vatnajökull, Hofsjökull, Langjökull and Mýrdalsjökull, from ERTS imagery acquired at low sun angle.

ERTS imagery is the first satellite imagery to have sufficient resolution to be useful to glaciologists. Individual glaciers and icecaps in Iceland (and other areas) were imaged by previously and currently operational weather satellites, such as Nimbus and NOAA-2, but neither had sufficient resolution to depict anything but gross glaciological features. Figure 19 is a 21 September 1970 image of Iceland taken by Nimbus IV. The four largest icecaps can be grossly delineated. Figure 18 is a NOAA-2 image of Iceland acquired on 22 May 1973. Considerably more detail is apparent on this image with the four largest icecaps more clearly delineated and some of the smaller icecaps as well. The Grímsvötn caldera in west-central Vatnajökull can be seen.

About one tenth of Iceland is covered by glaciers, nearly all of which are termed icecaps. Figure 20 shows the 33 IHD (International Hydrological Decade) glaciological observation stations in Iceland and all of the important glaciers (Rist, 1967b). Table 2, which accompanies Figure 20, lists most of these glaciers. All of the glaciers listed after Tungnafellsjökull encompass areas of 30 km^2 or less. Sufficient late summer and early fall 1973, ERTS-1 imagery of Iceland now exists to accurately map planimetrically the 10 percent of Iceland covered by glacial ice.

Optimum imagery has been obtained of Vatnajökull (Figures 21 and 22), Hofsjökull (Figure 23), Langjökull (Figure 23), Mýrdalsjökull (Figures 22 and 23), and Eyjafjallajökull (Figures 22 and 23), or five (including the four biggest) of the seven largest icecaps in Iceland and five of the smaller (less than 50 km^2) icecaps as well.

Special planimetric maps are being drafted from this ERTS imagery for comparison with previously published maps. All of Iceland's glaciers have a long history of change, some gradual, some rapid (Eyþórsson, 1963; Thorarinsson, 1964; and Sigbjarnarson, 1970).

Special emphasis is being given to Vatnajökull, the largest icecap in Iceland (Figure 24) (Eyþórsson, 1960). It has an area of approximately 8,400 km^2 (Thorarinsson, 1956) and is characterized by numerous outlet glaciers, particularly on the south and east margins; at least three subglacial volcanoes, Öræfajökull, Grímsvötn, and Kverkfjöll (Friedman and others, 1972); and numerous glacier-margin lakes. Grímsvötn, in particular, has had a long history of jökulhlaups, extraordinary discharges of water from the margins of a glacier caused by either the failure of ice dams which impound subglacial or glacier-margin lakes or subglacial volcanic and solfatara activity. Historic jökulhlaups are also known from other parts of Vatnajökull and also from Mýrdalsjökull (Thorarinsson, 1956), a result of a subglacial eruption of the volcano Katla (Rist, 1967a), Eyjafjallajökull and Öræfajökull (Thorarinsson, 1958).

Figure 12 shows a number of depressions on the surface of Vatnajökull, all the result of subglacial geothermal or volcanic activity, and some of which are related to recent jökulhlaups. The depressions seen on this ERTS image near the northern rim of the Grímsvötn caldera form or deepen after each jökulhlaup from Grímsvötn, the last one having occurred in March 1972. They are most certainly the result of permanent subglacial geothermal activity and subsidence of the overlying ice, following withdrawal of meltwater (Thorarinsson and others, 1973). The series of shallow depressions forming a chain east to south-southeast of the southeastern part of the caldera may possibly show the subglacial course of the flood water from the March 1972 jökulhlaup from Grímsvötn.

Between Grímsvötn and the western edge of Vatnajökull are three more depressions, almost certainly also the result of subglacial or volcanic (?) activity. The main depression (the easternmost one) was first observed by Thorarinsson and Hannesson during a reconnoitering flight over Vatnajökull on 7 September 1955. Since that time jökulhlaups have occurred every second year in Skaftá, a river which drains Vatnajökull on the southwest; the last one took place in August 1972. The depression has never been refilled by snow between jökulhlaups (See Figures 12 and 22). The depth of the depression after each jökulhlaup has been 100-150 m.

On Figures 12 and 22 the twin snow- and ice-filled craters and the ice-free valley at Kverkfjöll can be delineated. A jökulhlaup from Graenalón, a glacier-margin lake on the southwestern edge of Vatnajökull, which was unrelated to geothermal or volcanic activity, occurred in August 1973, and will be discussed under the River Flooding Experiment.

Changes in area, disappearance, and creation of glacier-margin lakes are quite common occurrences along the edges of icecaps or glaciers (Tómasson and Vilmundardóttir, 1967), particularly at the terminuses of glaciers. Vatnajökull is no exception (Price and Howarth, 1970). Numerous changes in and disappearance of such lakes have been reported in the literature (Thorarinsson, 1939). The surging glacier, Eyjabakkajökull (Figure 24), which surged during late 1972 and early 1973 (?) caused a lake to increase in size which lies between it and another surging glacier to the west, Brúarjökull. A number of changes in lakes along the edge of Brúarjökull, which last surged in 1963, are also evident.

Eyjabakkajökull was in the midst of a surge when ERTS-1 passed over on 14 October 1972 (Figure 25). Rist (1972) reported that the surge might have begun as early as 25 August 1972, and that travelers estimated a forward movement of 800-1,000 m as of 20 September 1972. Observations were made by two men on 7 and 21 October 1972; they estimated a movement of 370 m between those two dates or over 26 m per day. According to measurements made on the two ERTS-1 images (Figures 25 and 26), Eyjabakkajökull surged 1.8 km between 14 October 1972 and

22 September 1973, mostly in late 1972, but possibly including some motion in early 1973. If the field observations and the measurements from ERTS imagery are combined, then Eyjabakkajökull surged in excess of 3 km in a few months, perhaps in as little as a few weeks.

The most profound changes, however, were the successive changes in the area of Grænalón (Figures 12, 21, 22, 27, and 28). Successive ERTS images showed an increase in surface area, until the ice dam was partially breached, thereby resulting in a jökulhlaup and a sharp reduction in lake area. Glacier-margin lakes, or any lake which is receiving sediment-laden runoff from a glacier, have a distinctive robin's-egg blue color on MSS false-color composites (bands 4, 5, 7), placing them in sharp contrast with the white of the glacier, reds of vegetation, or other nonblue colors related to soil or bedrock.

Beyond the present margins of Vatnajökull are a number of interesting features related to past positions of Vatnajökull and Hofsjökull outlet glaciers. Recessional moraines are well displayed on Figure 12 in front of several outlet glaciers of Vatnajökull: Svínafellsjökull, Skeiðarárjökull, and Síðujökull. The beautiful little outlet glacier on the southeast side of the Hofsjökull icecap, has a striking series of concentric recessional moraines. Large medial moraines within the icecap proper (Vatnajökull) also show up well under the low sun angle, particularly on the eastern side of Dyngjujökull and southeast of Esjufjöll (Figure 12). On late summer imagery of Vatnajökull (Figures 21 and 22) the dark color of lateral and medial moraines can be sharply delineated. The distorted pattern of medial moraines in surging glaciers contrasts sharply with the undisturbed pattern of non-surging glaciers. These contorted medial moraine patterns can provide useful markers for the measurement of glacial motion over time. For example, on images of contorted medial moraines on Skeiðarárjökull (Figures 27 and 28) taken about 11 months apart, an estimated 600 m of glacier motion has taken place, on the eastern side of Skeiðarárjökull, east of lake Grænalón. This shows that ERTS imagery can be used, in certain instances where "marker" features are present, to measure directly surface flow rates of glaciers. This is important in the study of the dynamics of glacier movement, because the position of the snout or terminus of a glacier represents whether or not the glacier is in equilibrium with respect to accumulation and ablation or is in inequilibrium. In the case of Skeiðarárjökull the only direct measurement of the movement of this glacier was made by a Polish expedition during the summer of 1968. They found that the annual movement of Skeiðarárjökull, southeast of Grænalón to be about 430 m (Wójcik, 1973).

On false-color composite images, recently deglaciated terrain can be distinguished in some cases on the basis of vegetation difference (lack of grasses and lichens) from older deglaciated terrain, where the lichens have a purplish hue, and the grasses have a pink or red color. This distinction is particularly well defined in front of the small outlet glacier on the southeast side of the Hofsjökull icecap. On Figure 23, the band 7 ERTS image shows a dark band of concentric moraines between the glacier's terminus and the highly reflective grassy swamplands to the southeast. A similar dark fringe is common to many of Iceland's icecaps.

River Flooding Experiment

The lack of spring imagery of Iceland prevented the mapping of spring runoff and floods along major river valleys, the time of two prominent periods of higher than normal flow in drainage basins in Iceland. According to Rist (1969), high flow rates of Icelandic rivers do not necessarily follow the temperature pattern of peak discharge during the spring. High flow rates can occur during February-March (winter thaw), May-June (spring thaw), July-August (melting of glaciers), and October-November (autumn rainfall).

Changes in distributaries from glaciers could be mapped, however, particularly across the Skeiðarársandur (Figure 24) of the southern coast. Braided stream drainage on this large outwash plain is the result of melting snow and ice from Skeiðarárjökull and other outlet glaciers on the southwestern margin of Vatnajökull. Maximum flow across the Skeiðarársandur takes place during July and August. On Figure 12, very little discharge is taking place across the Skeiðarársandur, because it is winter. A snowstorm had crossed the area the day before, and the 0°C isotherm (during the storm) is represented by the snow-bare land contact at higher elevations on the outwash plain, inland about 20 km from the coast. Some ablation is taking

place, however, from the snout of Skeiðarárjökull even in midwinter. Maximum discharge of these glacial rivers can be seen on Figure 21, an image acquired on 30 July 1973. Reduced runoff only 7 weeks later, on 22 September 1973, can be seen on an early fall image (Figure 22).

It was anticipated that a jökulhlaup might occur during the ERTS-1 experiment. The effects of two jökulhlaups, one in March 1972 from Grímsvötn and the other in August 1972 from an area between Grímsvötn and Hamarinn, in the development of collapse features on the surface of Vatnajökull, has been discussed under the Glaciological Features Experiment. A jökulhlaup did occur from Grænalón in August 1973. The increase in area of this lake over a 10 month period to the jökulhlaup, and the decrease in area of the lake and new river channels across the Skeiðarársandur after the jökulhlaup can be clearly seen on ERTS imagery. Grænalón was first imaged on 14 October 1972 (Figure 27); the ice dam of a valley glacier from Skeiðarárjökull can be seen to the east. The lake was again imaged on 31 January 1973 but was completely frozen. The third time it was imaged was on 30 July 1973 (Figure 21) when it had reached its largest extent prior to the jökulhlaup. Less than 2 weeks later the ice dam was partially breached, and a small jökulhlaup partially drained Grænalón (Figure 28) along the Súla River which flows along the western margin of Skeiðarárjökull and then south across the Skeiðarársandur. The change in channel position of this river across the Skeiðarársandur can be seen by comparison of Figures 21 and 22. After the jökulhlaup, Grænalón did not return to the small area shown on Figure 27, but stabilized somewhat larger in area. Because of the shape of the Grænalón basin the lowering of water-level of Grænalón, resulting from the jökulhlaup, could be determined from the ERTS imagery with an error of less than ±2 m.

Jökulhlaups from this part of Vatnajökull are no longer solely of academic interest because of the completion in 1974 of the first all-weather road (Kristinsson, 1972) across the Skeiðarársandur. This road will permit considerable vehicular traffic to move along the south coast of Iceland for the first time. The prediction of the occurrence of jökulhlaups takes on added significance because of the need to provide advance warning. It is suggested that a combination of ERTS imagery and data collection system (DCS) platforms (ERTS or synchronous meteorological satellite) could provide the basis for such a warning system. The experience with ERTS imagery of Grænalón shows that imagery alone can at least monitor the increase in size of glacier-margin lakes.

OCEANOGRAPHIC STUDIES

Sea Ice Experiment

The presence of sea or floe ice off the northern and eastern coasts of Iceland has historically had a deleterious effect on grass growth in Iceland and has affected the shipping of goods to northern ports, such as the city of Akureyri. Particularly for shipping requirements the Icelandic Meteorological Office and the Icelandic Coast Guard monitor drift ice off the coast of Iceland. Sea ice, because it lowers sea-water temperatures below normal, may also affect the very important herring fisheries in Iceland (Jakobsson, 1969). However, sea ice concentration and persistence are only two of several variables which are thought to govern herring abundance.

Drift ice - its concentration and persistence - has had a marked influence on the economy of Iceland. Its impact on the natural environment has been studied by a number of Icelandic scientists, including Bergthórsson (1969), who found a good correlation between annual temperature and the resulting influence on the regime of Icelandic glaciers; Thorarinsson (1969) who discussed the effect of sea ice on glacier variations; and Friðriksson (1969), who has studied the effect of sea ice on annual grass yield. There is no question that the mapping of the drift ice margin and the concentration and movement of drift ice, if accomplished from satellite imagery, would be of value to the Icelandic economy.

Icelandic scientists have experimented with automatic picture transmission (APT) imagery from the ESSA satellite series (Jónsson, 1969); however, most of the Icelandic sea ice maps are compiled from observations made by aerial reconnaissance (Jakobsson, 1969, Sigurðsson, 1969) and the maps by Hlynur Sigtryggsson for the years 1960-1969 (Bárðarson, 1971). Subsequent weather satellites have shown a steady improvement in spatial resolution. Figure 29 shows sea ice between Iceland

and Greenland in the Denmark Strait or a Nimbus III Image Dissector Camera System (IDCS) image on 15 April 1969. Figure 18 is a NOAA-2 image mosaic of sea ice between Iceland and Greenland in the Denmark Strait on 22 May 1973. Only one ERTS image of the waters northwest of Iceland included any sea ice. That image (Skagi, B3, 23 May 73, 1304-12310) was acquired the day following the NOAA-2 image (Figure 18). The absence of other ERTS-1 coverage of northwestern Iceland and the sea north of the island, which is the usual closest approach of sea ice to Iceland; a mild sea-ice season; and the limitation in size of the test site to the north all prevented the objectives of the sea-ice experiment being attained.

Drawing from the work of Popham and Samuelson (1964), Predoehl (1966) and McClain and Baliles (1971), McClain (1972), Campbell (1972), Barnes and Bowley (1973a and 1974), and Wiesnet and McGinnis (1974), who have all studied sea ice from satellite sensors sensitive to reflected energy, and the work of Barnes, Chang, and Willand, in a series of reports (1969, 1970a, 1970b, 1972a, and 1972b), who have mapped sea ice on satellite thermography, it is obvious that the much higher resolution of the ERTS sensors and lesser frequency of coverage by the satellite, resulting from the relatively small field of view and orbital altitude to achieve the higher resolution, severely limits the usefulness of the ERTS imagery for mapping sea-ice concentration and movement. Persistent cloudiness around Iceland, combined with the infrequent coverage with ERTS-1, also limits availability of imagery. Another problem with sea-ice mapping with ERTS imagery north of Iceland is low solar illumination during nearly one-third of the year, that is the months of December and January and much of November and February. It is evident that a thermal channel on future MSS systems on ERTS-type satellites will be needed to overcome this deficiency. It would seem, therefore, that insofar as sea-ice mapping is concerned ERTS imagery can be best employed as a supplement to weather satellite imagery.

Finally, with respect to the addition of a thermal sensor on ERTS spacecraft, a valuable spinoff to having such a sensor to map sea ice during the winter months is that satellite thermography could provide much needed data on the variation in surface water temperatures of marine currents around Iceland, of great potential value to the fisheries industry. A preliminary evaluation of NOAA-2 thermography has established the promise such satellite thermography holds for mapping marine currents off the coast of Iceland.

AGRICULTURAL STUDIES

Grasslands and Forest Experiment

Animal husbandry, particularly sheep and cattle, is an important element of the Icelandic economy. Grass, therefore, is an important agricultural resource. Although Iceland was forested at the time of settlement, the excessive harvesting of timber, the introduction of large, free ranging flocks of sheep, and the apparent slight deterioration of the climate have resulted in almost total denudation of forested land. Birch, dwarf birch, and willow trees and various bushes exist in favorable locations, but only two sizeable areas of true forest still exist, Hallormsstaður in eastern Iceland, and Vaglaskógur near Akureyri. It was anticipated that the ERTS false-color composites would permit an accurate inventory to be made of areas covered by trees and bushes and assist in planning future reforestation work. Of greater importance, however, would be an accurate inventory of grasslands with such imagery. The sea ice and resulting lower summer and annual temperature had a devastating effect on hay yield in the northern, and to a lesser extent in the southern, part of Iceland in the 1960's decade (Friðriksson, 1969). It was expected that ERTS false-color composites of the grasslands would permit an assessment of areas subjected to winter-kill. More importantly, however, an assessment of the grasslands could perhaps be made on a regional basis during the growing season and a correlation made between distribution of vegetation and persistence of snow cover.

The agricultural industry of Iceland is heavily dependent on the areal extent, health, and growth rate of the grasslands. The grasslands are usually divided into lowlands and highlands, the latter being used for grazing by sheep during the summer months, and the former by cattle and Icelandic ponies during the late spring, summer and early fall. The highland grasslands are used in their natural state, while some of the lowland grasslands have been subjected to extensive ditching to lower the water table, thus improving the soil properties and increasing the grass

yield. On the homefields (Icel. tún), the application of fertilizer, ditching, and seeding have markedly increased the yield. The harvesting of hay from the homefields provides the feed for the animals kept through the winter months.

There is considerable effort being expended to reclaim the overgrazed lands through reseeding and fertilizing of barren areas (Friðriksson and Pálsson, 1970). Many areas are also being reforested to reverse the post-settlement trend of soil erosion (Bjarnason, 1961). The reclamation program is directed at an increase in the area of grazing lands to meet the future resource needs of a rapidly growing Icelandic population.

Although an excellent vegetation mapping program has been underway for several years (Thorsteinsson, 1972), it will be several more years before the mapping will be completed. Field observations are being plotted on aerial photographs acquired in ca. 1960 and later transferred to base maps. When completed, the vegetation mapping project will provide an inventory of Iceland's vegetation as mapped over a 15-year period. For resource management decisions, however, additional, timely data on the state of the grasslands is utilized. Seasonal imagery is needed so that gross changes in the rangelands can be mapped and evaluated. Not only is an operational ERTS needed to provide such data, but a means of making newly acquired imagery (MSS false-color composites) available to Icelandic agricultural experts within 10 days to 2 weeks after acquisition is also required. Information on dynamic phenomena, such as health and growth characteristics of rangelands, is "perishable."

A preliminary study of MSS false-color composites of various parts of Iceland has shown that at least five vegetation types can be mapped on ERTS imagery (Figures 23 and 30). These are: (1) bushes, dwarf trees, and shrubs; (2) natural grasslands; (3) reclaimed land; (4) cultivated homefields; and (5) lichen-covered lava fields. In addition, barren lands can be delineated by their absence of vegetation. One interesting finding from a preliminary study of the false-color composites is that the grasslands apparently must reach a certain density and/or size before they can be imaged even as a light pink. In other words, no pink or reddish color exists in the barren lands until an unknown areal distribution and/or density of grass is present. What this threshold value is must await careful field observations and correlation with preëxisting vegetation maps.

The variations in the climate of Iceland (Eyþórsson and Sigtryggsson, 1971), falls of volcanic ash, and presence, persistence, or absence of sea ice off the coast of Iceland all can have their effect on the state of the grasslands. Imagery from ERTS-type satellites offers, over a long period of time, the means of monitoring the effect of such phenomena on the grasslands and forests. Aside from the importance of an operational satellite to resource management decisions relative to the Icelandic grasslands, such long-term studies can have equal value in a better knowledge of the response of the grasslands to long-term climatic variation.

CARTOGRAPHIC STUDIES

Although not a separate experiment in the original proposal, the cartographic applications of ERTS-1 imagery of Iceland have grown to the point where a separate study has become both necessary and desirable. Several applications of ERTS imagery to improvement of existing small-scale Icelandic maps appear quite feasible and are being pursued.

Planimetric revisions of existing maps of Iceland to map scales of 1:250,000 or larger are quite feasible. With careful enlargement of a limited area, planimetric revisions to maps at a scale of 1:100,000 also can be accomplished. The cartographic experience with ERTS imagery of Iceland has determined that the 1:500,000-scale enlargement is the best. Tonal quality, resolution, and size of area presented all seem to be at an optimum at the 1:500,000 scale. Several experimental cartographic products of Iceland are planned, including: 1:500,000-scale orthoimage mosaics of summer band 5 and band 7 and winter band 7, and three 1:250,000-scale orthoimage mosaics of the largest icecaps. One of the advantages to using ERTS imagery for the latter three maps is that they will show how these icecaps existed at about the same time (within 7 weeks). Previous glaciological maps of Iceland are really hybrid composites, being compiled from data of different dates, and in the case of Vatnajökull, covering a number of years. Because glaciers are dynamic, such maps are partly fictitious in that they portray

a feature as it never was. Such cartographic license is common to maps published throughout the world, including those published of remote areas of the United States. ERTS imagery can portray features such as glaciers as they are at a point in time and also monitor changes quite frequently (MacDonald, 1974). Another cartographic product which is under preparation is a false-color composite mosaic of Iceland at a scale of 1:1,000,000 for use in the grasslands and forest experiment.

The success of ERTS-1 imagery in monitoring environmental phenomena of the Earth's surface has been solely through analysis of tonal variations (reflectance differences) on the imagery, a two-dimensional entity. However, some of the ERTS-1 scientists (Poulton, 1972; Williams and others, 1973b) have taken advantage of the limited sidelap available to map phenomena from a stereoimage.

Although stereophotogrammetric techniques applied to photographs of the Earth's surface are the basis for the production of modern topographic maps, ERTS-1 and its immediate successors were not designed for 3-dimensional mapping. Therefore the use of ERTS stereoimagery for the production of topographic maps is not an issue, rather it is the importance of ERTS stereoimagery to improving the extraction of certain types of 2-dimensional information. Stereoimagery from overlapping ERTS images of Iceland has been found to be of significant value in the study of geomorphic and structural geologic features or to phenomena related to morphology.

Photogeologists are trained to use stereophotographs to map geologic formations and structure on the basis of obvious or subtle differences in landforms. Such differences are often not evident on 2-dimensional photographs. With the current ERTS imagery, most investigators are unaware of the advantages of stereoimagery in mapping landform-related phenomena. It is curious, however, that a number of investigators, at the various ERTS-1 symposia (three to date) have commented on the importance of midwinter imagery to mapping certain types of phenomena (faults, lineations, landforms). This is because the lower sun angle of imagery at this time of year (in the Northern Hemisphere) enhances structural and morphologic details of the Earth's surface.

Interestingly enough, however, the low angle of solar illumination creates a sort of ersatz stereoimage in that the shadowing produces an effect similar to that achieved by selective shading on contour (topographic) maps. In Iceland, for example, ERTS imagery acquired at a 7° sun angle, revealed new subtle structural and morphologic details of unquestioned geologic value.

Because of the time of passage of ERTS over much of the Earth's surface, low sun angle imagery must be restricted to the higher latitudes. The provision of a stereocamera capability on a future ERTS, however, would permit the acquisition of stereoimagery of the entire Earth (McEwen, 1974). Stereoimagery would be of significant value to the mapping of many types of environmental phenomena. The ability to view the Earth in 3 dimensions and to relate dynamic and static environmental phenomena to these 3-dimensional images should not be treated lightly, but rather as a major step forward in our ability to view and record environmental conditions on our planet's surface.

An experiment was undertaken to try to determine whether stereopairs of adjacent (sidelap) ERTS-1 images of high relief areas of Iceland could give meaningful relative elevation differences. Some success was achieved using a Kern PG-2 measure of relative elevation of mountains where considerable overlap existed in successive orbits. A ground feature is imaged on three successive orbits at the latitude of Iceland, (65°N.) with about a 130 km baseline separation between the first and third orbits. Sufficient parallax existed on Herðubreið, a table mountain with 1,000 m of local relief, in north-central Iceland (Figure 2). The stereoplotter operator stated that he thought he could draft 10 contour lines within the 1,000 m elevation difference, giving a 100 m relative measurement capability from ERTS.

The repetitive ERTS-1 imagery acquisition over Iceland has caused a very large cataloging problem. For that reason a geographic matrix for Iceland has been created to place each image in its proper geographic area. Figure 31 shows how each image (and repetitive images of the same area) has been arbitrarily given a specific geographic name. Each matrix square (image) contains one or more images

of much the same area. Successive images differ only in their date and the amount of cloud cover. The handling of ERTS-1 imagery then becomes quite similar to map or aerial photo handling.

The arbitrary geographic matrix for ERTS-1 imagery of Iceland becomes a series of "quadrangle maps," easy to fit into existing map and aerial photographic coverage. NASA should consider holding the orbit quite closely over time and hold "framing" to the same area. In this way successive ERTS-1 images would become "maps" of specific areas. Study of dynamic phenomena could be more easily carried out, particularly computer-assisted, change-detection mapping. This suggestion, developed independently, is quite similar to Schoonmaker's (1973a and 1973b) and Colvocoresses' (1973b) excellent idea for an image format map series.

The high surface albedo (reflectivity) of snow permits imagery to be acquired under low intensity of solar illumination, that is at low solar angles. Consideration should be given to extending the programmed coverage of polar areas with the ERTS satellite to solar elevation angles as low as 5°, perhaps even lower. In addition, consideration should also be given to the acquisition of ERTS imagery during the polar summer when the midnight sun should offer sufficient illumination.

CONCLUSIONS

ERTS-1 imagery of Iceland provides the basis for the study of several different geological and geophysical phenomena which relate in an important way to the natural resources of Iceland. Preliminary analyses of available ERTS-1 imagery of Iceland clearly shows that timely analysis of repetitive ERTS data can enable Icelandic research institutes and governmental agencies to measure and map important environmental features which have great economic implications in Iceland.

Table 3 provides a brief summary of the most important results to date from the ERTS-1 experiment in Iceland as well as a comparison with expected results before ERTS-1 was launched. Full or partial success was achieved with each of these studies except for the sea ice study. The failure to reach 100 percent of the objectives for all the experiments was the result of the lack of seasonal data of Iceland from ERTS-1.

Because of the wide variety of geological and geophysical phenomena which can be observed in Iceland, and because of the very clear and direct relation to the management of the country's natural resources, Iceland is particularly well suited for experimental studies to establish operational feasibility of the use of operational earth resources technology satellite sensors and other systems to meet resource inventory and management needs on a timely and cost-effective basis. Success with such an operational system in Iceland will point the way to the use by other countries of the techniques and concepts proven in Iceland. Iceland shares with the United States and with most other countries of the world a need for accurate and timely information on the status of its natural resources, in order to make wise decisions concerning the optimum utilization of such resources. ERTS-1, the progenitor of a line of earth resources technology satellites, provides a "first-time" capability for the acquisition of environmental information, particularly for data on dynamic environmental phenomena.

An operational ERTS, with sufficient command-and-control capability, sufficient tape recorder capacity, and a thermal sensor still remains but a promise, however. All of this is available from existing ERTS technology if the technological and political leadership of the U. S. and the world will make the necessary hard decisions to build more ground receiving stations, provide long-term support for an operational ERTS system, an estimated U. S. $30 million per year, accelerate data dissemination to users, and restructure data user organizations to work with near real time information rather than obsolete or invalid data.

ACKNOWLEDGMENTS

The authors are indebted to the fine support provided to the project by Mr. Steingrímur Hermannsson, Director, Icelandic National Research Council, Dr. Vilhjálmur Lúðvíksson, the Icelandic National Research Council, and Prof. Magnús Magnússon, Director, Science Institute of the University of Iceland.

Financial and other support for the project was provided by the Earth Resources Observations Systems (EROS) Program Office of the U. S. Geological Survey. Special thanks are due to Dr. John M. DeMoyer, Director; Mr. Winston Sibert, Program Manager; Mr. William A. Fischer, Senior Scientist; and to Mr. W. Douglas Carter, Mr. William R. Hemphill, and Miss Mary Ann Milosavich, for their support in various aspects of the project.

The National Aeronautics and Space Administration's Goddard Space Flight Center provided MSS imagery and MSS false-color composites, under a no-fund ERTS-1 research experiment (SR 9651), Contract No. S-70243-AG, Task 43. We would like to acknowledge the fine support given to the project by Dr. Stanley C. Freden and Mr. Fred Gordon.

REFERENCES CITED

Anonymous, 1970a, Iceland volcano eruption causes fluoride pollution: Reuters dispatch published in the Christian Science Monitor, 15 July 1970.

Anonymous, 1970b, Polar research - a survey: Natl. Acad. of Sciences, Committee on Polar Research, Natl. Research Council, Washington, D. C., 204 p.

Anonymous, 1971, The Best of Nimbus: Allied Research Assoc., Inc., Rpt. #9G45-80, NASA Contr. No. NAS 5-10343, March, 119 p.

Barnes, J. C., and Bowley, C. J., 1966, Snow cover distribution as mapped from satellite photography: Final Rpt. for ESSA (NESS), Contr. No. Cwb-11269, Allied Res. Assoc., Inc., Rpt. No. 8G25-F, May, 108 p.

_____ 1968a, Snow cover distribution as mapped from satellite photography: Water Resources Research, v. 4, no. 2, p. 257-272.

_____ 1968b, Operational guide for mapping snow cover from satellite photography: Final Rpt. for ESSA, Contr. No. E-162-67(N), Allied Res. Assoc., Inc.

_____ 1969a, Satellite photography for snow surveillance in western mountains: Rpt. presented at Western Snow Conf., Salt Lake City, Utah, April, 20 p.

_____ 1969b, Satellite surveillance of mountain snow in the western United States: Final Rpt., Contr. for ESSA, No. E-195-67(N), Allied Res. Assoc., Inc.

_____ 1970, The use of environmental satellite data for mapping annual snow-extent decrease in the western United States: Final Rpt. for Environmental Science Services Administration, Contr. No. E-252-69(N), Allied Res. Assoc., Inc., Rpt. No. 8G72-F, June, 105 p.

_____ 1972, Snow studies using thermal infrared measurements from Earth Satellites: Final Rpt. for NOAA (NESS), Contr. No. 1-35350, Allied Res. Assoc., Inc., Rpt. No. 8G92-F, July, 112 p.

_____ 1973a, Use of ERTS data for mapping Arctic sea ice: in Symp. on Significant Results Obtained from the Earth Resources Technology Satellite-1, v. I, Tech. Presentation, Sect. B, NASA SP-327, p. 1377-1384.

_____ 1973b, Use of ERTS data for mapping snow cover in the western United States: in Symp. on Significant Results Obtained from the Earth Resources Technology Satellite-1, v. I, Tech. Presentation, Sec., A, NASA SP-327, p. 855-862.

_____ 1974, Monitoring Arctic sea ice using ERTS imagery: in Proc. of the Third ERTS Symp., NASA Special Paper (in press).

Barnes, J. C., Bowley, C. J., and Simmes, D. A., 1973, Use of satellite data for mapping snow cover in western U. S.: in Proc. of the Symp. on Management and Utilization of Remote Sensing Data, Sioux Falls, S. Dak., Amer. Soc. Photogram., p. 166-176.

_____, 1974, Mapping snow extent in the Salt-Verde watershed and the southern Sierra Nevada using ERTS imagery: in Proc. of the Third ERTS Symp., NASA Special Paper (in press).

Barnes, J. C., Chang, D. T., and Willand, J. H., 1969, Use of satellite high resolution infrared imagery to map Arctic sea ice: Final Rpt. for NASA/ NAVOCEANO, Spacecraft Oceanography Project, Contr. No. N62306-68-C-0276, Allied Res. Assoc., Inc., Rpt. No. 8G60-F, August, 109 p.

_____ 1970a, Improved techniques for mapping sea ice from satellite infrared data: Final Rpt. for NOAA (NESS), Contr. No. E-67-70(N), Allied Res. Assoc., Inc., Rpt. No. 8G74-F, November, 95 p.

_____ 1970b, Satellite infrared observation of Arctic sea ice: AIAA Earth Resources Observations and Information Systems Meeting, Annapolis, Md., AIAA Paper No. 70-301, March, 6 p.

_____ 1972a, Application of ITOS and Nimbus infrared measurements to mapping sea ice: Final Rpt. for National Oceanic and Atmospheric Administration, National Environmental Satellite Service, Contr. No. 1-36025, Allied Res. Assoc., Inc., Rpt. No. 8G93-F, June, 87 p.

_____ 1972b, Image enhancement techniques for improving sea ice depiction in satellite infrared data: Jour. Geophys. Res. (Oceans and Atmosphere Edition), v. 77 (3), p. 453-462.

Bárðarson, H. R., 1971, Ice and fire: H. R. Bárðarson, Reykjavík, 171 p.

Barth, Tom. F. W., 1950, Volcanic geology, hot springs and geysers of Iceland: Washington, Carnegie Institution of Washington, Pub. 587, 174 p.

Bergthórsson, Páll, 1969, An estimate of drift ice and temperature in Iceland in 1000 years: Jökull, v. 19, p. 94-101.

Billingsley, F. C., and Goetz, A. F. H., 1973, Computer techniques used for some enhancements of ERTS images: in Symp. on Significant Results Obtained from the Earth Resources Technology Satellite-1, v. I, Tech. Presentations, Sect. B, NASA SP-327, p. 1159-1167.

Bjarnason, Hákon, 1961, Forestry in Iceland: Jour. of the Royal Scottish Forestry Society, v. 22, no. 1, p. 55-60.

Björnsson, Sveinbjörn, ed., 1967, Iceland and mid-ocean ridges: Vísindafélag, Íslandinga, Reykjavík, 209 p.

Björnsson, Sveinbjörn; Arnórsson, Stefan; and Tómasson, Jens, 1972, Economic evaluation of Reykjanes thermal brine area, Iceland: Amer. Assoc. Petrol. Geol. Bull., v. 56, p. 2380-2391.

Böðvarsson, Gunnar, 1960, Hot springs and the exploitation of natural heat resources: in On the Geology and Geophysics of Iceland: Intl. Geol. Cong., 21st, Copenhagen, 1960, Guide to Excursion A2, p. 46-54.

Campbell, W. I., 1972, Analysis of Arctic ice features: in Earth Resources Technology Satellite-1, Symposium Proceedings, NASA, Goddard Space Flight Ctr., Document X-650-73-10, p. 129-130.

Colvocoresses, A. P., 1972, Cartographic applications of ERTS imagery: Earth Resources Technology Satellite-1, Symp. Proceedings, NASA, Goddard Space Flight Ctr., Document X-650-73-10, p. 88-94.

_____ 1973a, Advantages of ERTS (TV) system over film return systems: Memorandum for the Record (EC-15-ERTS), U. S. Geological Survey, Topographic Division, 21 February, 2 p.

_____ 1973b, The ERTS image format as the basis for a map series: in Proc. of the Symp. on Management and Utilization of Remote Sensing Data, Sioux Falls, So. Dak., Amer. Soc. Photogram., p. 142-143.

_____ 1973c, Unique characteristics of ERTS: in Symp. on Significant Results Obtained from the Earth Resources Technology Satellite-1, v. I, Tech. Presentations, Sect. B, NASA SP-327, p. 1523-1525.

_____ 1974, Towards an operational ERTS: in Proc. of the Third ERTS Symp., NASA Special Paper (in press).

Colvocoresses, A. P., and McEwen, R. B., 1973, Progress in Cartography, EROS Program: in Symp. on Significant Results Obtained from the Earth Resources Technology Satellite-1, v. I, Tech. Presentations, Sect. B, NASA SP-327, p. 887-898.

Eyþórsson, Jón, 1960, Vatnajökull: Almenna Bókafélagið, Reykjavík, Iceland, 44 p.

_____ 1963, Variation of Iceland glaciers: Jökull, v. 13, p. 31-33.

Eyþórsson, Jón, and Sigtryggsson, Hlynur, 1971, The climate and weather of Iceland: in The Zoology of Iceland, v. I., pt. 3, p. 1-62.

Friðriksson, Sturla, 1969, The effects of sea ice on flora, fauna, and agriculture: Jökull, v. 19, p. 146-157.

Friðriksson, Sturla, and Pálsson, Jóhann, 1970, Landgræðslutilraun á Sprengisandi: Íslenzkar Landbúnaðarrannsóknir, v. 2, no. 2, p. 34-49.

Friðriksson, Sturla, Sveinbjörnsson, Bjartmar, and Magnússon, Skúli, 1972, On the vegetation of Heimaey, Iceland - Pt. II: Surtsey Research Progress Rpt., v. VI, The Surtsey Research Society, p. 36-53.

Friedman, J. D.; Williams, R. S., Jr.; Thorarinsson, Sigurður; Pálmason, Guðmundur; 1972, Infrared emission from Kverkfjöll subglacial volcanic and geothermal area, Iceland: Jökull, v. 22, p. 27-43.

Fritz, S., 1962, Snow surveys from satellite meteorology: Rocket and Satellite Meteorology, North-Holland Pub. Co., Amsterdam, p. 419-421.

Heezen, B. C., Tharp, Marie, and Ewing, Maurice, 1959, The floors of the oceans: Geol. Soc. Amer., Spec. Paper, 65.

Jakobsson, Jakob, 1969, On herring migrations in relation to changes in sea temperature: Jökull, v. 19, p. 134-145.

Jakobsson, Jónas, 1969, Winds and ice drift north of Iceland, especially in the year 1965: Jökull, v. 19, p. 69-76.

Jakobsson, S. P., 1972a, On the consolidation and palagonitization of the tephra of the Surtsey volcanic island, Iceland: Surtsey Res. Prog. Rpt., VI, The Surtsey Research Society, Reykjavík, Iceland, p. 121-128.

_____ 1972b, Chemistry and distribution patterns of Recent basaltic rocks in Iceland: Lithos, v. 5, p. 365-386.

Jónsson, B. H., 1969, Sea ice in satellite pictures: Jökull, v. 19, p. 62-68.

Kjartansson, Guðmundur, 1960, The Móberg Formation: in On the geology and geophysics of Iceland: Internatl. Geol. Cong., 21st, Copenhagen, 1960, Guide to excursion A2, p. 21-28.

Kristinsson, Valdimar, 1972, Bridging the gap and closing the circle: in Atlantica and Iceland Review, v. 10, no. 3, p. 21-25.

McClain, E. P., 1972, Detection of ice conditions in the Queen Elizabeth Islands: in Earth Resources Technology Satellite-1, Symposium Proceedings, NASA, Goddard Space Flight Ctr., Document X-650-73-10, p. 127-128.

McClain, E. P., and Baliles, M. D., 1971, Sea ice surveillance from Earth Satellites: Mariners Weather Log, v. 15, no. 1, p. 1-4.

McEwen, R. B., 1974, Stereo capability of a convergent RBV system on ERTS: Memorandum for the Record (EC-22-ERTS), U. S. Geological Survey, Topographic Division, 9 January, 6 p.

MacDonald, W. R., 1974, New space technology advances knowledge of the remote polar regions: in Proc. of the Third ERTS Symp., NASA Special Paper (in press).

Meier, M. F., 1973, Evaluation of ERTS imagery for mapping and detection of changes of snowcover on land and on glaciers: in Symp. on Significant Results Obtained from the Earth Resources Technology Satellite-1, v. I, Tech. Presentations, Sect. A, NASA SP-327, p. 863-875.

Norrman, J. O., 1970, Trends in postvolcanic development of Surtsey island. Progress report on geomorphological activities in 1968: Surtsey Research Prog. Rpt., V, The Surtsey Research Society, Reykjavík, Iceland, p. 95-112.

_____ 1972a, Coastal development of Surtsey island, 1968-69: Surtsey Research Prog. Rpt., VI, The Surtsey Research Society, Reykjavík, Iceland, p. 137-143.

_____ 1972b, Coastal changes in Surtsey island, 1969-1970: Surtsey Research Prog. Rpt., VI, The Surtsey Research Society, Reykjavík, Iceland, p. 145-149.

Pálmason, Guðmundur, and Sæmundsson, Kristján, 1974, Iceland in relation to the Mid-Atlantic Ridge: Ann. Rev. of Earth and Planetary Sciences, v. 2, p. 25-50.

Popham, R. W., and Samuelson, R. E., 1964, Polar exploration with Nimbus: Observations from the Nimbus I Meteorological Satellite, NASA SP-89, p. 47-59.

Popham, R. W., Flanders, A., and Weiss, H., 1966, Second progress report on satellite applications to snow hydrology: Proc. of the 23rd Ann. Mtng., Eastern Snow Conf.

Poulton, C. E., 1972, The advantages of side-lap stereo interpretation of ERTS-1 imagery in northern latitudes: Earth Resources Technology Satellite-1, Symp. Proceedings, NASA, Goddard Space Flight Ctr., Document X-650-73-10, p. 157-161.

Predoehl, M. C., 1966, Antarctic pack ice: Boundaries established from Nimbus I pictures: Science, v. 153, no. 3738, p. 861-863.

Price, R. J., and Howarth, P. J., 1970, The evolution of the drainage system (1904-1965) in front of Breiðamerkurjökull, Iceland: Jökull, v. 20, p. 27-37.

Rittman, Alfred, 1962, Volcanoes and their activity: New York, Interscience Publishers, 305 p. [Translated from 2nd German edition by E. A. Vincent].

Rist, Sigurjón, 1967a, The thickness of the ice cover of Mýrdalsjökull, southern Iceland: Jökull, v. 17, p. 237-242.

_____ 1967b, Jöklabreytingar 1964/65, 1965/66, og 1966/67: Jökull, v. 17, p. 321-325.

_____ 1969, Climatic trend and flood danger: Jökull, v. 19, p. 128-133.

_____ 1969, Lake-ice of Mývatn: Jökull, v. 19, p. 121-127.

_____ 1972, Jöklabreytingar (Glacier variations) 1931/64, 1964/71 og 1971/72: Jökull, v. 22, p. 89-95.

Sæmundsson, Kristján, 1974, Evolution of the axial rifting zone in northern Iceland and the Tjörnes Fracture Zone: Geol. Soc. Amer. Bull., v. 85, no. 3, p. 495-504.

Schoonmaker, J. W., Jr., 1973a, Status of the ERTS image format as the basis for a map series: Memorandum for the Record (EC-19-ERTS), U. S. Geological Survey, Topographic Division, 29 June, 3 p.

_____ 1973b, Progress of ERTS-1 nominal scene: Memorandum for the Record (EC-20-ERTS), U. S. Geological Survey, Topographic Division, 6 December, 4 p.

Sigbjarnarson, Guttormur, 1970, On the recession of Vatnajökull: Jökull, v. 20, p. 50-61.

_____ 1972, Vatnafræði Þórisvatnssvæðis: Orkustofnun, 65 p. (mimeo.)

Sigurðsson, F. H., 1969, Report on sea ice off the Icelandic coasts October 1967 to September 1968: Jökull, v. 19, p. 77-93.

Tarble, R. D., 1963, Areal distributions of snow as determined from satellite photographs: Publ. No. 65 of the I.A.S.H., p. 372-375.

Thorarinsson, Sigurður, 1939, The ice dammed lakes of Iceland with particular reference to their value as indicators of glacier oscillations: Geografiska Annaler, v. 21, p. 216-242.

Thorarinsson, Sigurður, 1956, The thousand years struggle against ice and fire: Museum of Natural History, Dept. of Geology and Geography, Reykjavík, Miscellaneous papers no. 14, 52 p.

_____ 1958, The Öræfajökull eruption of 1362: Acta Naturalia Islandica, II, 2, p. 1-100.

_____ 1960, The postglacial volcanism: in On the geology and geophysics of Iceland: Internatl. Geol. Cong., 21st, Copenhagen, 1960, Guide to excursion A2, p. 33-45.

_____ 1963, Eldur í Öskju Askja on Fire: Reykjavík, Almenna Bókafélagið, 101 p.

_____ 1964, Sudden advance of Vatnajökull outlet glaciers 1930-1964: Jökull, v. 14, p. 76-89.

_____ 1966, The median zone of Iceland: in The World Rift System, Geological Survey of Canada, Dept. of Mines and Technical Surveys, Paper 66-14, p. 187-211.

_____ 1968, Síðustu þættir Eyjaelda (The last phases of the Surtsey eruption): Náttúrufræðingurinn, v. 38, p. 113-135.

_____ 1969, The effect of glacier changes in Iceland resulting from increase in the frequency of drift ice years (abs.): Jökull, v. 19, p. 103.

_____ 1970, Hekla - A notorious volcano: Almenna Bókafélagið, Reykjavík, 62 p.

Thorarinsson, Sigurður, and Sigvaldason, G. E., 1962, The eruption in Askja, 1961 - A preliminary report: Amer. Jour. Sci., v. 260, p. 641-651.

Thorarinsson, Sigurður; Einarsson, Trausti; and Kjartansson, Guðmundur; 1959, On the geology and geomorphology of Iceland: Geografiska Annaler, v. 41, no. 2-3, p. 135-169.

Thorarinsson, Sigurður; Sæmundsson, Kristján; Williams, R. S., Jr.; 1973, ERTS-1 image of Vatnajökull: Analysis of glaciological, structural, and volcanic features: Jökull, v. 23 (in press).

Thorsteinsson, Ingvi, 1972, Gróðurvernd: Reykjavík, Rit Landverndar 2, 128 p.

Tómasson, Haukur, and Vilmundardóttir, E. G., 1967, The lakes Stórisjór and Langisjór, v. 17, p. 280-299.

Ward, P. L., 1971, New interpretation of the geology of Iceland: Geol. Soc. Amer. Bull., v. 82, no. 11, p. 2991-3012.

White, D. E., and Miller, L. D., 1968, Geothermal infrared anomalies of low intensity, Yellowstone National Park: in First Earth Resources Aircraft Program Status Review, NASA, v. I, p. 16-1 - 16-4.

Wiesnet, D. R., 1972, Detection of snow conditions in mountainous terrain: in Earth Resources Technology Satellite-1, Symposium Proceedings, NASA, Goddard Space Flight Ctr., Document X-650-73-10, p. 131-132.

Wiesnet, D. R., and McGinnis, D. F., 1974, Snow-extent mapping and lake ice studies using ERTS-1 MSS together with NOAA-2 VHRR: in Proc. of the Third ERTS Symp., NASA Special Paper (in press).

Williams, R. S., Jr., 1972, Satellite geological and geophysical remote sensing of Iceland (summ.): in Proc. Eighth Intl. Symp. on Remote Sensing of Environment, Univ. of Mich., Ann Arbor, Mich., p. 1465-1466.

Williams, R. S., Jr., and Moore, J. G., 1973, Iceland chills a lava flow: Geotimes, v. 18, no. 8, p. 14-17.

Williams, R. S., Jr.; Friedman, J. D.; Thorarinsson, Sigurður; Sigurgeirsson, Thorbjörn; and Pálmason, Guðmundur; 1968, Analysis of 1966 infrared survey of Surtsey, Iceland: in Surtsey Research Progress Rpt., The Surtsey Research Society, Reykjavík, Iceland, v. IV, p. 177-192.

Williams, R. S., Jr.; Böðvarsson, Ágúst; Friðriksson, Sturla; Pálmason, Guðmundur; Rist, Sigurjón; Sigtryggsson, Hlynur; Thorarinsson, Sigurður; and Thorsteinsson, Ingvi; 1973a, Satellite geological and geophysical remote sensing of Iceland - Preliminary results from analysis of MSS imagery: in Proc. of Symp. of Significant Results Obtained from ERTS-1, NASA, Goddard Space Flight Center, Greenbelt, Md., p. 317-327.

Williams, R. S., Jr.; Böðvarsson, Ágúst; Friðriksson, Sturla; Pálmason, Guðmundur; Rist, Sigurjón; Sigtryggsson, Hlynur; Sæmundsson, Kristján; Thorarinsson, Sigurður; and Thorsteinsson, Ingvi; 1973b, Iceland: Preliminary results of geologic, hydrologic, oceanographic, and agricultural studies with ERTS-1 imagery: in Proceedings of Symposium on Management and Utilization of Remote Sensing Data, American Society of Photogrammetry, Sioux Falls, South Dakota, p. 17-35.

Williams, R. S., Jr.; Thorarinsson, Sigurður; and Sæmundsson, Kristján, 1973c, Vatnajökull area, Iceland: New volcanic and structural features on ERTS-1 imagery: in Geol. Soc. Amer. Abstracts with Programs, 1973 Ann. Mtngs., Dallas, Texas, p. 864-865.

Wójcik, Gabriel, 1973, Glaciological studies on the Skeidarárjökull, in Rajmund Galon, Ed., Scientific results of the Polish Geographical Expedition to Vatnajökull (Iceland): Polish Acad. Sci., Geographia Polonica, v. 26, p. 185-208.

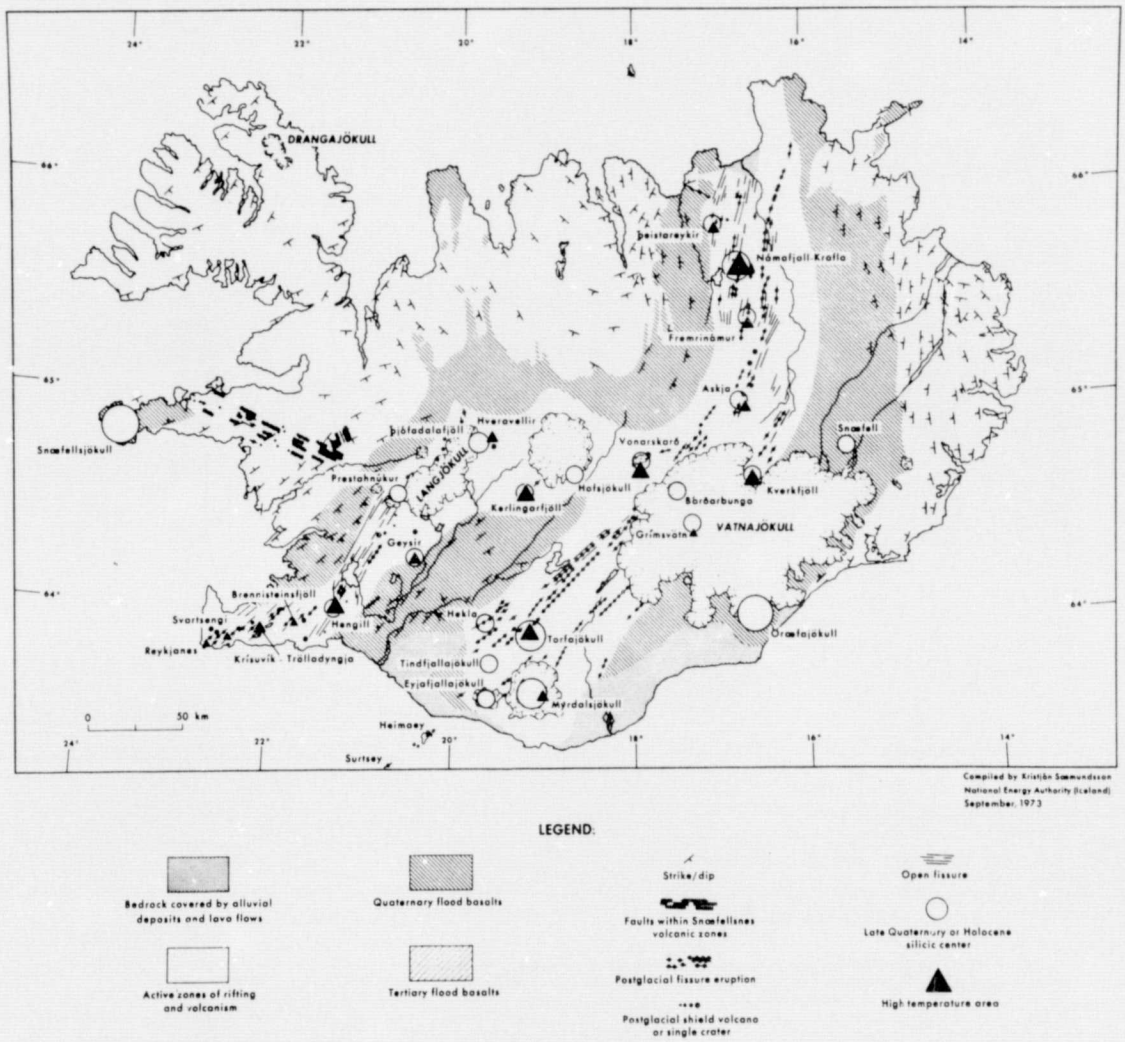

FIGURE 1. Geologic Map of Iceland modified from Pálmason and Sæmundsson, 1974, fig. 2.

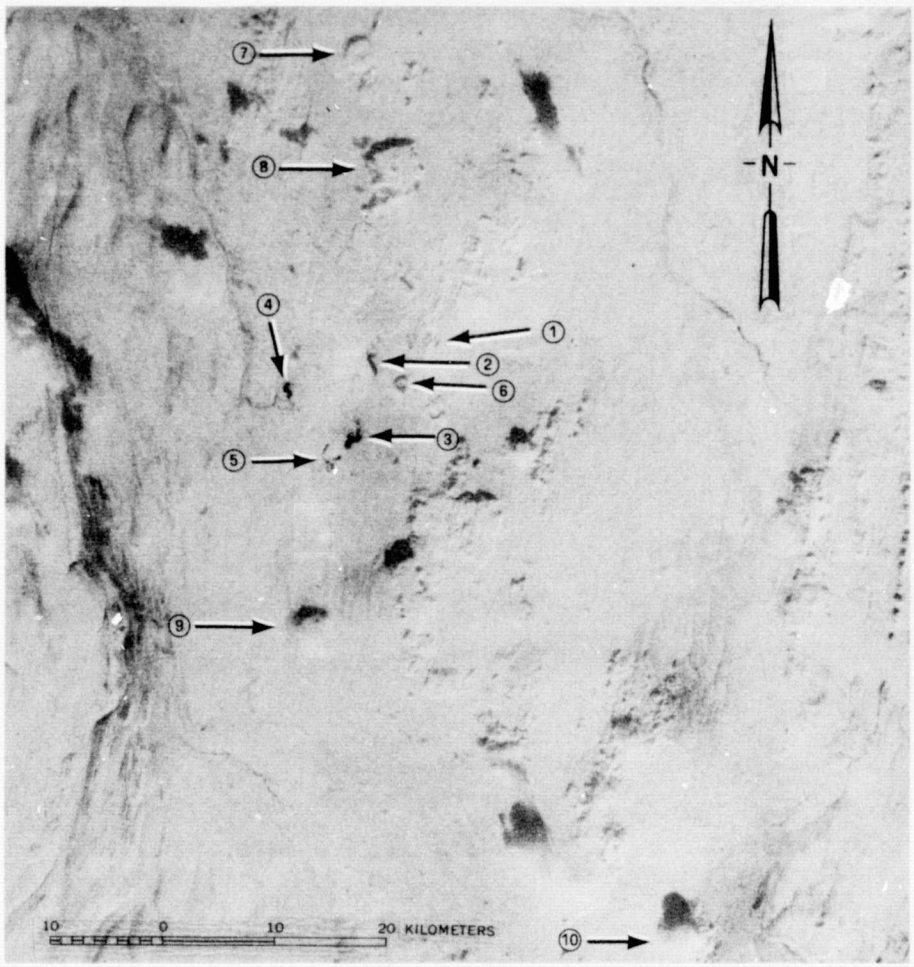

Figure 2. The Námafjall geothermal area (1) appears on wintertime imagery as a light grey, linear, "ragged area," which is surrounded by bright white snow (Mývatn, C6, 9 Mar. 73, 1229-12142-7). Open water in lake Mývatn due to thermal spring discharge can be seen at (2), due to a high volume of spring discharge at Kálfaströnd (3), at the main river outlet of the lake at Álabrot (4), and at lake Grænavatn (5), just to the south of Mývatn. The tephra ring, Hverfjall, can be seen at (6). The table mountains, Bæjarfjall (7), Gæsafjöll (8), Sellandafjall (9), and Herðubreið (10), also stand out sharply. Compare with Figure 3.

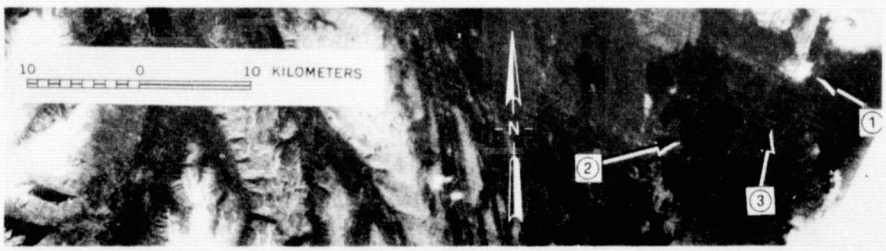

Figure 3. The Námafjall geothermal area (1) appears as a light greenish area on an MSS color composite (bands 4, 5, 7), here shown on band 5 (Akureyri, C5, 19 Aug. 73, 1392-12185-5). The area of altered ground is the result of intense geothermal activity, which has altered the basaltic lava flows and hyaloclastites. Lake Mývatn can be seen at (2) and the tephra ring, Hverfjall, at (3). Compare with Figure 2.

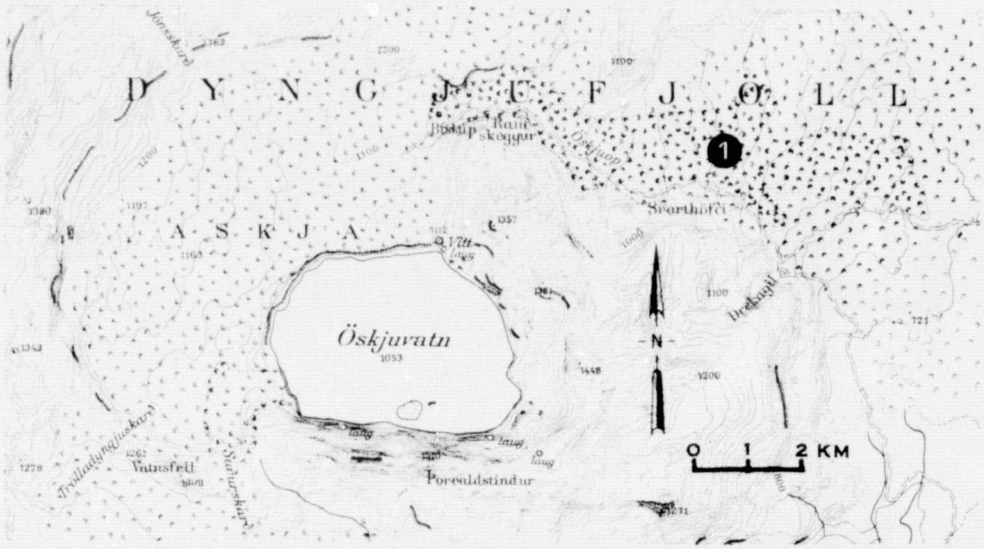

Figure 4. Topographic map of the 1961 lava flows (1) in the Askja area, Dyngjufjöll massif, Iceland (Uppdráttur Íslands, Blað 84, Herðubreið, Landmælingar Íslands, 1:100,000 scale, 1969). Based on 1937-38 survey by Geodætisk Institut, Copenhagen, Denmark. Revised by Landmælingar Íslands in 1965. Compare shape of lava flows as shown on Figures 5 and 6.

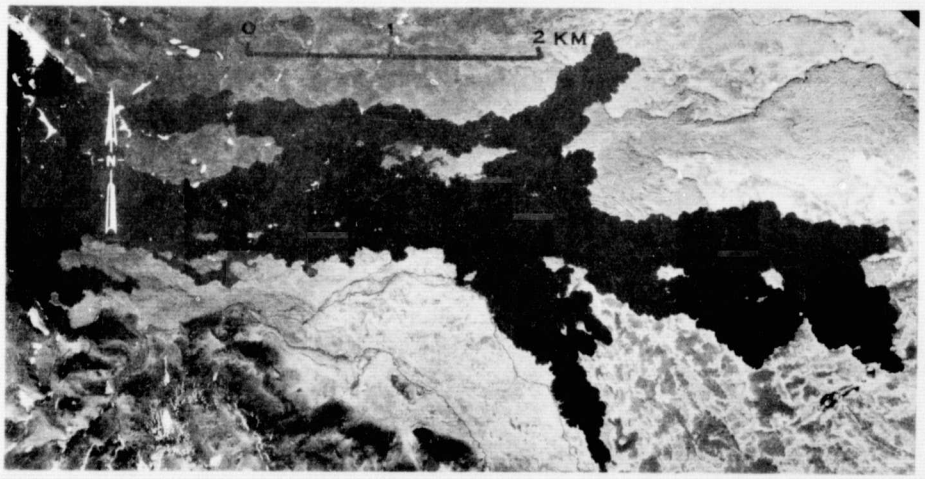

Figure 5. Vertical aerial photograph (#5240B) taken by Landmælingar Íslands (Icelandic Geodetic Survey) on 21 August 1970. Lava flows of 1961 have flowed over a pumiceous layer deposited in the explosive eruption of 1875. Compare with Figures 4 and 6.

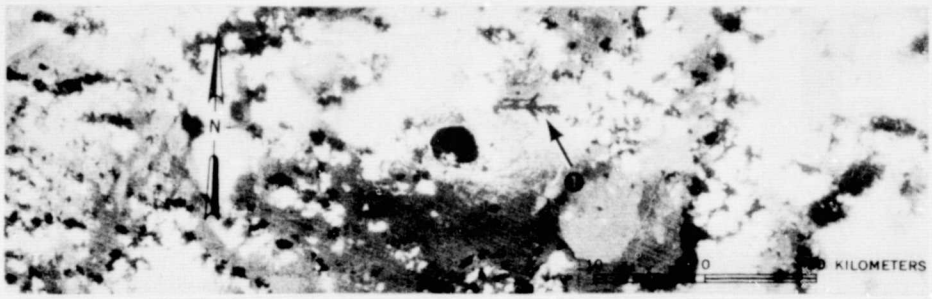

Figure 6. The 1961 lava flows (1) are sharply delineated on the mostly cloudy ERTS-1, MSS image (Ódáðahraun, C7, 30 July 73, 1372-12074-5). Note the detail in the outline of the flows, including the two prominent windows within the flows. Compare with Figures 4 and 5.

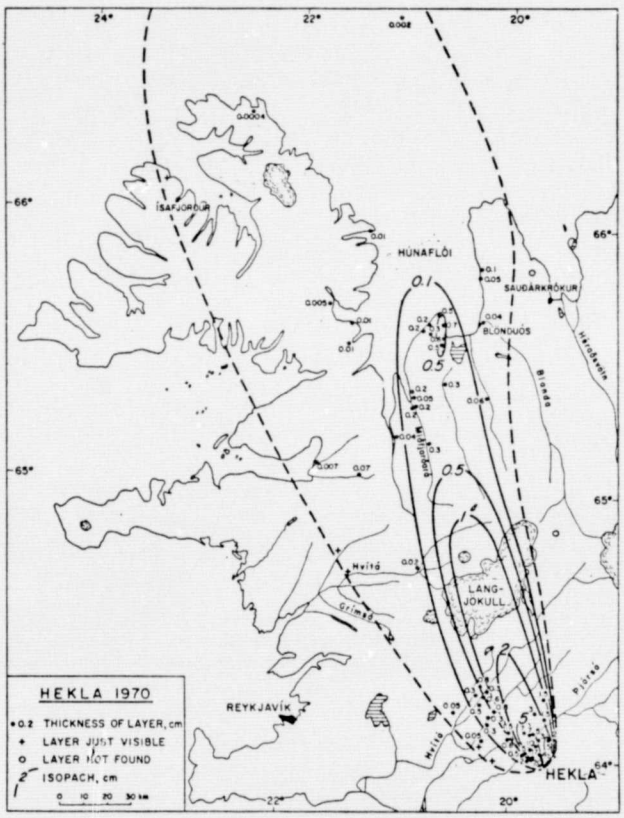

Figure 7. Isopach map of tephra layer from eruption of Hekla in May-July 1970. (From Thorarinsson, 1970, fig. 13).

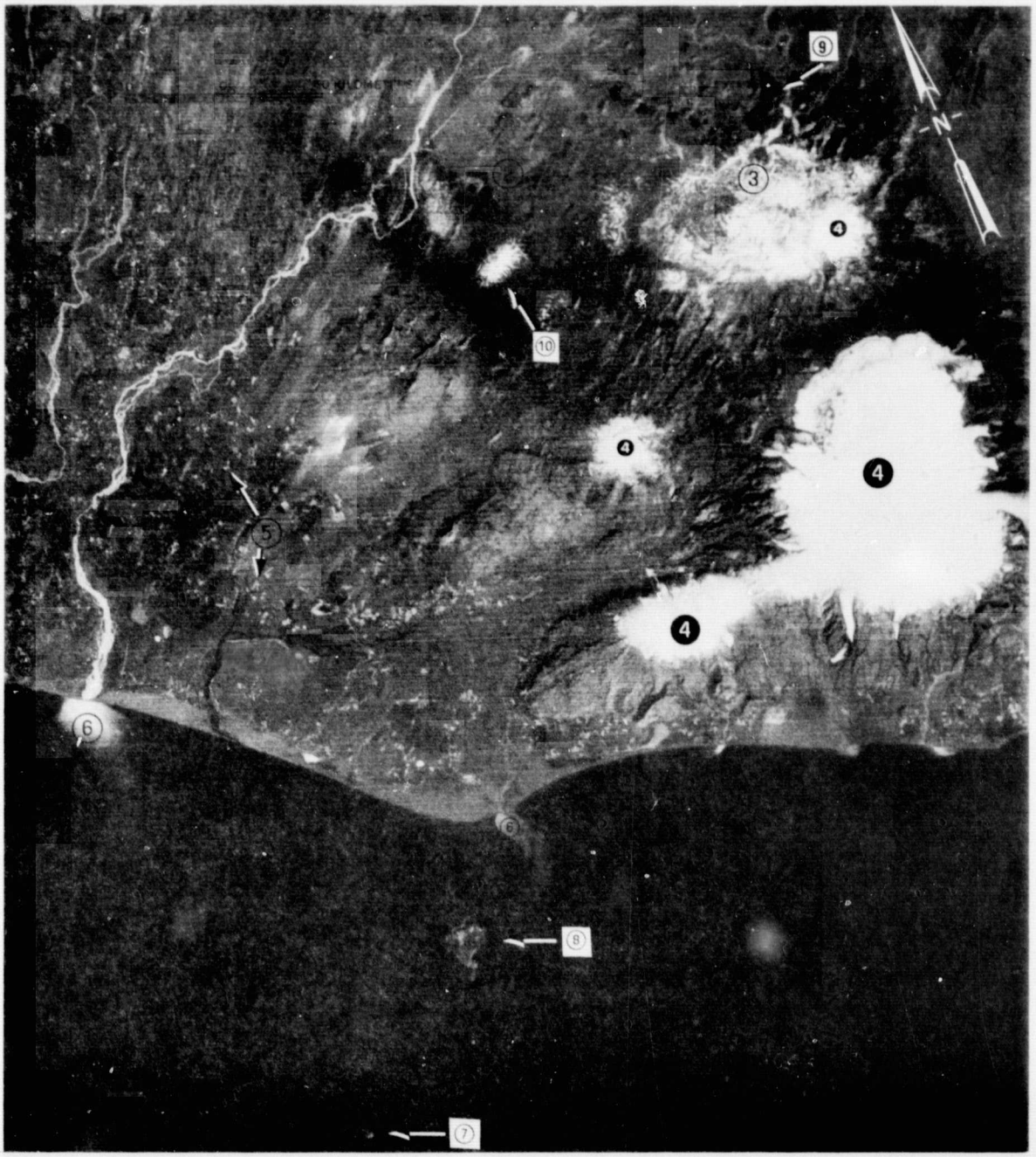

Figure 8. Part of an ERTS-1, MSS image of the Hekla area, Iceland (Hekla, D5, 19 Aug. 73, 1392-12191-5). Important features are the tephra fallout pattern from the 1970 eruption of Hekla (1), three areas of new lava flows from Hekla's 1970 eruption (2), rhyolitic rocks and a clear trace of a caldera fault in Torfajökull area (3), several icecaps (4), numerous cultivated areas (5), sediment plumes from rivers laden with glacial rock flour (6), new shapes of the islands of Surtsey (7) and Heimaey (8), a maar (9), and stratified ridge (10).

Figure 9. Geologic map of Hekla and environs showing the three areas of new lava flows in 1970 (cross-hatched patterns) and areas of previous lava flows. (From Thorarinsson, 1970, fig. 14). Geologic map explanation: 1, 1970 lava flows; 2, 1947-1948 lava flows; 3, 4, and 5, different historic and prehistoric lava flows, Hekla and Hekla region; 6, Þjórsá lava flows; and 7, craters.

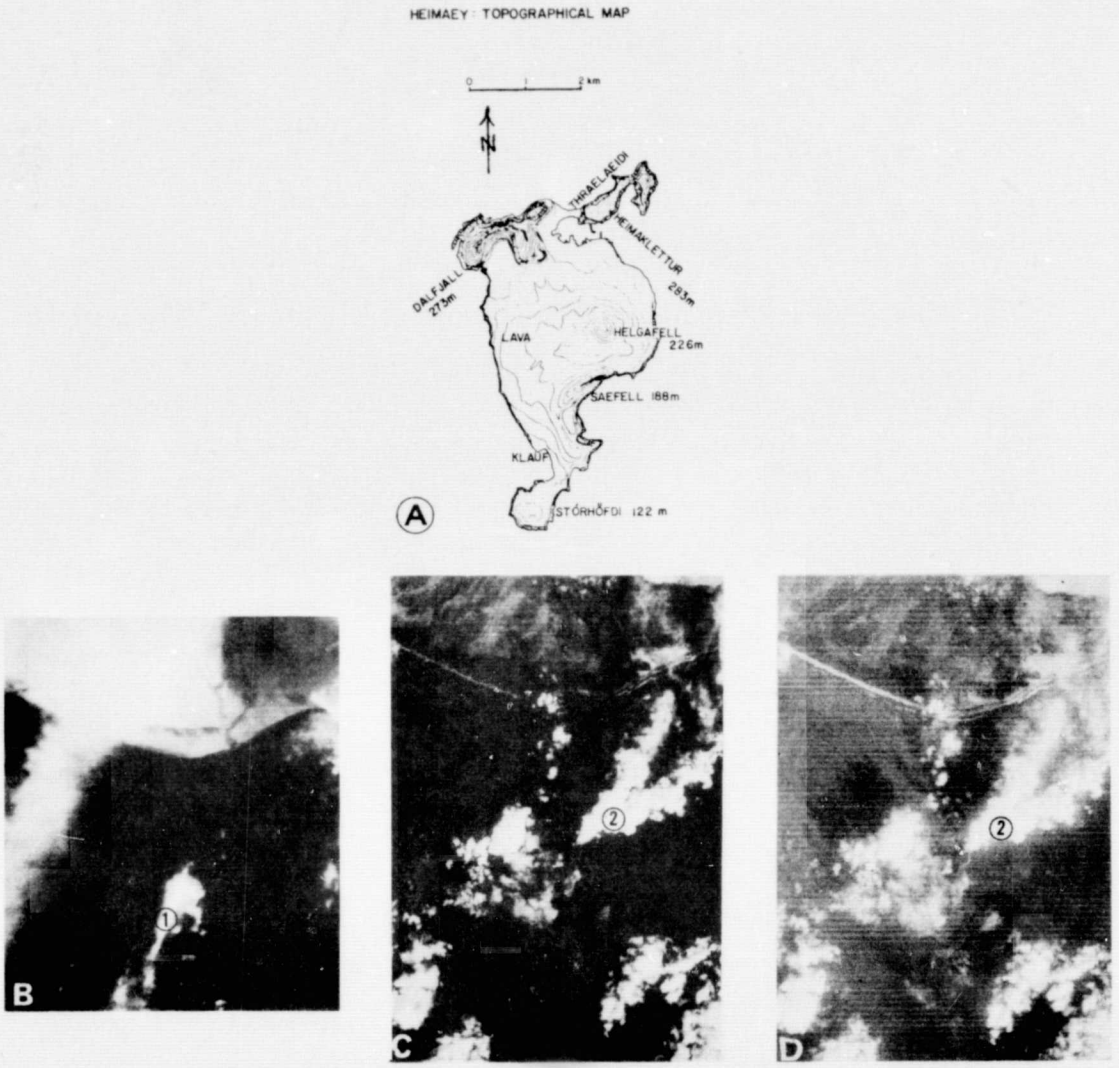

Figure 10. Simplified topographic map of Heimaey, Vestmann Islands, Iceland, (A) showing the configuration of the island prior to the onset of volcanic activity on 23 January 1973. (Map is from figure in Friðriksson and others, 1972, p. 53). The ERTS image on the left (B) (Þórisvatn, D6, 21 Nov. 72, 1121-12143-7) shows the island prior to the eruption, with the western shoreline partially obscured by a long, linear cloud (1). (See also Figure 16 for an enlargement of this image.) The center (C) and right-hand (D) ERTS images (Vestmannaeyjar, E6, 9 Mar. 73, 1229-12151, bands 7 and 5, respectively) were acquired during an active phase of the eruption. Although partially obscured by clouds, the outline of the island can be seen, with the eruption plume (2) ascending to the east from the east side of the island. The eruption plume, however, nearly obscures all of the new land.

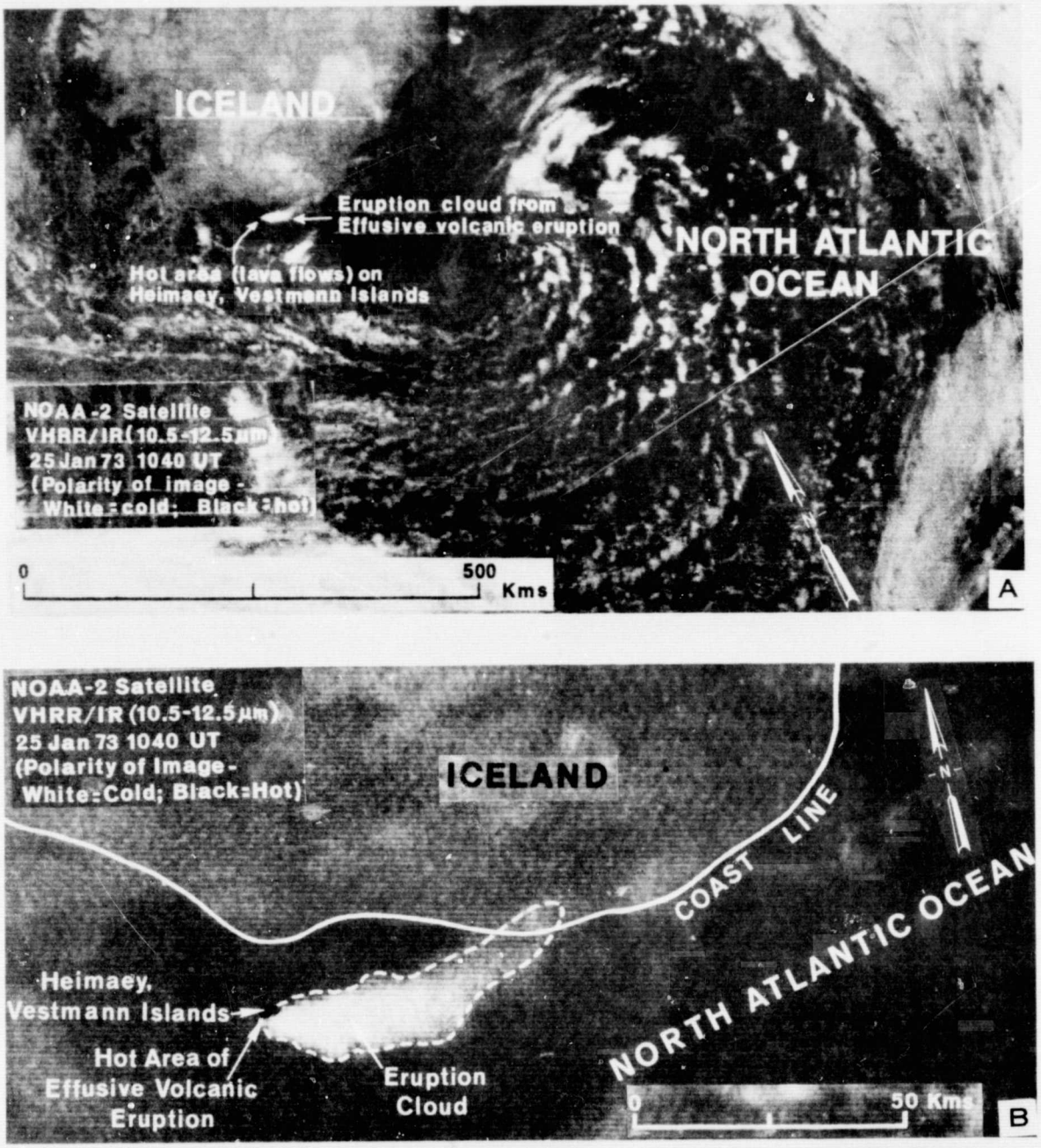

Figure 11. Satellite thermograph obtained by the VHRR (Very High Resolution Radiometer) instrument of the NOAA-2 satellite on 25 January 1973, less than 33 hours after the beginning of the volcanic eruption on Heimaey, Vestmann Islands, Iceland. This thermal infrared image was furnished to the authors by E. Paul McClain and Donald Wiesnet of NOAA's National Environmental Satellite Service. The bottom thermograph (B) is a 10X enlargement of the top thermograph (A).

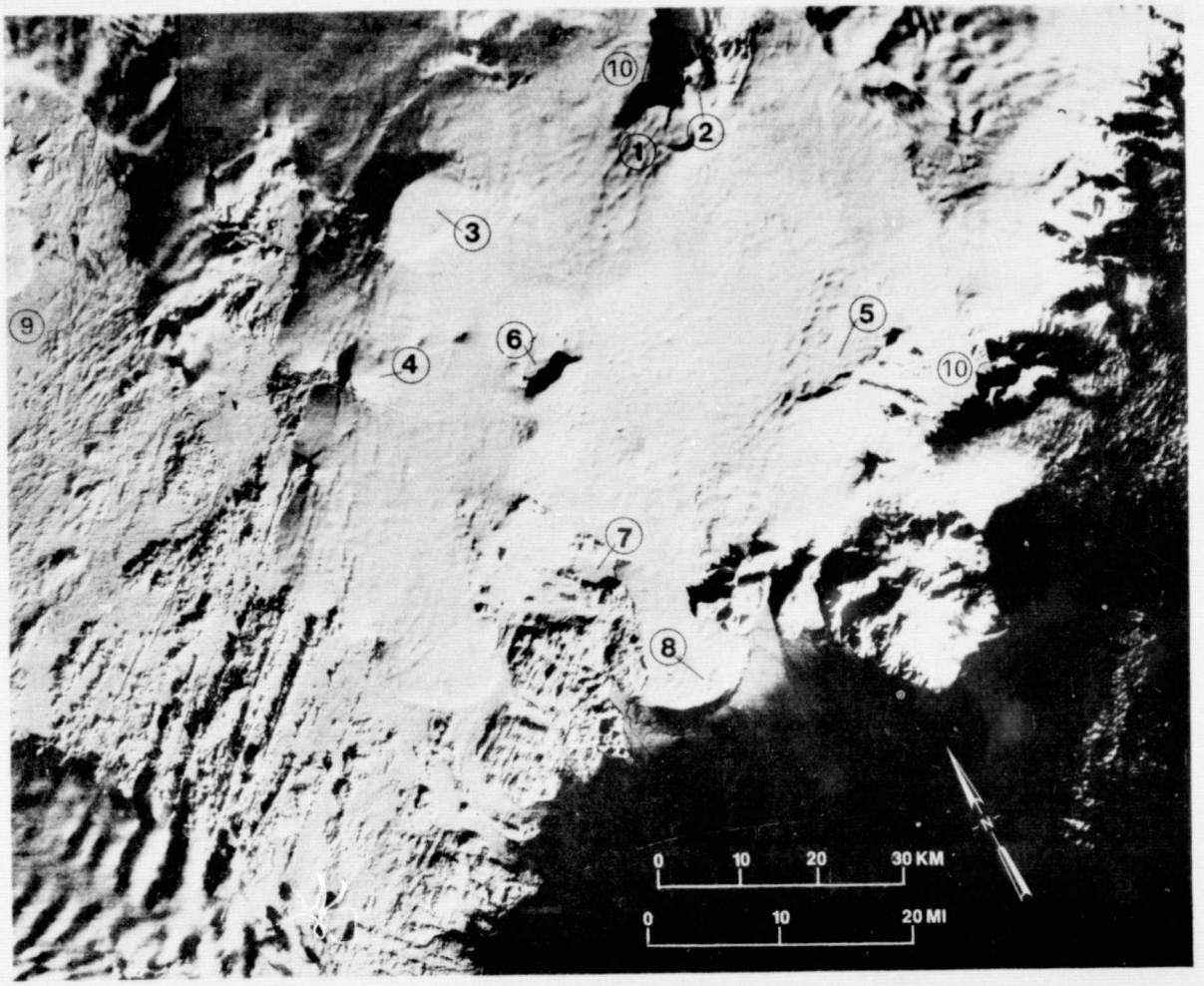

Figure 12. Low sun angle (7°) ERTS-1 image (Vatnajökull, D7, 31 Jan. 73, 1192-12084-5) of the snow-covered Vatnajökull area, Iceland, which shows a number of volcanic and glaciologic features within the Vatnajökull icecap. Features shown include: (1) elliptical shape of a hitherto unknown subglacial caldera southwest of Kverkfjöll; (2) elliptical shape of partially subglacial caldera at Kverkfjöll. Although dark, two subglacial craters can be seen on the western edge of this caldera with a partially subglacial geothermal area extending southwest into the icecap through the westernmost crater; (3) and (4) elliptically shaped central volcanoes at Bárðarbunga and east of Hamarinn, respectively; (5) faint elliptical features and associated nunataks at Esjufjöll which may represent a partially ice covered large central volcano; (6) the large depression of Grímsvötn, a well-known subglacial caldera, and source of many catastrophic jökulhlaups (glacial floods) to the south, including one in March 1972; (7) the frozen lake, Grænalón, another source of jökulhlaups, including one which occurred in August 1973; and (8) the partially snow covered snout of Skeiðarárjökull. Around the periphery of the Grímsvötn caldera are a number of punctate features resulting from collapse after the March 1972 jökulhlaup. Several more collapse features, resulting from the August 1972 jökulhlaup can be seen in a line between Hamarinn (4) and the Grímsvötn caldera. Southwest of Vatnajökull are superb examples of NE-trending grabens, crater rows, and hyaloclastite ridges. Two prominent volcano-tectonic lineaments can be seen on this image. One extends N.45°E. for 80 km between Kverkfjöll (1 and 2), the eastern edge of Grímsvötn (6), to the southwestern edge of Vatnajökull. The second lineament extends N.35°W., just north of Grænalón (7). Concentric recessional moraines in front of one of Hofsjökull's outlet glaciers can be seen at (9). Medial moraines are visible at (10).

Decreasing temperature / Increasing explosivity	Main products of eruption	Number of eruptions	FORM OF RUPTURE: Punctual •	FORM OF RUPTURE: Linear /
	LAVA (Flowing material)	1		Lava fissure ELDGJÁ Type: ÖGMUNDARGJÁ
		1	Lava cone ELDBORG Type: ELDBORG	Lava cone row ELDBORGARÖÐ Type: SVÖRTUBORGIR
		>1	Shield volcano DYNGJA Type: SKJALDBREIÐUR	
	LAVA and TEPHRA (Flowing and air borne material)	1	Spatter cone KLEPRAGÍGUR Type: BÚÐAKLETTUR	Spatter cone row KLEPRAGÍGARÖÐ Type; LÁKAGÍGAR
		>1	Stratovolcano ELDKEILA Type: SNÆFELLSJÖKULL	Stratified ridge ELDHRYGGUR Type: HEKLA
	TEPHRA (Airborne material)	1	Scoria cone GJALLGÍGUR Type: RAUÐASKÁL	Scoria cone row GJALLGÍGARÖÐ Type: VATNAÖLDUR
		1	Tephra ring HVERFJALL Type: HVERFJALL	Explosion fissure SPRENGIGJÁ Type: VÁLAGJÁ
		1	Maar KER Type: GRÆNAVATN	

Table 1. The main types of basaltic Icelandic volcanoes (from Thorarinsson, 1960, p. 35).

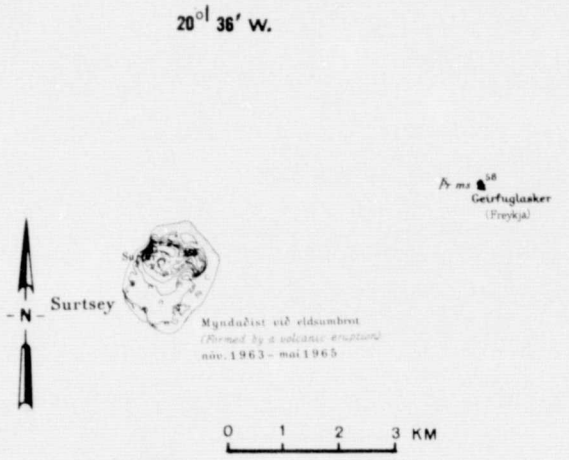

Figure 13. Topographic map of Surtsey, Vestmann Islands, Iceland/Uppdráttur Íslands, Blað 49, Vestmannaeyjar, Landmælingar Íslands, 1:100,000 scale, 1966). Outline of Surtsey drafted from aerial photography acquired by Landmælingar Íslands on 24 August 1965 (Photo No. 375).

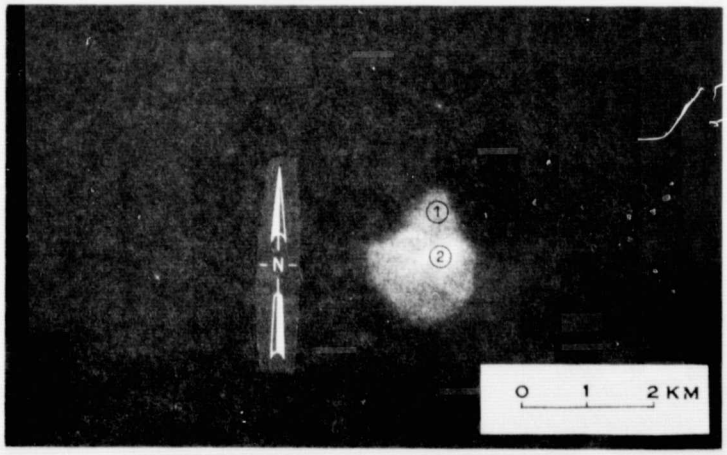

Figure 14. Positive enlargement (40X) of 3d generation, NDPF, 70 mm negative (original scale of 1:3,369,000) of ERTS image of Surtsey, Vestmann Islands, Iceland (Surtsey, E-5, 19 Aug. 73, 1392-12194-6). Original enlargement scale was 1:84,225. Note prominent ness at (1) and the highly reflective area at (2), where the tephra pile is undergoing palogonitization. Although the image is somewhat grainy, the coastline of the island can be delineated.

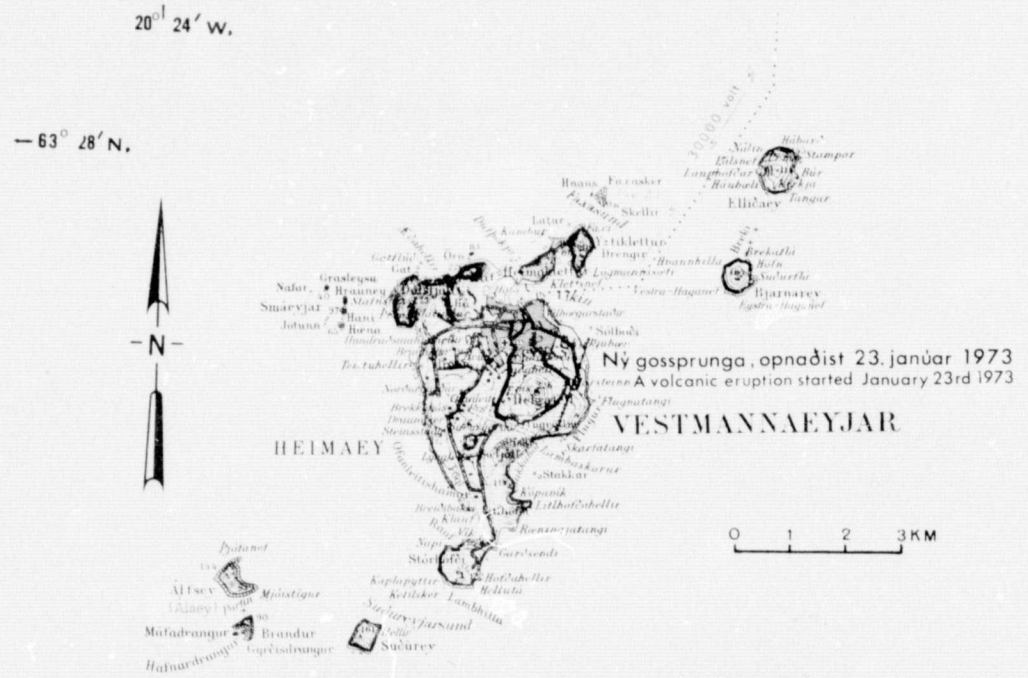

Figure 15. Recently revised (23 January 1973) topographic map of Heimaey, Vestmann Islands, Iceland (Uppdráttur Íslands, Blað 49, Vestmannaeyjar, Landmælingar Íslands, 1:100,000 scale, 1966). The outline of the island predates the volcanic eruption; however, the location of the eruptive fissure has been overprinted in red (on original map).

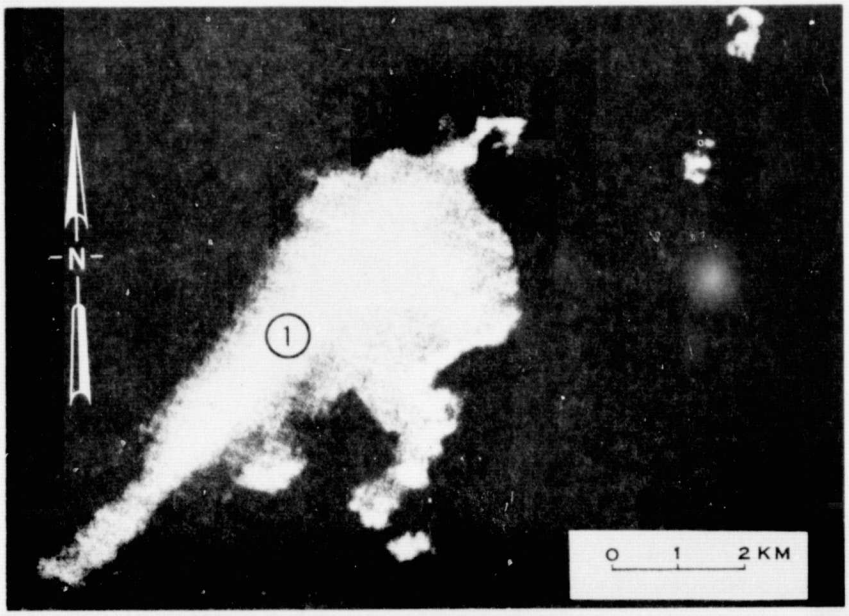

Figure 16. Positive enlargement (40X) of 3d generation, NDPF, 70 mm negative (original scale of 1:3,369,000) of ERTS image of Heimaey, Vestmann Islands, Iceland (Þórisvatn, D6, 21 Nov. 72, 1121-12143-6). Original enlargement scale was 1:84,225. Island is partially obscured by long, lenticular cloud (1) on its western side.

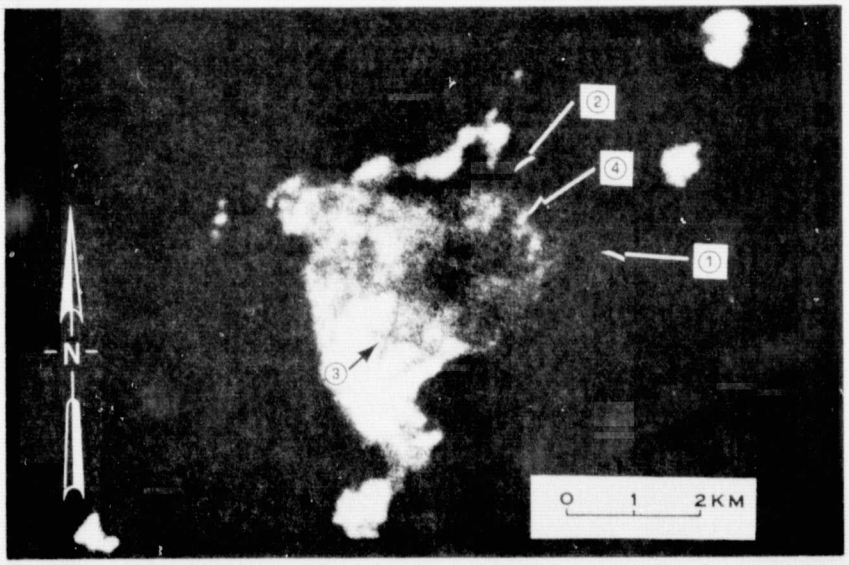

Figure 17. Positive enlargement (40X) of 3d generation, NDPF, 70 mm negative (original scale of 1:3,369,000) of ERTS image of Heimaey, Vestmann Islands, Iceland (Hekla, D5, 19 Aug. 73, 1392-12191-6). Original enlargement scale was 1:84,225. Note the new land area (1) resulting from lava flows to the east and northeast, near closure of the harbor entrance by new flows at (2), and change in reflectivity of the island at near-infrared wavelengths (0.7-0.8μm), the result of burial of vegetation by tephra, and the plus-shaped, gravel and crushed tephra landing strip at (3). Areas of sublimate deposition and clouds of steam, which are still rising through fractures in the lava flows, even though the surface eruption had ceased 7 weeks earlier, can be seen at (4).

Figure 18. NOAA-2 image mosaic, (Iceland, 22 May 73, NOAA-2 VHRR, VIS/VREC #11 and #12, Rev. 2741) of Iceland and surroundings. Vatnajökull (1), Hofsjökull (2), Langjökull (3), and Mýrdalsjökull (4) can be delineated. Note snow cover in the highland areas. Grímsvötn can be discerned in west-central Vatnajökull. Drift ice (5) can be seen in the Denmark Strait between Iceland and Greenland (6). The island of Jan Mayen can be seen at the top of the image (7). Image courtesy of E. Paul McClain and Donald R. Wiesnet, NOAA, National Environmental Satellite Service, Suitland, Maryland.

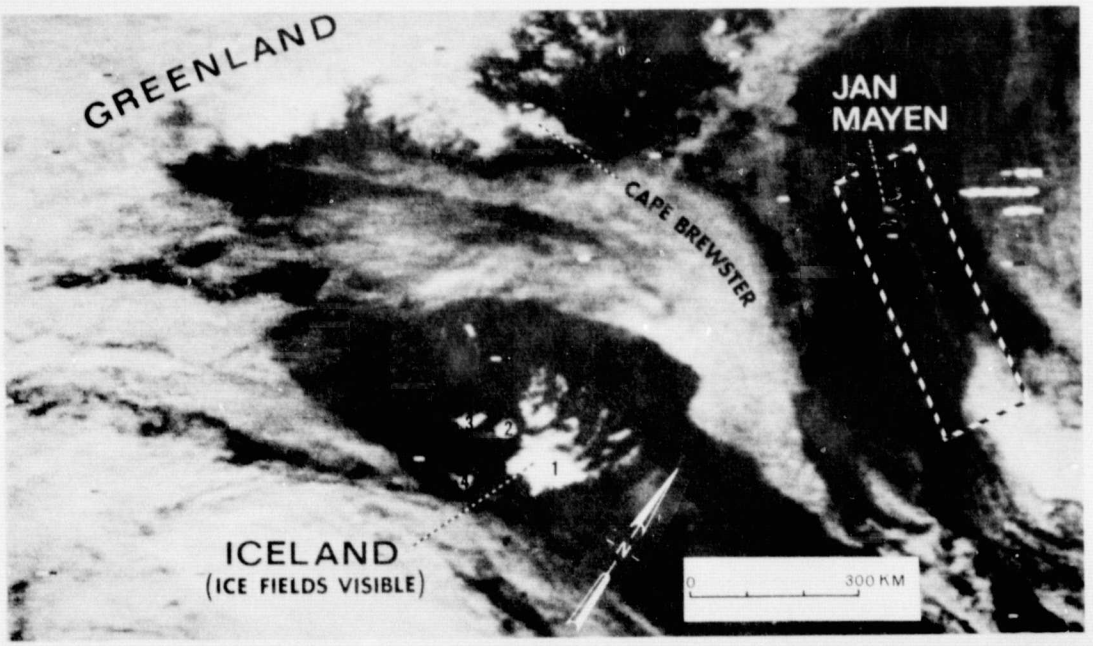

Figure 19. Nimbus IV image (Iceland, 21 Sep. 70, Nimbus IV, IDCS, 1200 UT) of Iceland and surroundings. Vatnajökull (1), Hofsjökull (2), Langjökull (3), and Mýrdalsjökull (4) can be delineated in a gross way. Note also the eruption plume from Beerenberg Volcano on the island of Jan Mayen. Image courtesy of NASA, Goddard Space Flight Center, Greenbelt, Md. From figure in Anon., 1971, p. 85).

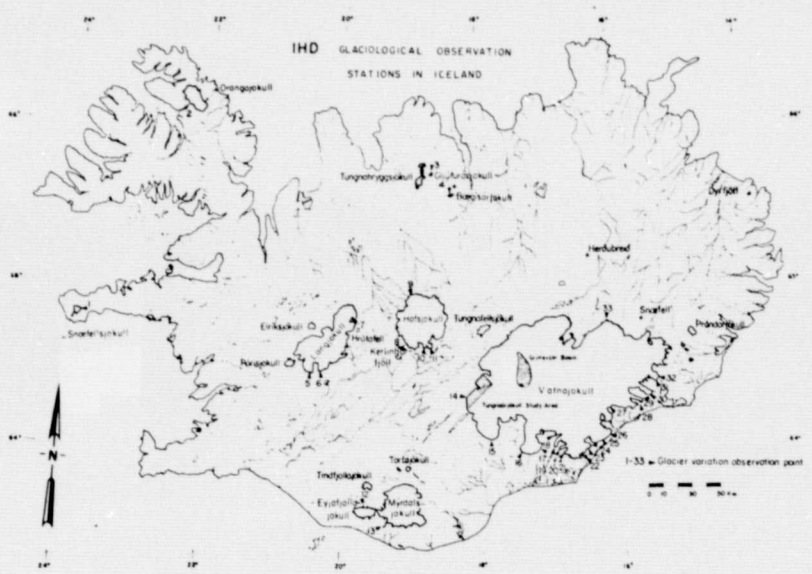

Figure 20. Icelandic Glaciers and International Hydrological Decade Glaciological Observation Stations. (From Rist, 1967b, p. 324).

Vatnajökull	(8400 km^2)	Snæfellsjökull
Langjökull	(1020 km^2)	Eiríksjökull
Hofsjökull	(996 km^2)	Þrándarjökull
Mýrdalsjökull	(700 km^2)	Tindfjallajökull
Drangajökull	(200 km^2)	Tungnahryggsjökull
Eyjafjallajökull	(107 km^2)	Torfajökull
Tungnafellsjökull	(50 km^2)	Gljúfurárjökull
Þórisjökull		Bægisárjökull

Table 2. Selected Icelandic Glaciers
(Areas from Bárðarson, 1971)

Figure 21. Midsummer, ERTS-1 image of the Vatnajökull icecap (Vatnajökull, D7, 30 July 73, 1372-12080-4). The high sun angle (42°) and high reflectivity of the snow-covered glacier limit the amount of surface detail as compared with the low sun angle, wintertime image (Figure 12). Older snowpack can be seen at (1), where it has drifted. Sediment plumes can be distinguished in the northwest arm of Þórisvatn (2) and all along the coast. A number of glacier-margin lakes are visible; note the maximum area encompassed by Grænalón (3), prior to the August 1973 jökulhlaup across Skeiðarársandur, the large glacial outwash plain to the south. A number of braided glacial rivers cross this outwash plain. Undistorted moraines (4) can be seen on Breiðamerkurjökull; contorted moraines (5) are visible on Skeiðarárjökull. The retreat of the snowline can be seen on most of the glaciers, including Mýrdalsjökull (6) and Eyjafjallajökull (7).

Figure 22. Early fall ERTS-1, cloud-free image mosaic of Vatnajökull (Vatnajökull, D7, 22 Sept. 73, 1426-12070-4; Vík, E7, 22 Sept. 73, 1426-12073-4). As the sun angle drops (25°), surface detail begins to again appear on Vatnajökull, although not as pronounced as on the wintertime image (Figure 12). Note the reduction in sediment plumes along the coast and the decreased discharge of glacial rivers across Skeiðarársandur. The entire western arm of lake Þórisvatn has suspended sediment (1). Note the retreat of the snowline on Vatnajökull and Mýrdalsjökull when compared with Figure 21. Note the reduction in area of Grænalón (2) after the August 1973 jökulhlaup, as compared with Figure 21.

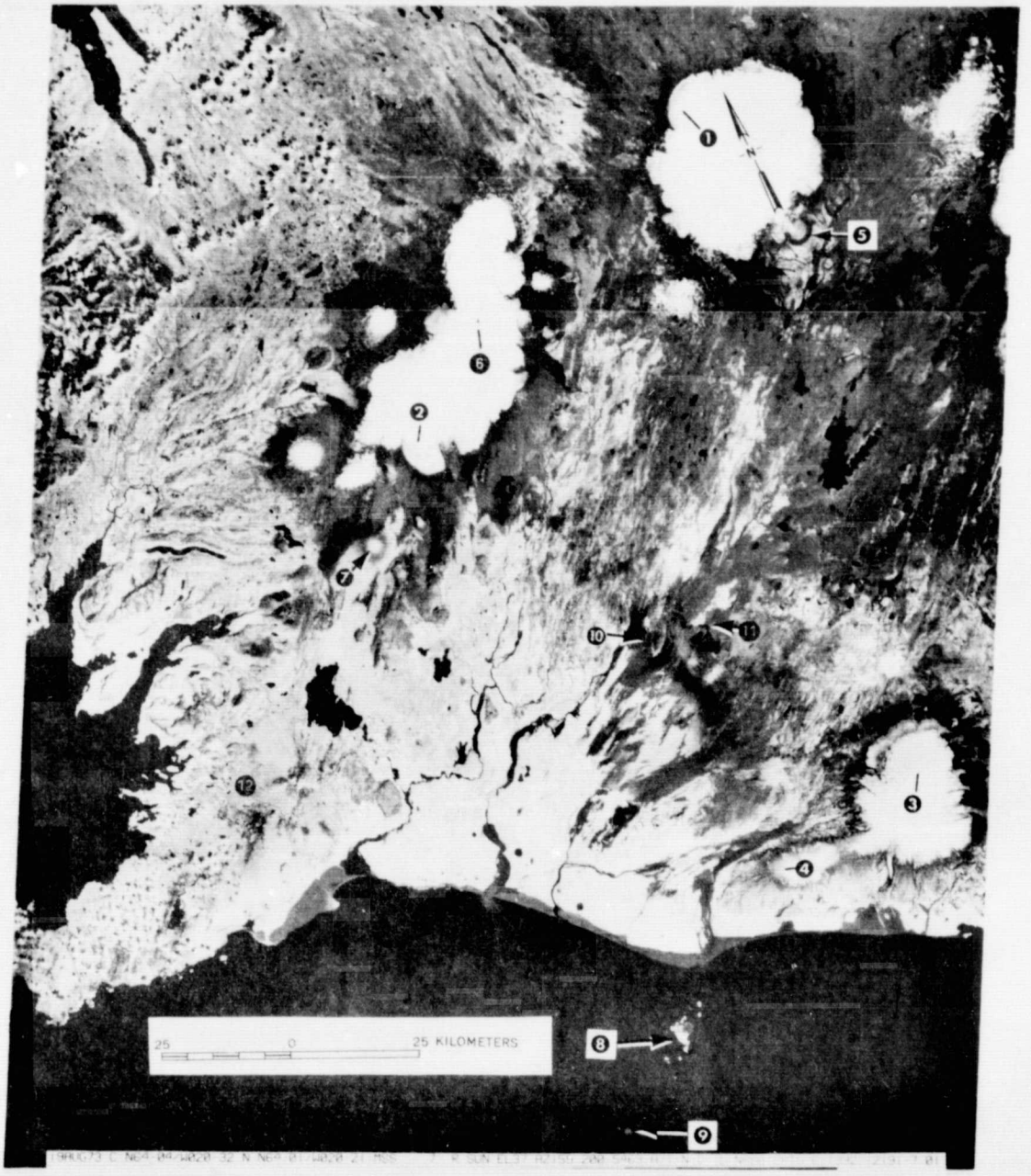

Figure 23. ERTS image mosaic (Akureyri, C5, 19 Aug. 73, 1392-12185-7; Hekla, D5, 19 Aug. 73, 1392-12191-7) of west-central and southwestern Iceland. The snowline can be delineated on the Hofsjökull (1), Langjökull (2), Mýrdalsjökull (3), and Eyjafjallajökull (4) icecaps. Note area of no vegetation (5), from where one of the outlet glaciers of Hofsjökull has receded. A prominent nunatak can be seen in the center of Langjökull (6) with a caldera- or cirque-like feature to the west within the icecap. The snow-capped, shield volcano, Skjaldbreiður, can be seen at (7), with tectonic fissures (gjár) extending southwest, south of Skjaldbreiður. The highly reflective vegetation can be delineated most accurately on false-color composites, including the new vegetation pattern on Heimaey (8). Surtsey (9) is also visible, southwest of Heimaey. The tephra fallout pattern (10) and new lava flows (11) from the 1970 volcanic activity on Hekla can be seen. (See also Figure 8). Lichen-covered basalts are visible at (12).

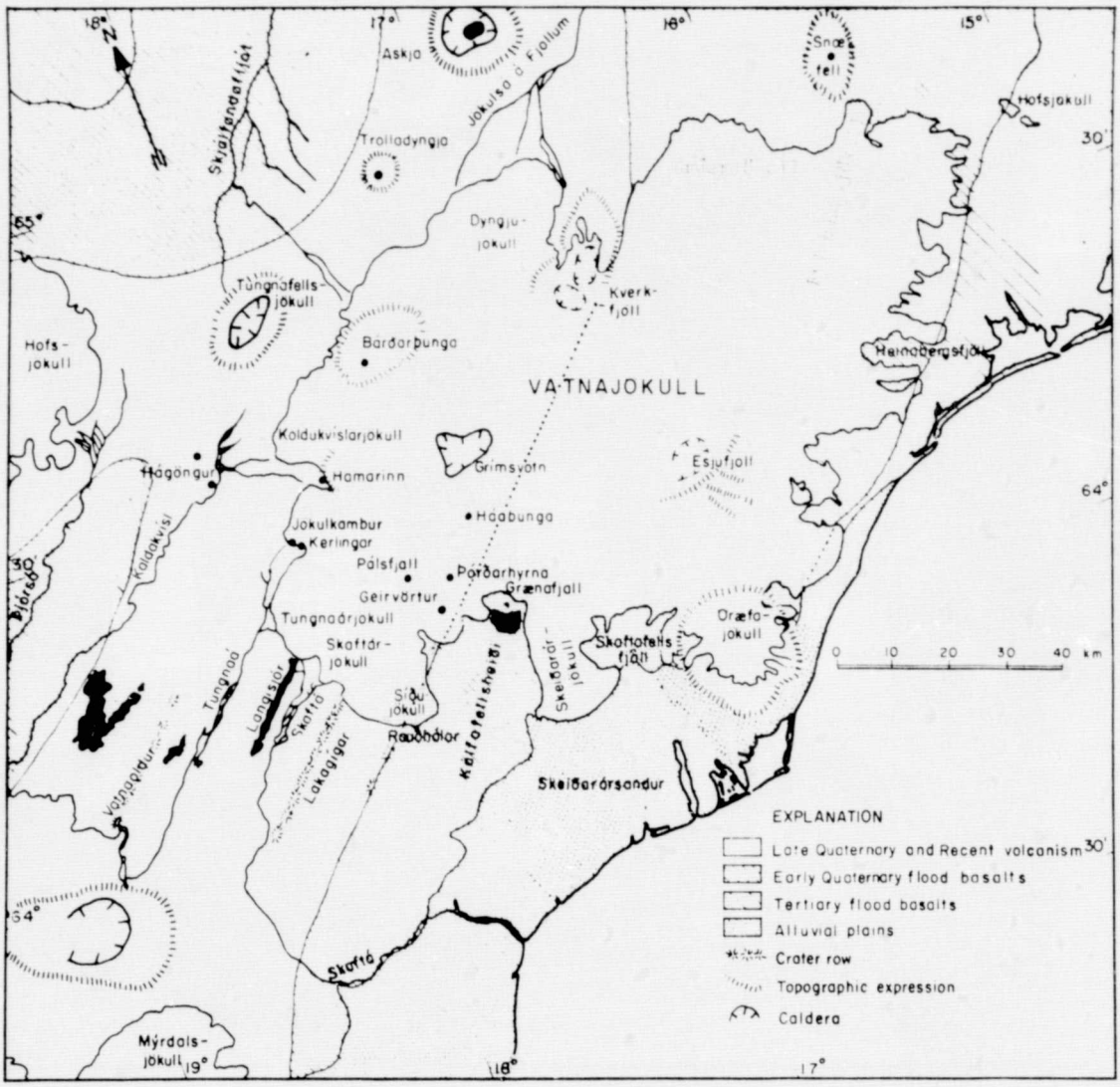

Figure 24. Geologic sketch map for Vatnajökull and surrounding area, Iceland. It covers most of the area shown on Figures 12, 21 and 22. [From Thorarinsson and others, (in press)].

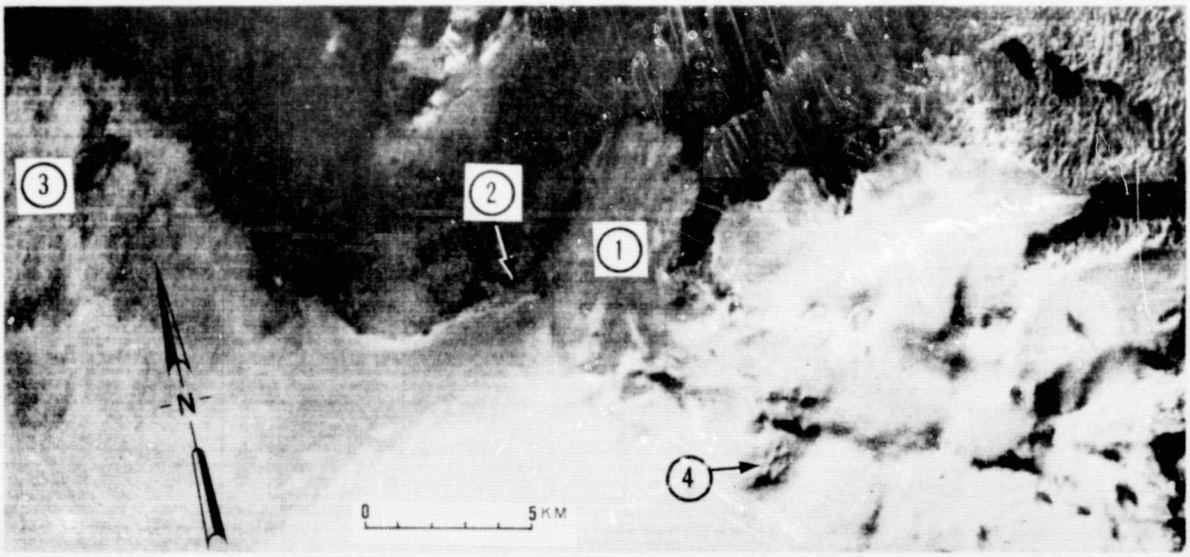

Figure 25. Positive enlargement (20X) of 3d generation, NDPF, 70 mm negative (original scale of 1:3,369,000) of ERTS image of Eyjabakkajökull, Iceland [Ingólfshöfði, D8, 14 Oct. 72, (1083-12023-5; partial, uncatalogued image)]. Original enlargement was 1:168,450. Eyjabakkajökull (1), an outlet glacier on the northeast part of Vatnajökull, was in the process of surging when it was imaged. A glacier-margin lake is visible at (2). Part of another surging glacier, Brúarjökull is visible to the left (3). Possible crevasse patterns resulting from the surge are visible at (4).

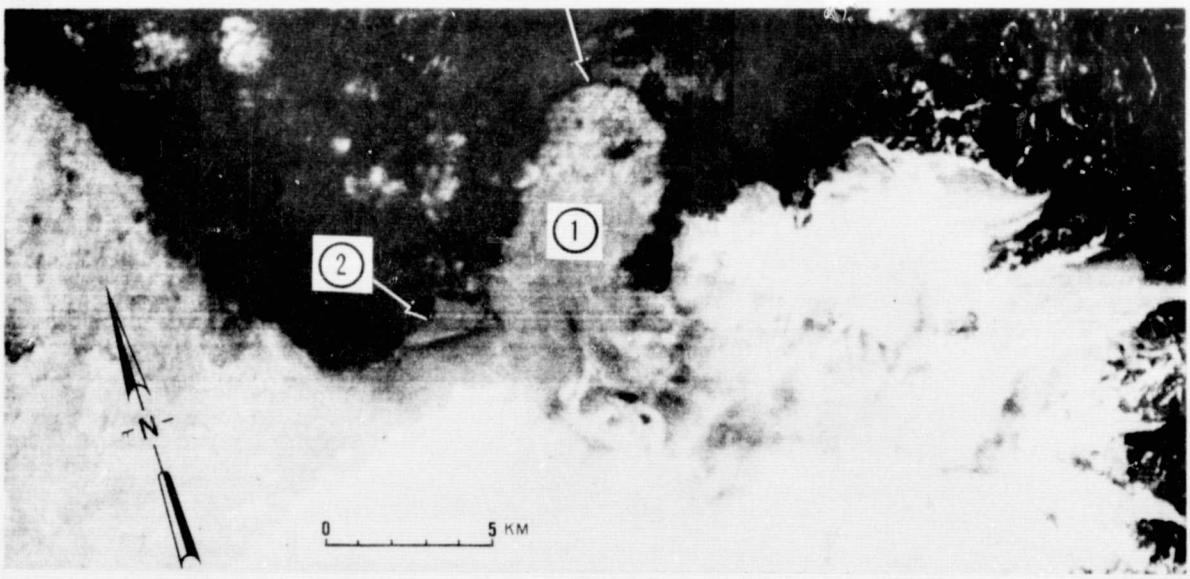

Figure 26. Positive enlargement (20X) of 3d generation, NDPF, 70 mm negative (original scale of 1:3,369,000) of ERTS image of Eyjabakkajökull, Iceland (Vatnajökull, D7, 22 Sep 73, 1426-12070-5). Original enlargement was 1:168,450. Eyjabakkajökull (1) had apparently completed its surge. Between 14 Oct. 72 and 22 Sept. 73, Eyjabakkajökull had surged approximately 1.8 km. Note the increase in surface area of the glacier-margin lake (2).

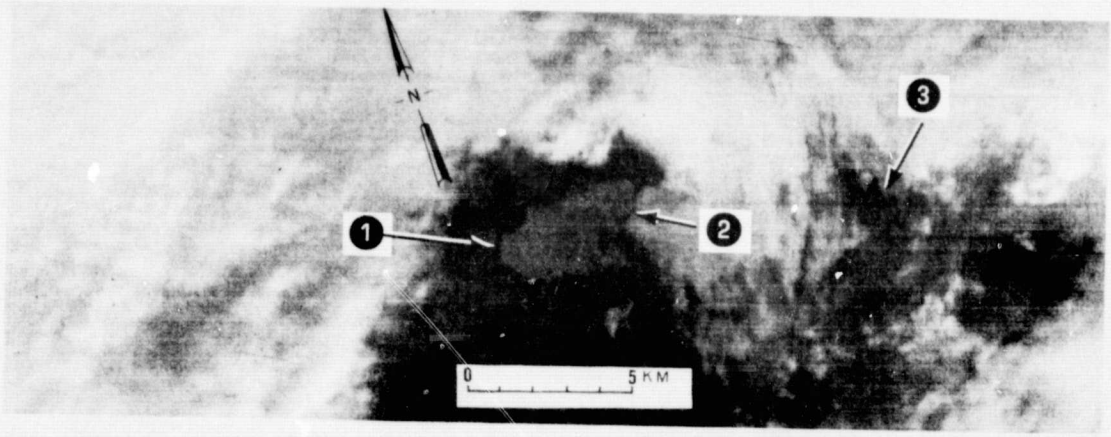

Figure 27. Positive enlargement (20X) of 3d generation, NDPF, 70 mm negative (original scale of 1:3,369,000) of ERTS image of Grænalón, Iceland [Ingólfshöfði, D8, 14 Oct. 72, (1083-12023-5; partial, uncatalogued image)]. Original enlargement of 1:168,450. First image of the ice-dammed lake Grænalón (1) taken by ERTS-1. Ice dam is visible at (2). A distinctive pattern of distorted medial moraines is visible at (3), although somewhat obscured by clouds.

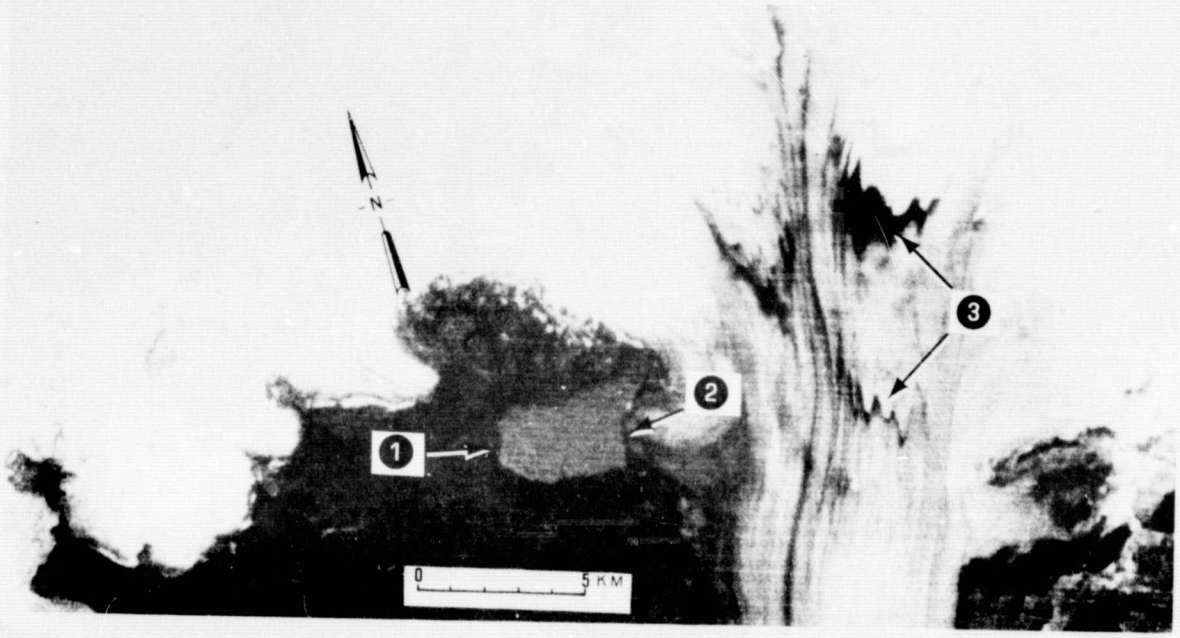

Figure 28. Positive enlargement (20X) of 3d generation, NDPF, 70 mm negative (original scale of 1:3,369,000) of ERTS image of Grænalón, Iceland (Vatnajökull, D7, 22 Sept. 73, 1426-12070-5). Original enlargement of 1:168,450. Image of the ice-dammed lake Grænalón (1) after the August 1973 jökulhlaup. Ice dam is visible at (2). Note the distinctive patterns of distorted medial moraines at (3). The interv between the two may represent the time between two successive jökulhlaups. If the motion of Skeiðarárjökull, as measured on Figures 27 and 28, is 600 m and this represents an average annual rate of motion, then the interval represents about 6 or 7 years. The increase in area of lake Grænalón can be monitored on Figure 27 (14 Oct. 72), Figure 12 (31 Jan. 73), and Figure 21 (30 Jul. 73). The latter shows the largest area prior to the jökulhlaup. Note that the area of Grænalón after the jökulhlaup (Figure 28) is still slightly larger than the area shown on Figure 27.

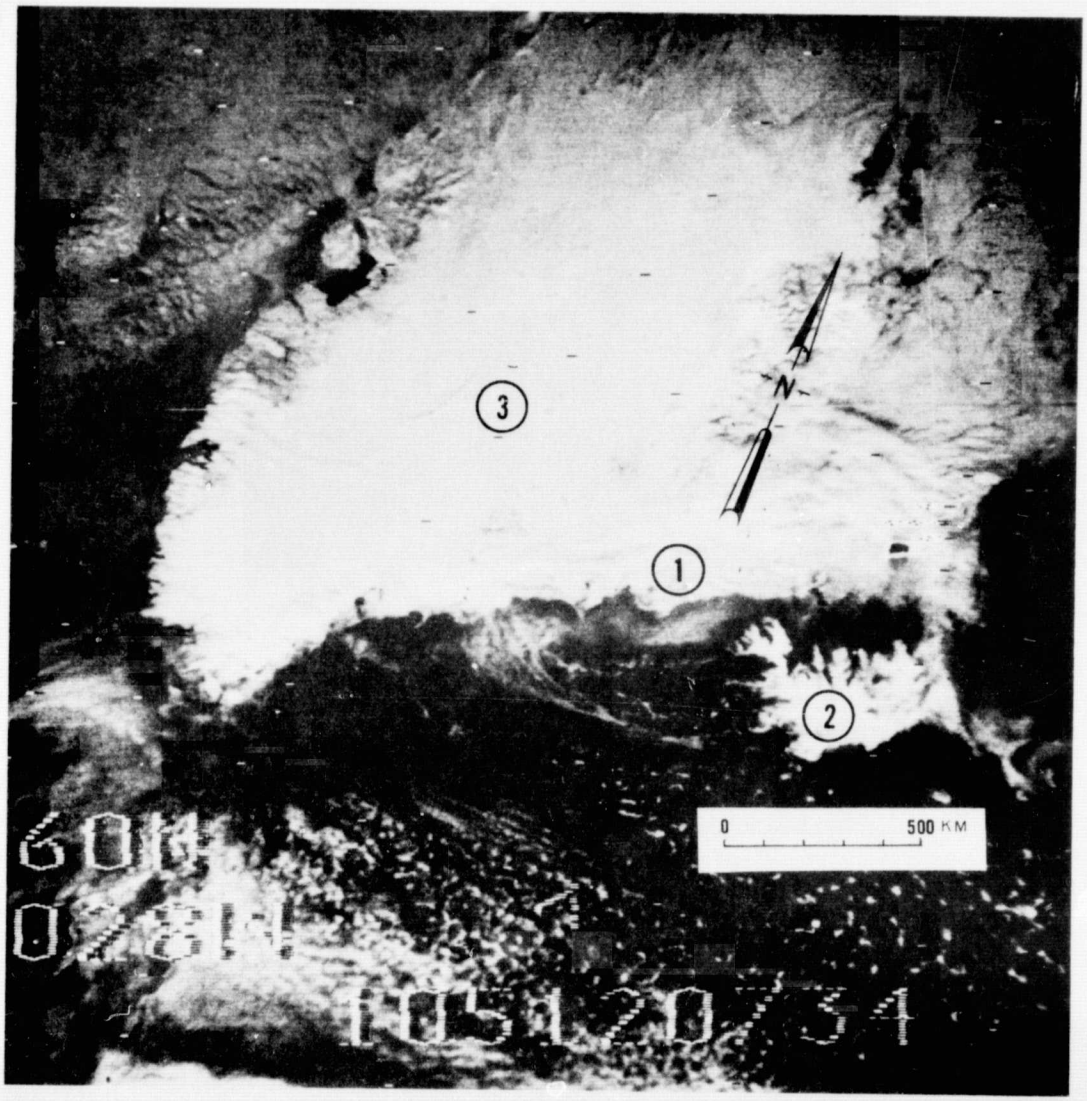

Figure 29. Nimbus III image of sea ice (1) in the Denmark Strait between Iceland (2) and Greenland (3). (Iceland, 15 Apr. 69, Nimbus III, IDCS, Orbit 16). Compare with Figure 18, a NOAA-2 image of sea ice in the Denmark Strait. Image courtesy of NASA, Goddard Space Flight Center, Greenbelt, Md. From figure in Anon., 1971, p. 63.

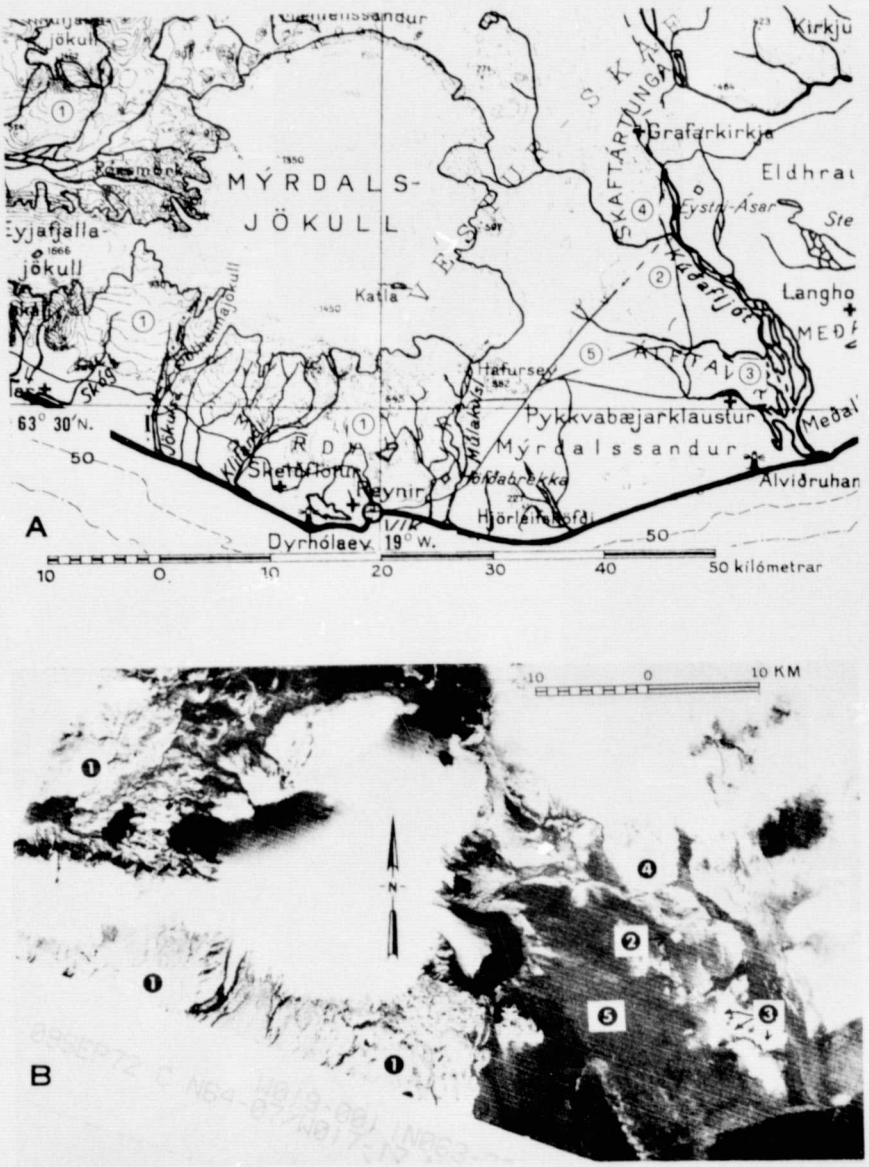

Figure 30. Comparison of 1:500,000-scale map (A) of Iceland (Ísland, Geodætisk Institut, Copenhagen, Denmark, 1945) with an ERTS-1 image (B) of the same area (Vatnajökull, D7, 9 Sept. 72, 1048-12080-7). Note the different outline of Mýrdalsjökull and some of its outlet glaciers. Four of the five different vegetation classes discernible on ERTS imagery of Iceland (not including barren lands -5) can be mapped on the false-color, MSS composite of this scene: natural grassland, 1; reclaimed land, 2; cultivated land, 3; and dwarf forests, 4; by their different hues of red and purple. Not shown on this image but visible on Figure 23, is an example of the vegetation class, lichen-covered basalts, which have a distinctive purplish hue on flase-color, MSS composites of Iceland.

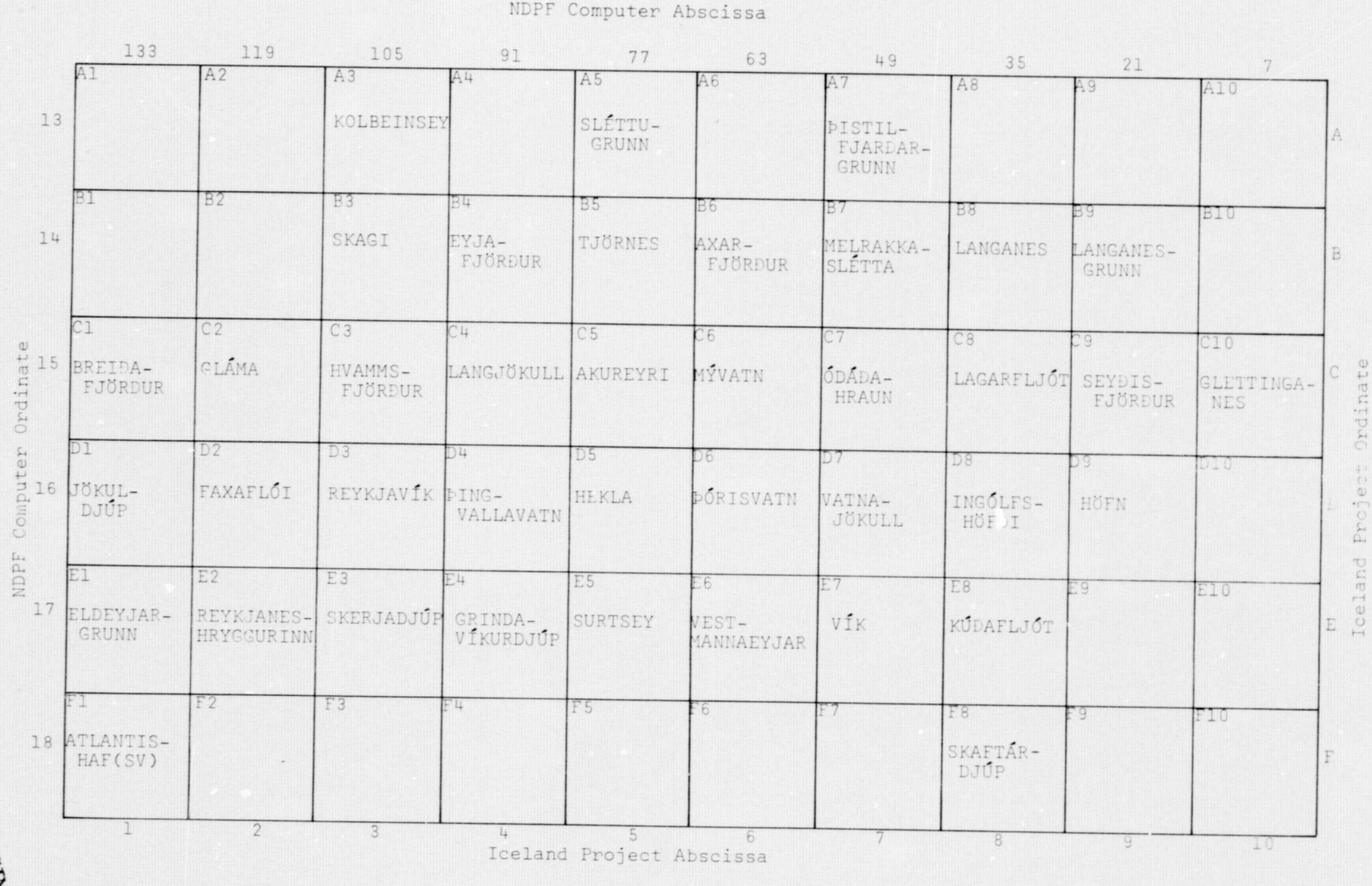

Figure 31. Geographic names and data acquisition matrix for ERTS-1 imagery of Iceland.

TABLE 3. SUMMARY OF STUDIES IN ICELAND WITH ERTS-1 IMAGERY

Discipline	Experiments	Research Objectives	Research Results
GEOLOGY	Geothermal	Delineation of geothermal areas by extent of snow-melt pattern	Delineation of part of geothermal area by snowmelt pattern. Delineation of geothermally altered ground in 3 geothermal areas.
GEOLOGY	Volcanic Eruptive	Delineation of areas of new basalt flows and tephra falls	Delineation of new basalt flows in 3 areas and tephra fallout pattern in 1 area. Image of effusive volcanic eruption.
GEOLOGY	Geologic Structure	Mapping, on a regional basis, of faults, fissures, lineaments, and other structural features in the neovolcanic zone	Mapping of many new structural geologic and volcanic features, particularly within icecaps, and on snow-covered terrain at low sun angle (<10°).
GEOLOGY	Volcanic Geomorphology	Mapping of the regional aspect of volcanic landforms	Regional distribution of different volcanic landforms mappable, particularly unique landforms.
GEOLOGY	Marine Geology and	Mapping of any changes in the coastline of Iceland and any submarine features visible	Planimetric revisions of maps (to 1:100,000 scale) of Surtsey (erosion) and Heimaey (volcanic eruption) feasible. Mapping of seasonal change of sediment plumes from glacial rivers.
HYDROLOGY	Ephemeral Snow and Ice	Mapping of changes in snow cover over time; mapping of surface water distribution, and mapping of ice freeze-ups and thaws on major lakes	Mapping of surface water distribution can be achieved. Some mapping (lack of seasonal imagery) of changes in snow cover and thaw of lake ice.
HYDROLOGY	Glaciological Features	Delineation of areas covered by glaciers; mapping of changes in ice-margin lakes; mapping of nunataks; and mapping of depositional glacial features	Delineation of 90% of the area covered by icecaps; mapping of changes in glacier-margin lakes; mapping of some nunataks and some depositional glacial features. Mapping of surging glacier (1.8km movement and flow of another glacier (600m/11 mos.).
HYDROLOGY	River Flooding	Mapping of spring runoff, floods along river valleys, and changes in distributaries from glaciers	Mapping of changes in distributaries from glaciers. Mapping of changes in lake and outwash plain caused by a jökulhlaup.

TABLE 3 - CONTINUED

Discipline	Experiments	Research Objectives	Research Results
OCEANOGRAPHY	Sea Ice	Mapping of changes in ice floe concentrations with time off northern and eastern coasts	No usable imagery.
AGRICULTURE/ FORESTRY	Grasslands and Forest	Delineation of grasslands and particularly change in vigor with time	Mapping of 5 classes of vegetation: grasslands, cultivated areas, reclaimed land, forested areas, lichen-covered lava flows, and barren areas on false-color composites.
CARTOGRAPHY	-	-	Compilation of an orthoimage mosaic of Iceland at 1:1,000,000 (false-color composite) and planned 1:500,000- and 1:250,000-scale orthoimage mosaic maps. Study of landforms with stereoscopic images. Measurement of 100m elevation difference. Planimetric revisions on existing maps.

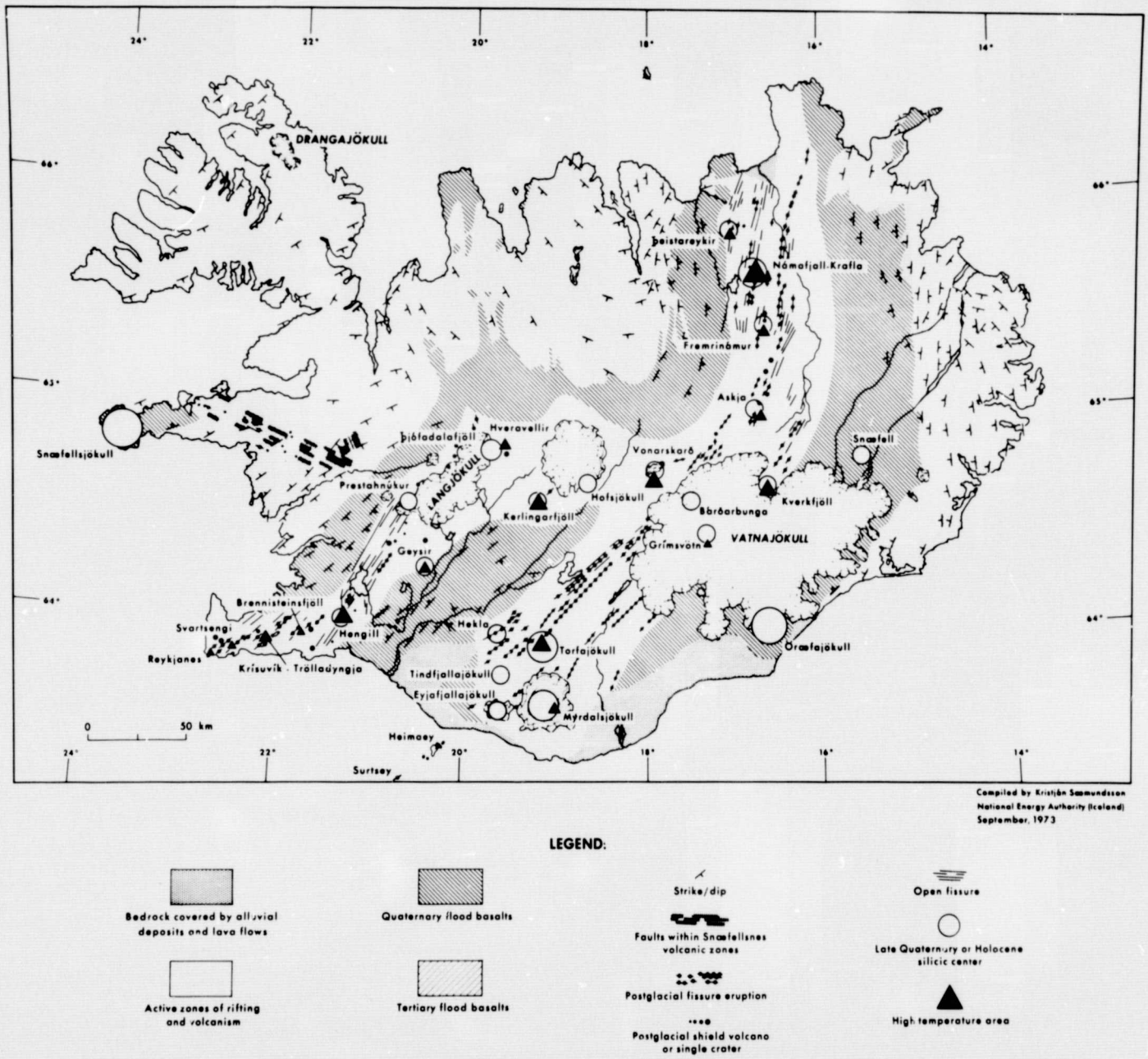

FIGURE 1. Geologic Map of Iceland modified from Pálmason and Sæmundsson, 1974, fig. 2.

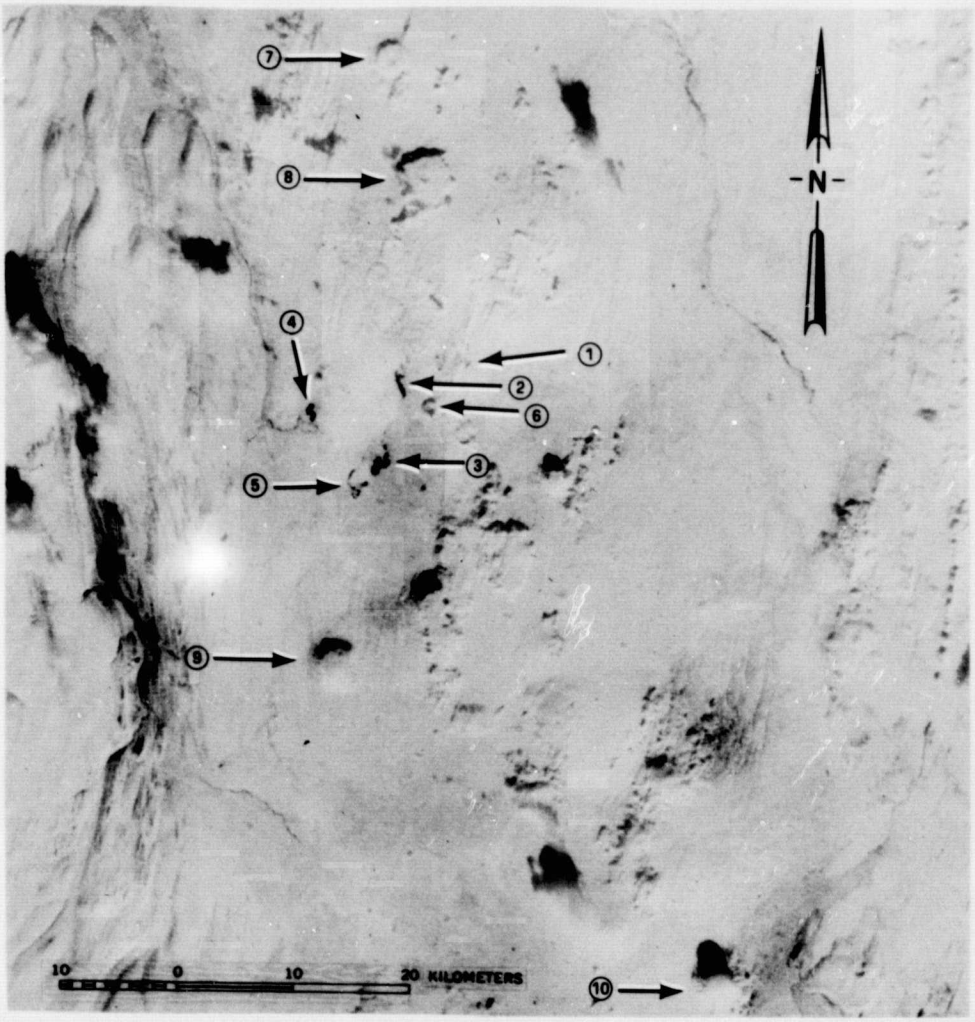

Figure 2. The Námafjall geothermal area (1) appears on wintertime imagery as a light grey, linear, "ragged area," which is surrounded by bright white snow (Mývatn, C6, 9 Mar. 73, 1229-12142-7). Open water in lake Mývatn due to thermal spring discharge can be seen at (2), due to a high volume of spring discharge at Kálfaströnd (3), at the main river outlet of the lake at Álabrot (4), and at lake Grænavatn (5), just to the south of Mývatn. The tephra ring, Hverfjall, can be seen at (6). The table mountains, Bæjarfjall (7), Gæsafjöll (8), Sellandafjall (9), and Herðubreið (10), also stand out sharply. Compare with Figure 3.

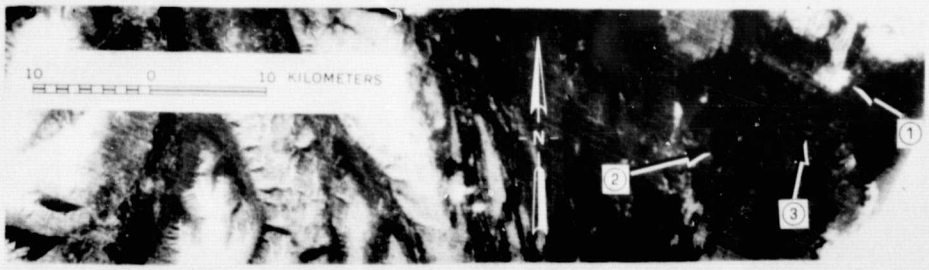

Figure 3. The Námafjall geothermal area (1) appears as a light greenish area on an MSS color composite (bands 4, 5, 7), here shown on band 5 (Akureyri, C5, 19 Aug. 73, 1392-12185-5). The area of altered ground is the result of intense geothermal activity, which has altered the basaltic lava flows and hyaloclastites. Lake Mývatn can be seen at (2) and the tephra ring, Hverfjall, at (3). Compare with Figure 2.

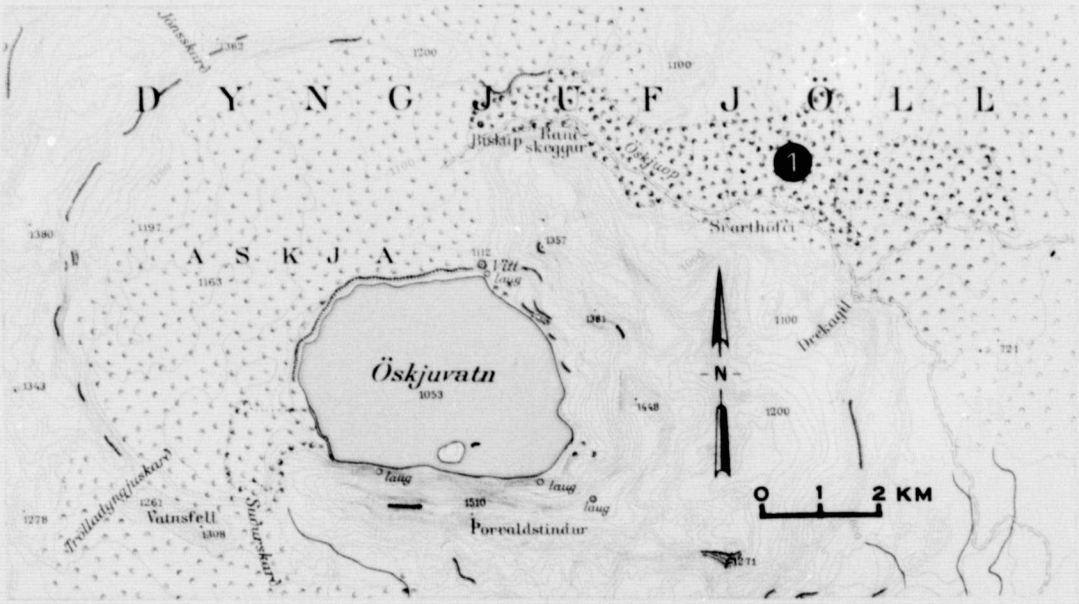

Figure 4. Topographic map of the 1961 lava flows (1) in the Askja area, Dyngjufjöll massif, Iceland (Uppdráttur Íslands, Blað 84, Herðubreið, Landmælingar Íslands, 1:100,000 scale, 1969). Based on 1937-38 survey by Geodætisk Institut, Copenhagen, Denmark. Revised by Landmælingar Íslands in 1965. Compare shape of lava flows as shown on Figures 5 and 6.

Figure 5. Vertical aerial photograph (#5240B) taken by Landmælingar Íslands (Icelandic Geodetic Survey) on 21 August 1970. Lava flows of 1961 have flowed over a pumiceous layer deposited in the explosive eruption of 1875. Compare with Figures 4 and 6.

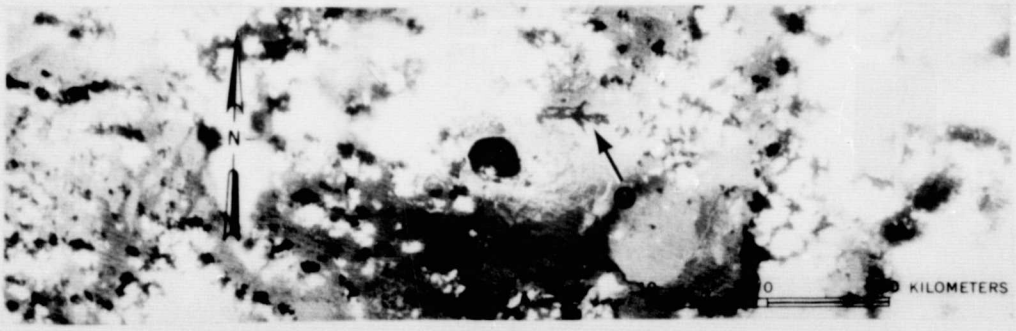

Figure 6. The 1961 lava flows (1) are sharply delineated on the mostly cloudy ERTS-1, MSS image (Ódáðahraun, C7, 30 July 73, 1372-12074-5). Note the detail in the outline of the flows, including the two prominent windows within the flows. Compare with Figures 4 and 5.

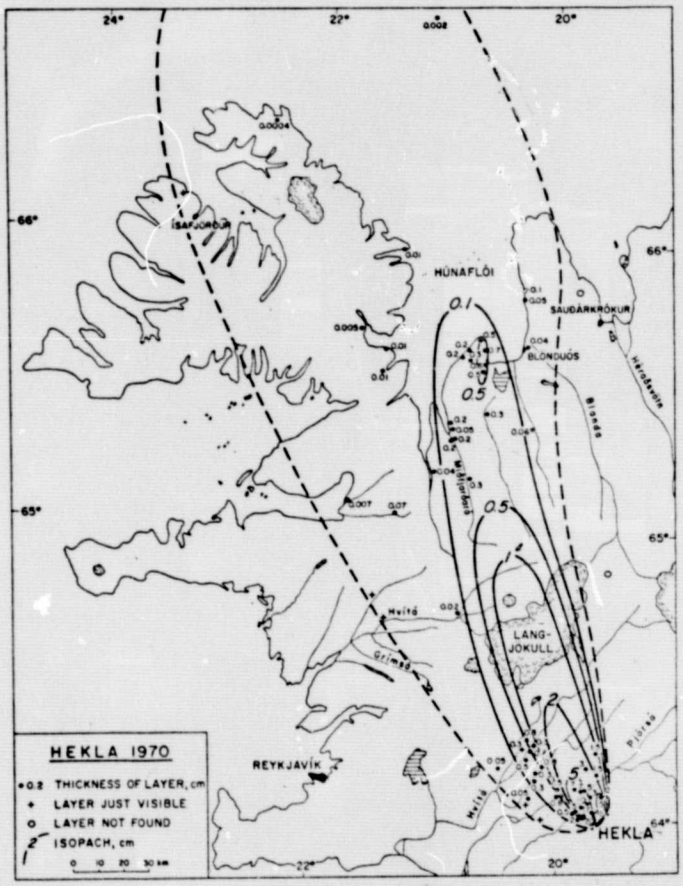

Figure 7. Isopach map of tephra layer from eruption of Hekla in May-July 1970. (From Thorarinsson, 1970, fig. 13).

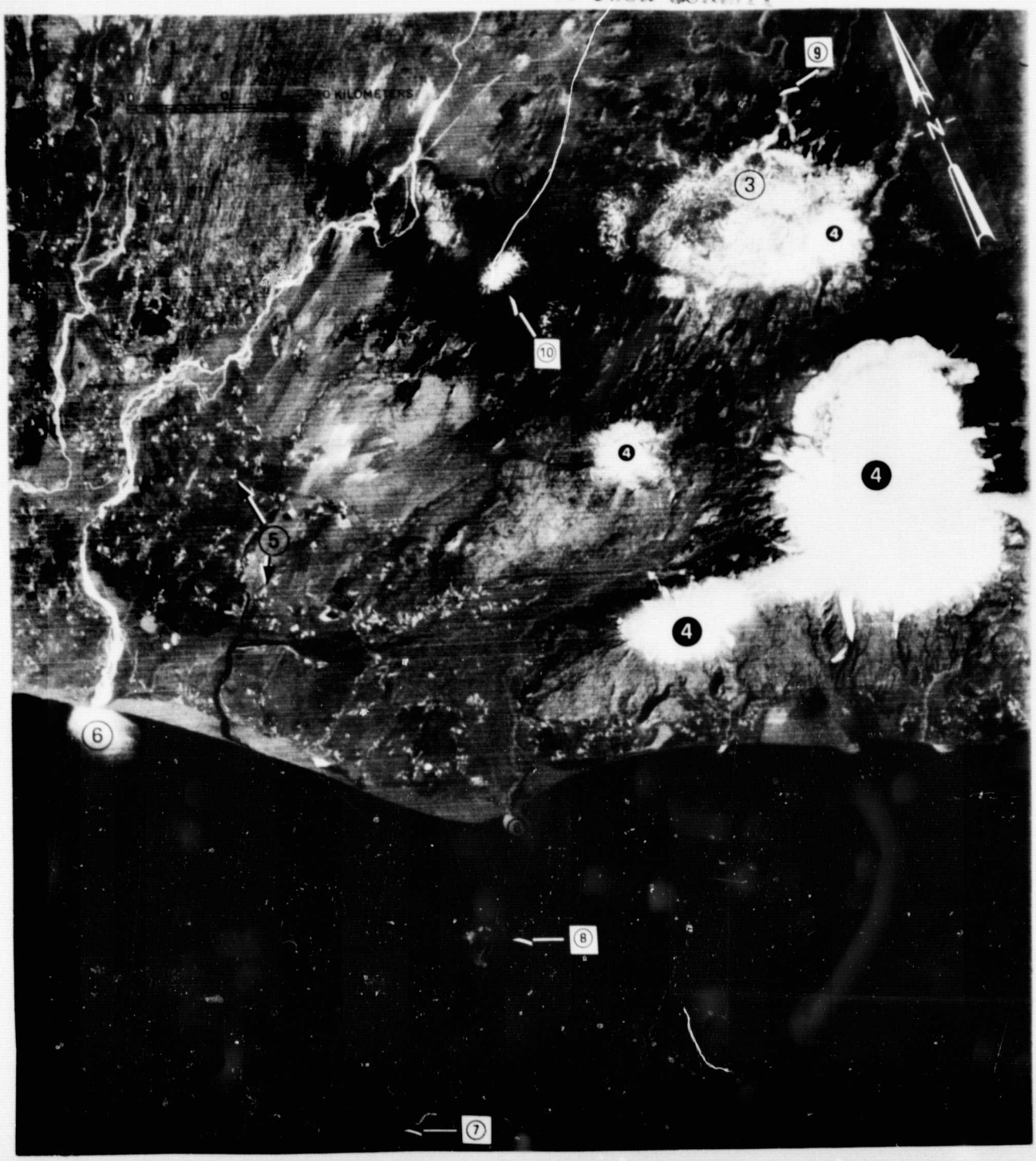

Figure 8. Part of an ERTS-1, MSS image of the Hekla area, Iceland (Hekla, D5, 19 Aug. 73, 1392-12191-5). Important features are the tephra fallout pattern from the 1970 eruption of Hekla (1), three areas of new lava flows from Hekla's 1970 eruption (2), rhyolitic rocks and a clear trace of a caldera fault in Torfajökull area (3), several icecaps (4), numerous cultivated areas (5), sediment plumes from rivers laden with glacial rock flour (6), new shapes of the islands of Surtsey (7) and Heimaey (8), a maar (9), and stratified ridge (10).

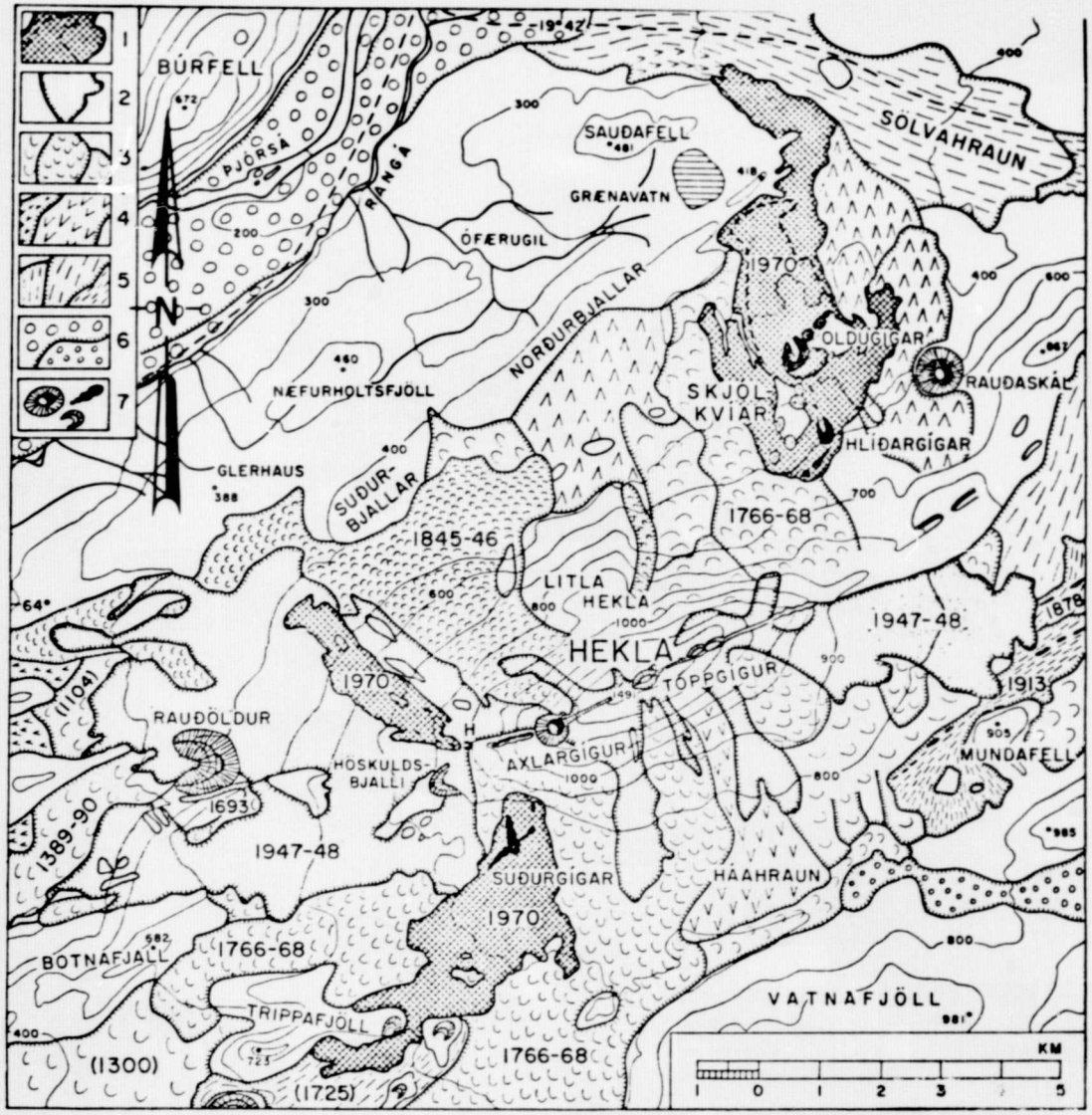

Figure 9. Geologic map of Hekla and environs showing the three areas of new lava flows in 1970 (cross-hatched patterns) and areas of previous lava flows. (From Thorarinsson, 1970, fig. 14). Geologic map explanation: 1, 1970 lava flows; 2, 1947-1948 lava flows; 3, 4, and 5, different historic and prehistoric lava flows, Hekla and Hekla region; 6, Þjórsá lava flows; and 7, craters.

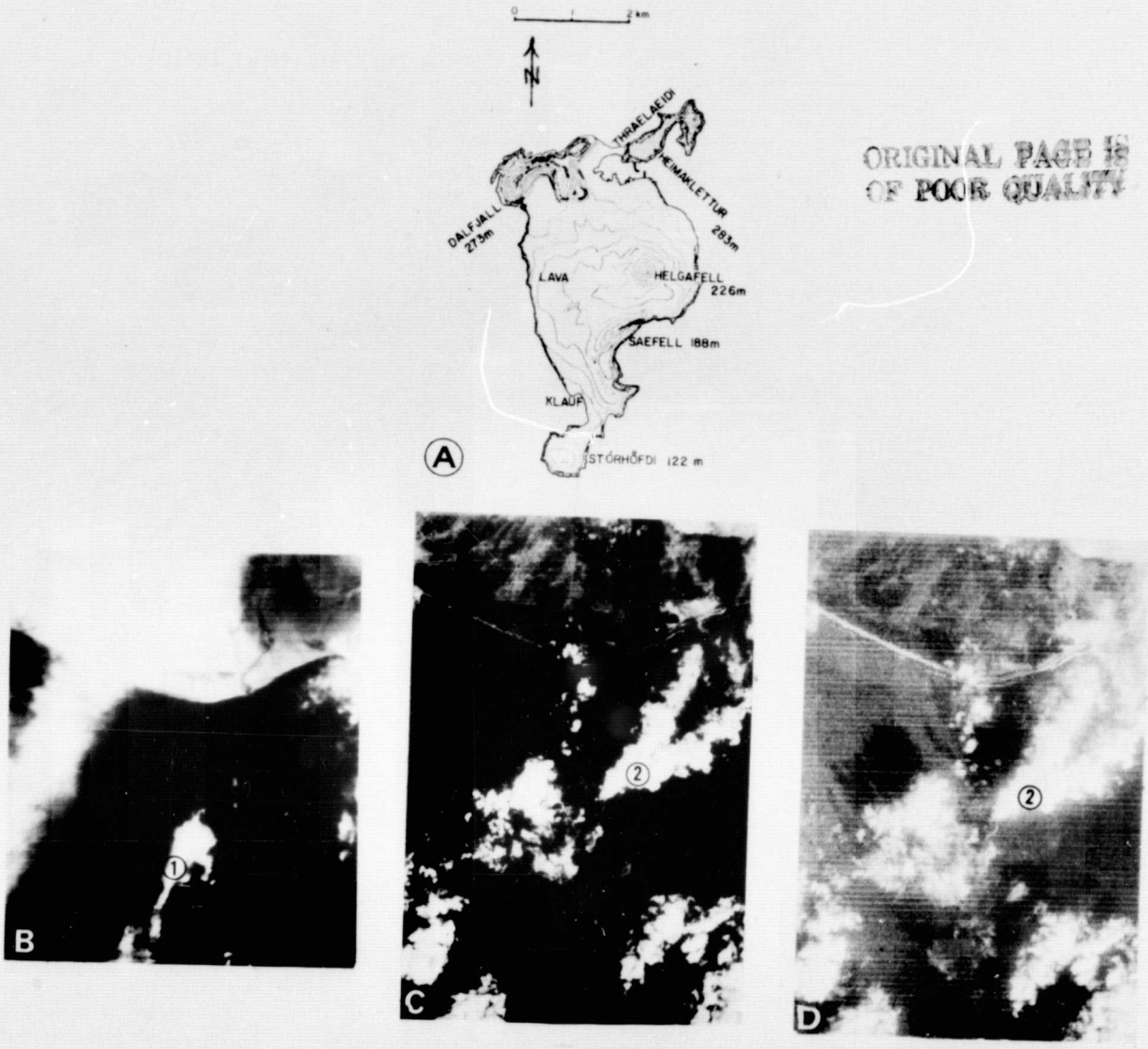

Figure 10. Simplified topographic map of Heimaey, Vestmann Islands, Iceland, (A) showing the configuration of the island prior to the onset of volcanic activity on 23 January 1973. (Map is from figure in Friðriksson and others, 1972, p. 53). The ERTS image on the left (B) (Þórisvatn, D6, 21 Nov. 72, 1121-12143-7) shows the island prior to the eruption, with the western shoreline partially obscured by a long, linear cloud (1). (See also Figure 16 for an enlargement of this image.) The center (C) and right-hand (D) ERTS images (Vestmannaeyjar, E6, 9 Mar. 73, 1229-12151, bands 7 and 5, respectively) were acquired during an active phase of the eruption. Although partially obscured by clouds, the outline of the island can be seen, with the eruption plume (2) ascending to the east from the east side of the island. The eruption plume, however, nearly obscures all of the new land.

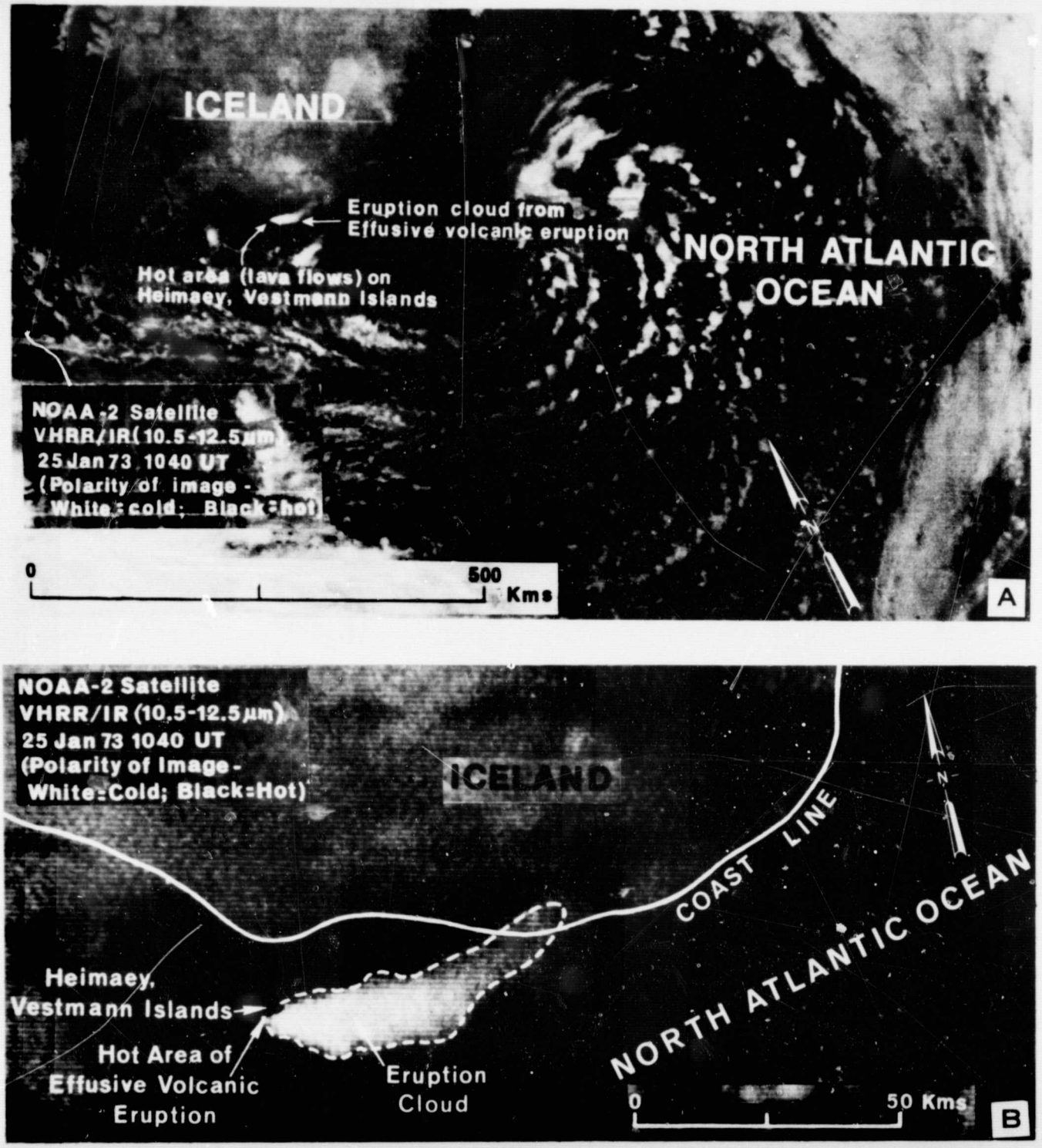

Figure 11. Satellite thermograph obtained by the VHRR (Very High Resolution Radiometer) instrument of the NOAA-2 satellite on 25 January 1973, less than 33 hours after the beginning of the volcanic eruption on Heimaey, Vestmann Islands, Iceland. This thermal infrared image was furnished to the authors by E. Paul McClain and Donald Wiesnet of NOAA's National Environmental Satellite Service. The bottom thermograph (B) is a 10X enlargement of the top thermograph (A).

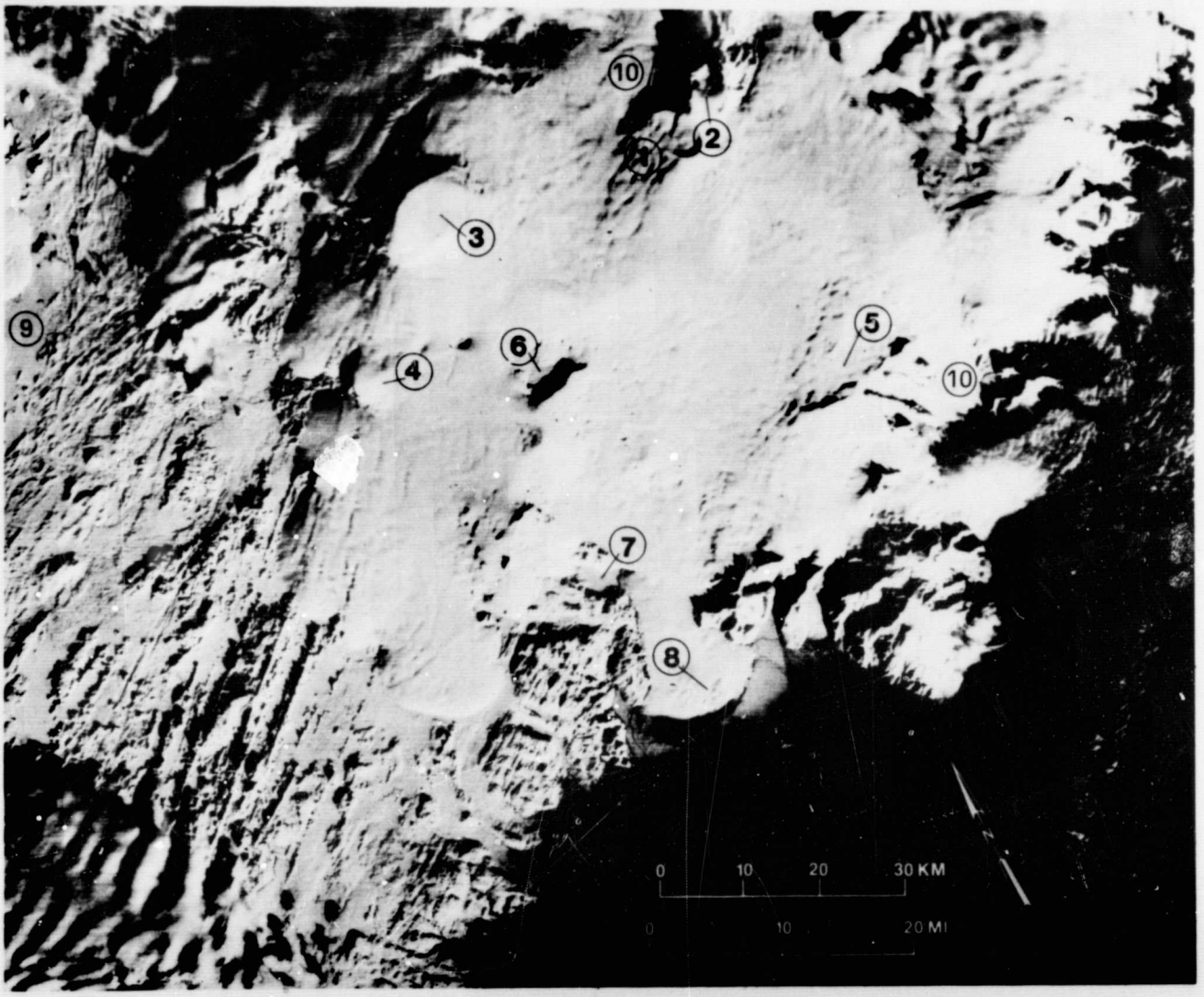

Figure 12. Low sun angle (7°) ERTS-1 image (Vatnajökull, D7, 31 Jan. 73, 1192-12084-5) of the snow-covered Vatnajökull area, Iceland, which shows a number of volcanic and glaciologic features within the Vatnajökull icecap. Features shown include: (1) elliptical shape of a hitherto unknown subglacial caldera southwest of Kverkfjöll; (2) elliptical shape of partially subglacial caldera at Kverkfjöll. Although dark, two subglacial craters can be seen on the western edge of this caldera with a partially subglacial geothermal area extending southwest into the icecap through the westernmost crater; (3) and (4) elliptically shaped central volcanoes at Bárðarbunga and east of Hamarinn, respectively; (5) faint elliptical features and associated nunataks at Esjufjöll which may represent a partially ice covered large central volcano; (6) the large depression of Grímsvötn, a well-known subglacial caldera, and source of many catastrophic jökulhlaups (glacial floods) to the south, including one in March 1972; (7) the frozen lake, Grænalón, another source of jökulhlaups, including one which occurred in August 1974; and (8) the partially snow covered snout of Skeiðarárjökull. Around the periphery of the Grímsvötn caldera are a number of punctate features resulting from collapse after the March 1972 jökulhlaup. Several more collapse features, resulting from the August 1972 jökulhlaup can be seen in a line between Hamarinn (4) and the Grímsvötn caldera. Southwest of Vatnajökull are superb examples of NE-trending grabens, crater rows, and hyaloclastite ridges. Two prominent volcano-tectonic lineaments can be seen on this image. One extends N.45°E. for 80 km between Kverkfjöll (1 and 2), the eastern edge of Grímsvötn (6), to the southwestern edge of Vatnajökull. The second lineament extends N.35°W., just north of Grænalón (7). Concentric recessional moraines in front of one of Hofsjökull's outlet glaciers can be seen at (9). Medial moraines are visible at (10).

	Main products of eruption	Number of eruptions	FORM OF RUPTURE	
			Punctual •	Linear —
Decreasing temperature Increasing explosivity ↓	LAVA (Flowing material)	1		Lave fissure ELDGJÁ Type: ÖGMUNDARGJÁ
		1	Lava cone ELDBORG Type: ELDBORG	Lava cone row ELDBORGARÖÐ Type: SVÖRTUBORGIR
		>1	Shieldvolcano DYNGJA Type: SKJALDBREIÐUR	
	LAVA and TEPHRA (Flowing and air borne material)	1	Spatter cone KLEPRAGÍGUR Type: BÚÐAKLETTUR	Spatter cone row KLEPRAGÍGARÖÐ Type; LAKAGÍGAR
		>1	Stratovolcano ELDKEILA Type: SNÆFELLSJÖKULL	Stratified ridge ELDHRYGGUR Type: HEKLA
	TEPHRA (Airborne material)	1	Scoria cone GJALLGÍGUR Type: RAUÐASKÁL	Scoria cone row GJALLGÍGARÖÐ Type: VATNAÖLDUR
		1	Tephra ring HVERFJALL Type: HVERFJALL	Explosion fissure SPRENGIGJÁ Type: VALAGJÁ
		1	Maar KER Type: GRÆNAVATN	

Table 1. The main types of basaltic Icelandic volcanoes (from Thorarinsson, 1960, p. 35).

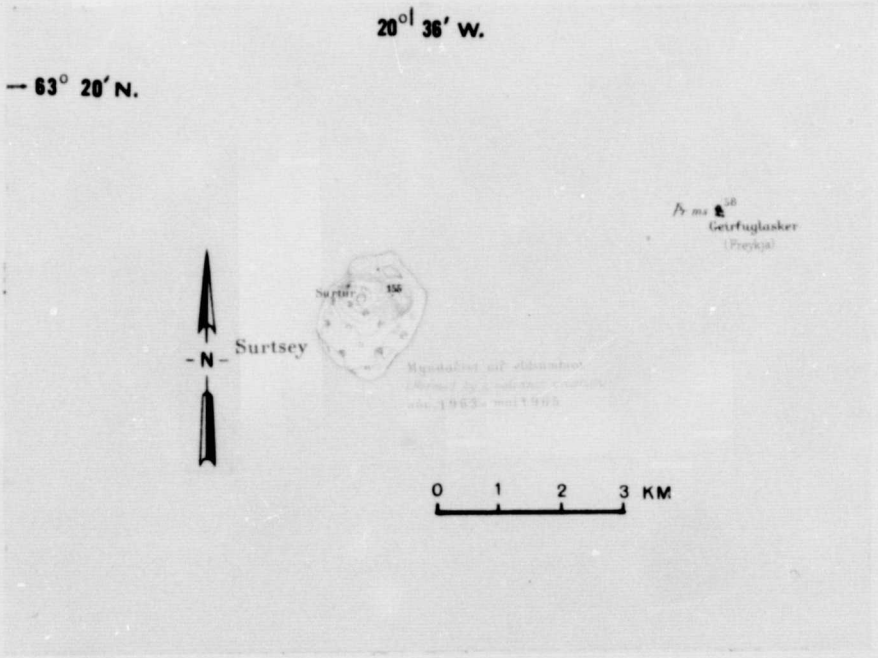

Figure 13. Topographic map of Surtsey, Vestmann Islands, Iceland/Uppdráttur Íslands, Blað 49, Vestmannaeyjar, Landmælingar Íslands, 1:100,000 scale, 1966). Outline of Surtsey drafted from aerial photography acquired by Landmælingar Íslands on 24 August 1965 (Photo No. 375).

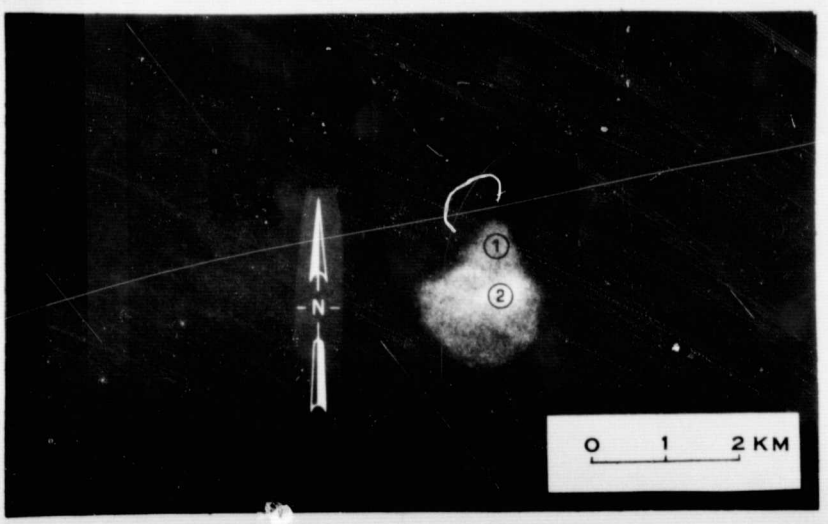

Figure 14. Positive enlargement (40X) of 3d generation, NDPF, 70 mm negative (original scale of 1:3,369,000) of ERTS image of Surtsey, Vestmann Islands, Iceland (Surtsey, E-5, 19 Aug. 73, 1392-12194-6). Original enlargement scale was 1:84,225. Note prominent ness at (1) and the highly reflective area at (2), where the tephra pile is undergoing palogonitization. Although the image is somewhat grainy, the coastline of the island can be delineated.

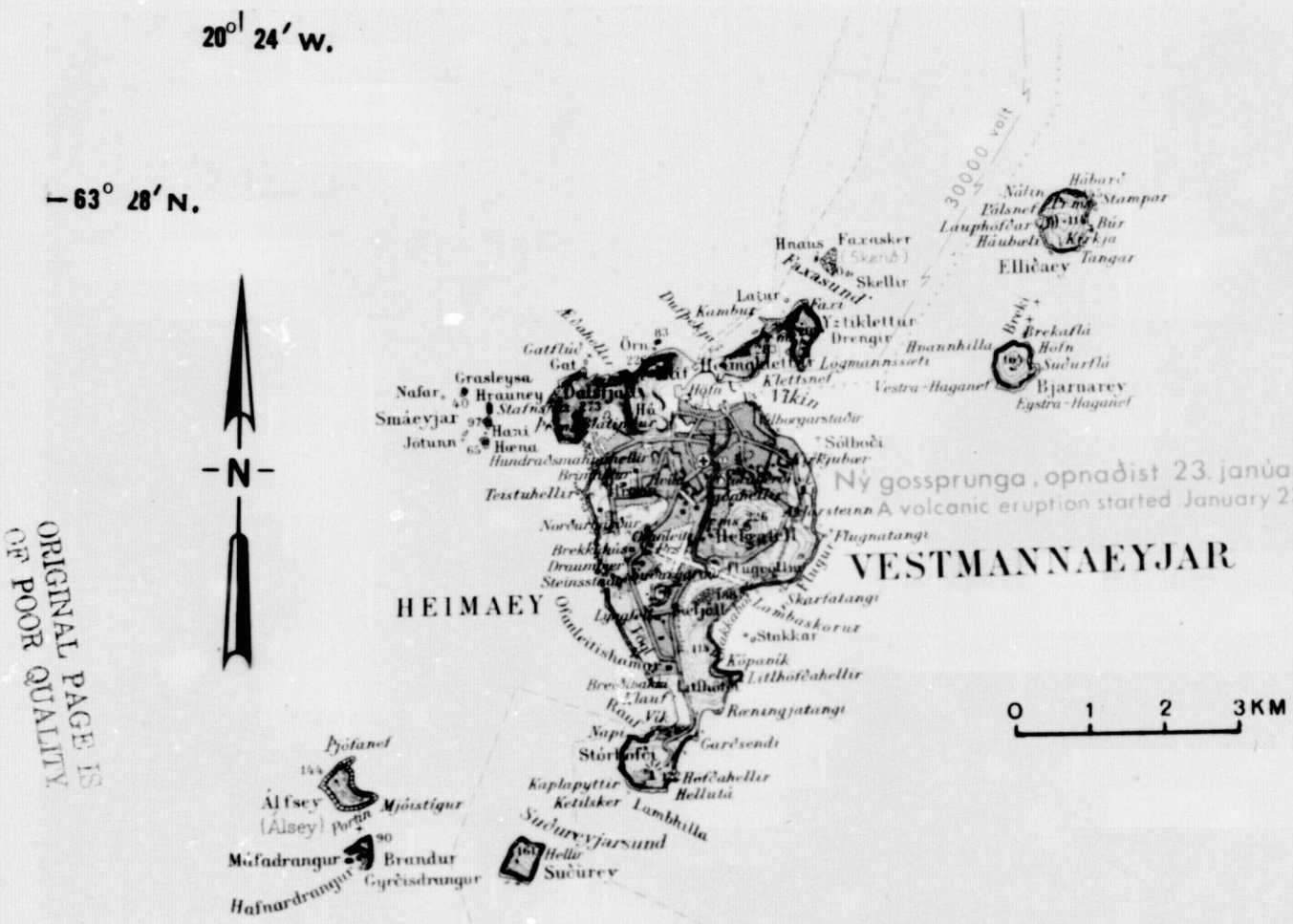

Figure 15. Recently revised (23 January 1973) topographic map of Heimaey, Vestmann Islands, Iceland (Uppdráttur Íslands, Blað 49, Vestmannaeyjar, Landmælingar Íslands, 1:100,000 scale, 1966). The outline of the island predates the volcanic eruption; however, the location of the eruptive fissure has been overprinted in red (on original map).

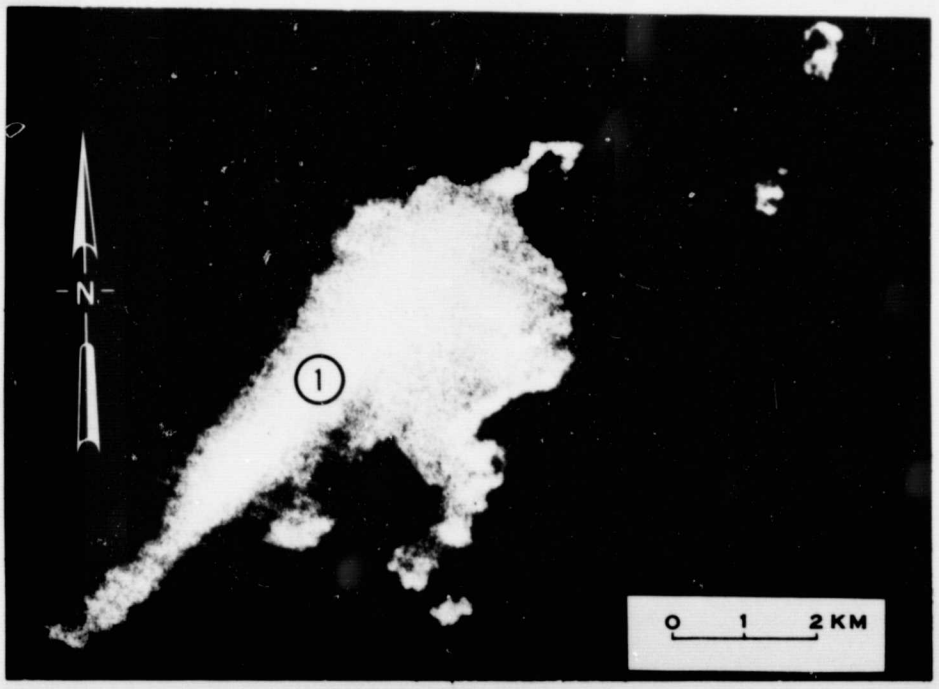

Figure 16. Positive enlargement (40X) of 3d generation, NDPF, 70 mm negative (original scale of 1:3,369,000) of ERTS image of Heimaey, Vestmann Islands, Iceland (Þórisvatn, D6, 21 Nov. 72, 1121-12143-6). Original enlargement scale was 1:84,225. Island is partially obscured by long, lenticular cloud (1) on its western side.

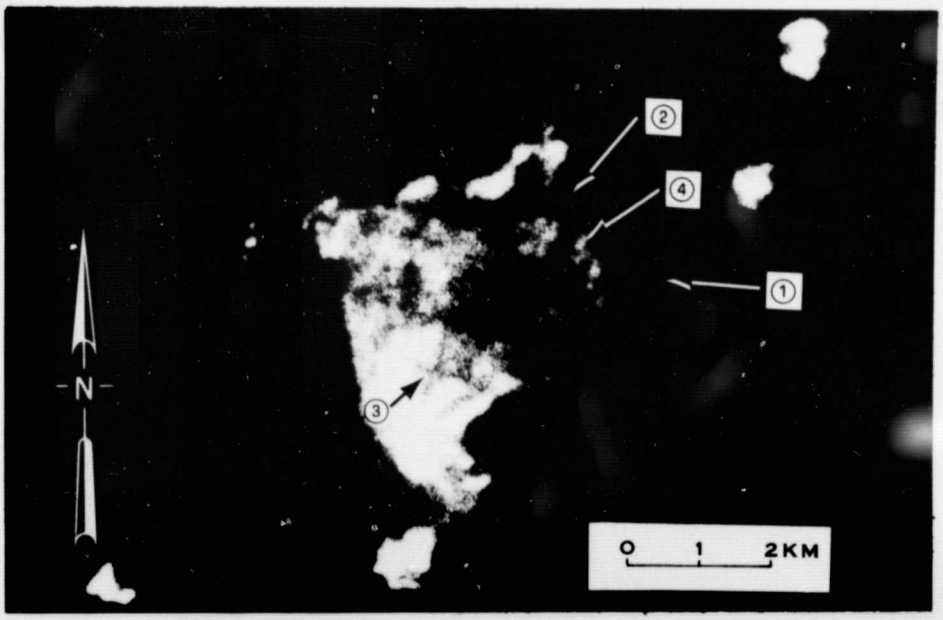

Figure 17. Positive enlargement (40X) of 3d generation, NDPF, 70 mm negative (original scale of 1:3,369,000) of ERTS image of Heimaey, Vestmann Islands, Iceland (Hekla, D5, 19 Aug. 73, 1392-12191-6). Original enlargement scale was 1:84,225. Note the new land area (1) resulting from lava flows to the east and northeast, near closure of the harbor entrance by new flows at (2), and change in reflectivity of the island at near-infrared wavelengths (0.7-0.8μm), the result of burial of vegetation by tephra, and the plus-shaped, gravel and crushed tephra landing strip at (3). Areas of sublimate deposition and clouds of steam, which are still rising through fractures in the lava flows, even though the surface eruption had ceased 7 weeks earlier, can be seen at (4).

Figure 18. NOAA-2 image mosaic, (Iceland, 22 May 73, NOAA-2 VHRR, VIS/VREC #11 and #12, Rev. 2741) of Iceland and surroundings. Vatnajökull (1), Hofsjökull (2), Langjökull (3), and Mýrdalsjökull (4) can be delineated. Note snow cover in the highland areas. Grímsvötn can be discerned in west-central Vatnajökull. Drift ice (5) can be seen in the Denmark Strait between Iceland and Greenland (6). The island of Jan Mayen can be seen at the top of the image (7). Image courtesy of E. Paul McClain and Donald R. Wiesnet, NOAA, National Environmental Satellite Service, Suitland, Maryland.

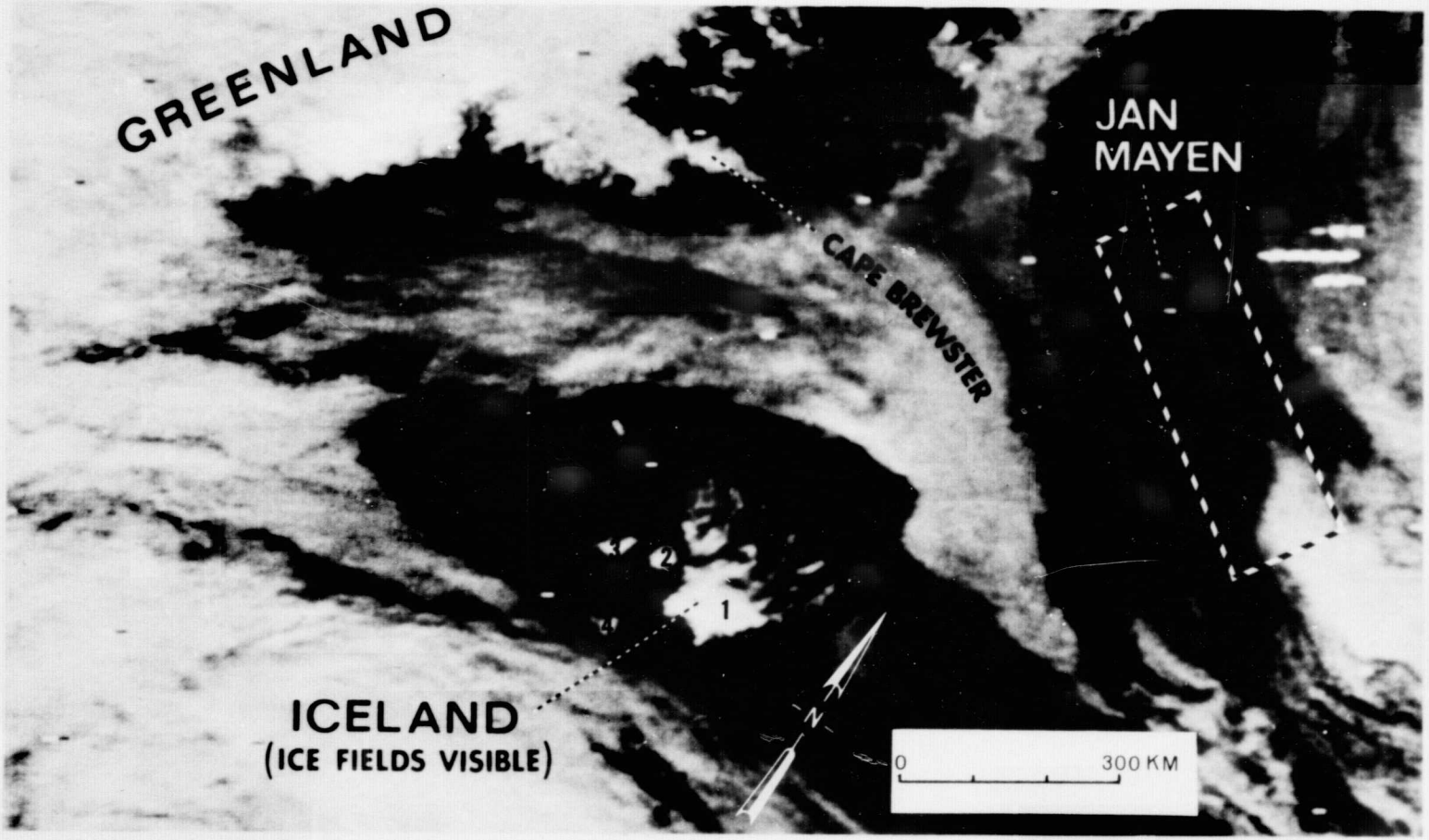

Figure 19. Nimbus IV image (Iceland, 21 Sep. 70, Nimbus IV, IDCS, 1200 UT) of Iceland and surroundings. Vatnajökull (1), Hofsjökull (2), Langjökull (3), and Mýrdalsjökull (4) can be delineated in a gross way. Note also the eruption plume from Beerenberg Volcano on the island of Jan Mayen. Image courtesy of NASA, Goddard Space Flight Center, Greenbelt, Md. From figure in Anon., 1971, p. 85).

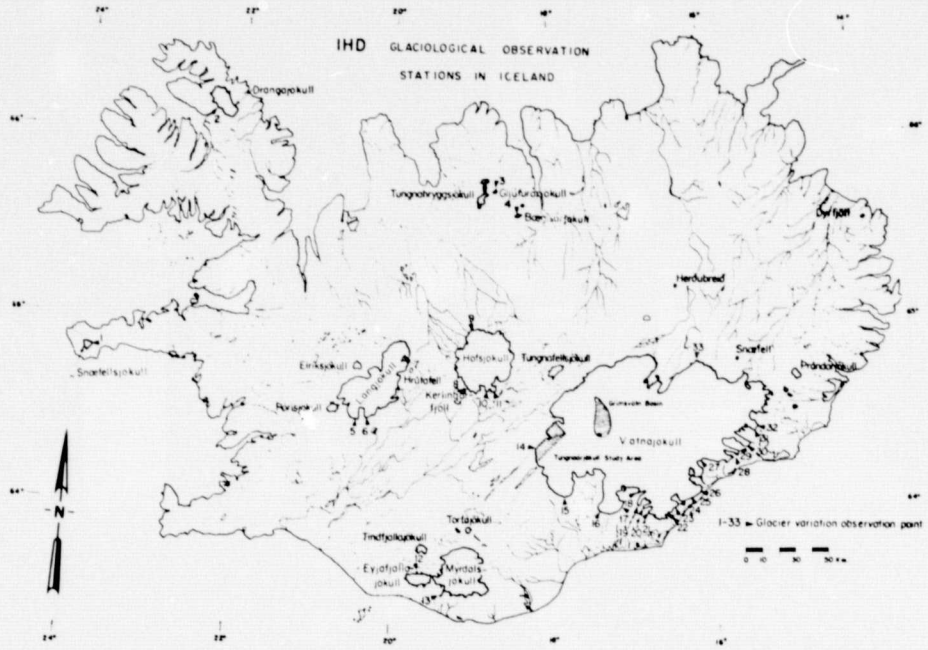

Figure 20. Icelandic Glaciers and International Hydrological Decade Glaciological Observation Stations. (From Rist, 1967b, p. 324).

Vatnajökull	(8400 km^2)	Snæfellsjökull
Langjökull	(1020 km^2)	Eiríksjökull
Hofsjökull	(996 km^2)	Þrándarjökull
Mýrdalsjökull	(700 km^2)	Tindfjallajökull
Drangajökull	(200 km^2)	Tungnahryggsjökull
Eyjafjallajökull	(107 km^2)	Torfajökull
Tungnafellsjökull	(50 km^2)	Gljúfurárjökull
Þórisjökull		Bægisárjökull

Table 2. Selected Icelandic Glaciers
(Areas from Bárðarson, 1971)

Figure 21. Midsummer, ERTS-1 image of the VatnajÖkull icecap (VatnajÖkull, D7, 30 July 73, 1372-12080-4). The high sun angle (42°) and high reflectivity of the snow-covered glacier limit the amount of surface detail as compared with the low sun angle, wintertime image (Figure 12). Older snowpack can be seen at (1), where it has drifted. Sediment plumes can be distinguished in the northwest arm of Þórisvatn (2) and all along the coast. A number of glacier-margin lakes are visible; note the maximum area encompassed by Grænalón (3), prior to the August 1973 jökulhlaup across Skeiðarársandur, the large glacial outwash plain to the south. A number of braided glacial rivers cross this outwash plain. Undistorted moraines (4) can be seen on Breiðamerkurjökull; contorted moraines (5) are visible on Skeiðarárjökull. The retreat of the snowline can be seen on most of the glaciers, including Mýrdalsjökull (6) and Eyjafjallajökull (7).

Figure 22. Early fall ERTS-1, cloud-free image mosaic of Vatnajökull (Vatnajökull, D7, 22 Sept. 73, 1426-12070-4; Vík, E7, 22 Sept. 73, 1426-12073-4). As the sun angle drops (25°), surface detail begins to again appear on Vatnajökull, although not as pronounced as on the wintertime image (Figure 12). Note the reduction in sediment plumes along the coast and the decreased discharge of glacial rivers across Skeiðarársandur. The entire western arm of lake Þórisvatn has suspended sediment (1). Note the retreat of the snowline on Vatnajökull and Mýrdalsjökull when compared with Figure 21. Note the reduction in area of Grænalón (2) after the August 1973 jökulhlaup, as compared with Figure 21.

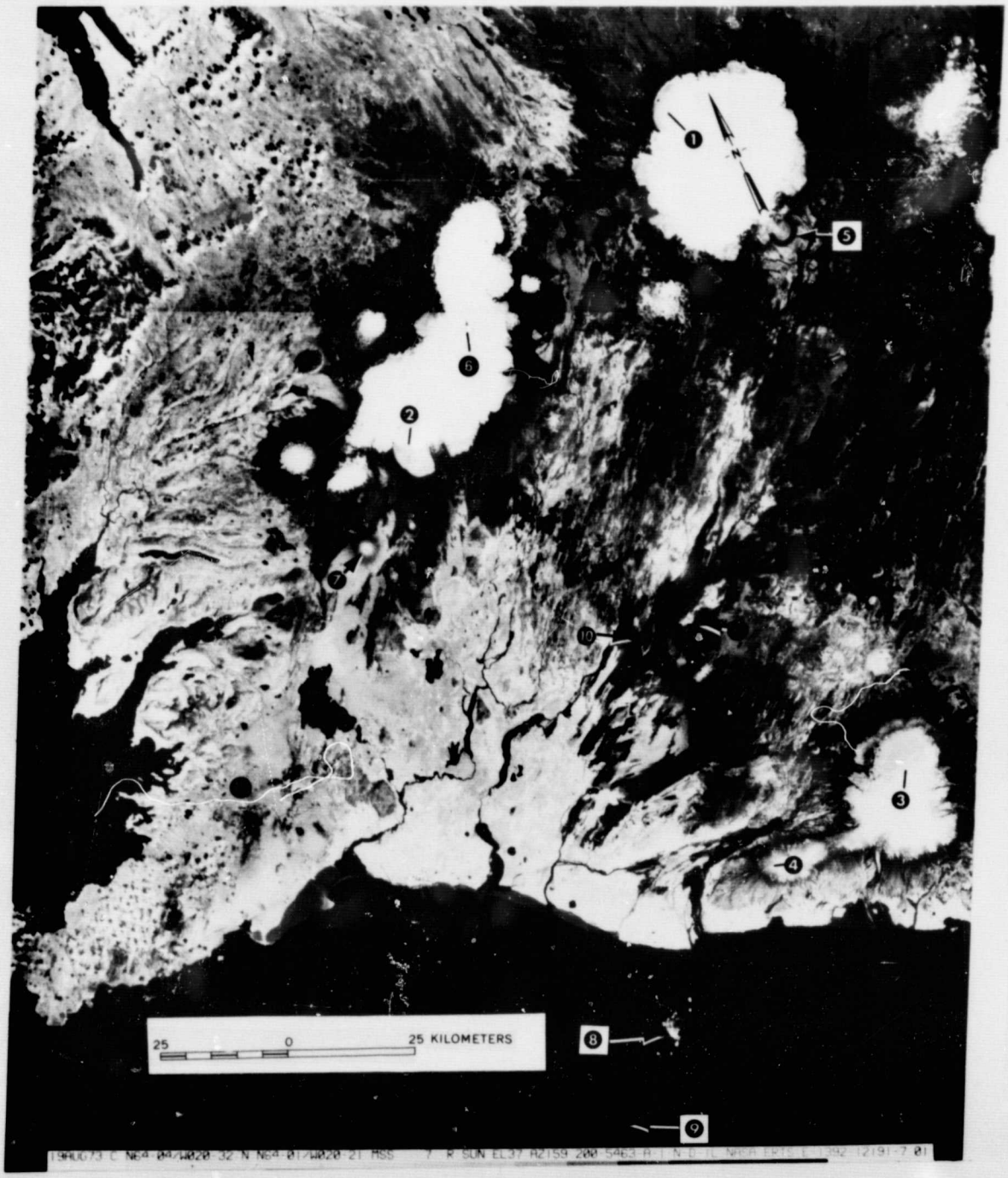

Figure 23. ERTS image mosaic (Akureyri, C5, 19 Aug. 73, 1392-12185-7; Hekla, D5, 19 Aug. 73, 1392-12191-7) of west-central and southwestern Iceland. The snowline can be delineated on the Hofsjökull (1), Langjökull (2), Mýrdalsjökull (3), and Eyjafjallajökull (4) icecaps. Note area of no vegetation (5), from where one of the outlet glaciers of Hofsjökull has receded. A prominent nunatak can be seen in the center of Langjökull (6) with a caldera- or cirque-like feature to the west within the icecap. The snow-capped, shield volcano, Skjaldbreiður, can be seen at (7), with tectonic fissures (gjár) extending southwest, south of Skjaldbreiður. The highly reflective vegetation can be delineated most accurately on false-color composites, including the new vegetation pattern on Heimaey (8). Surtsey (9) is also visible, southwest of Heimaey. The tephra fallout pattern (10) and new lava flows (11) from the 1970 volcanic activity on Hekla can be seen. (See also Figure 8). Lichen-covered basalts are visible at (12).

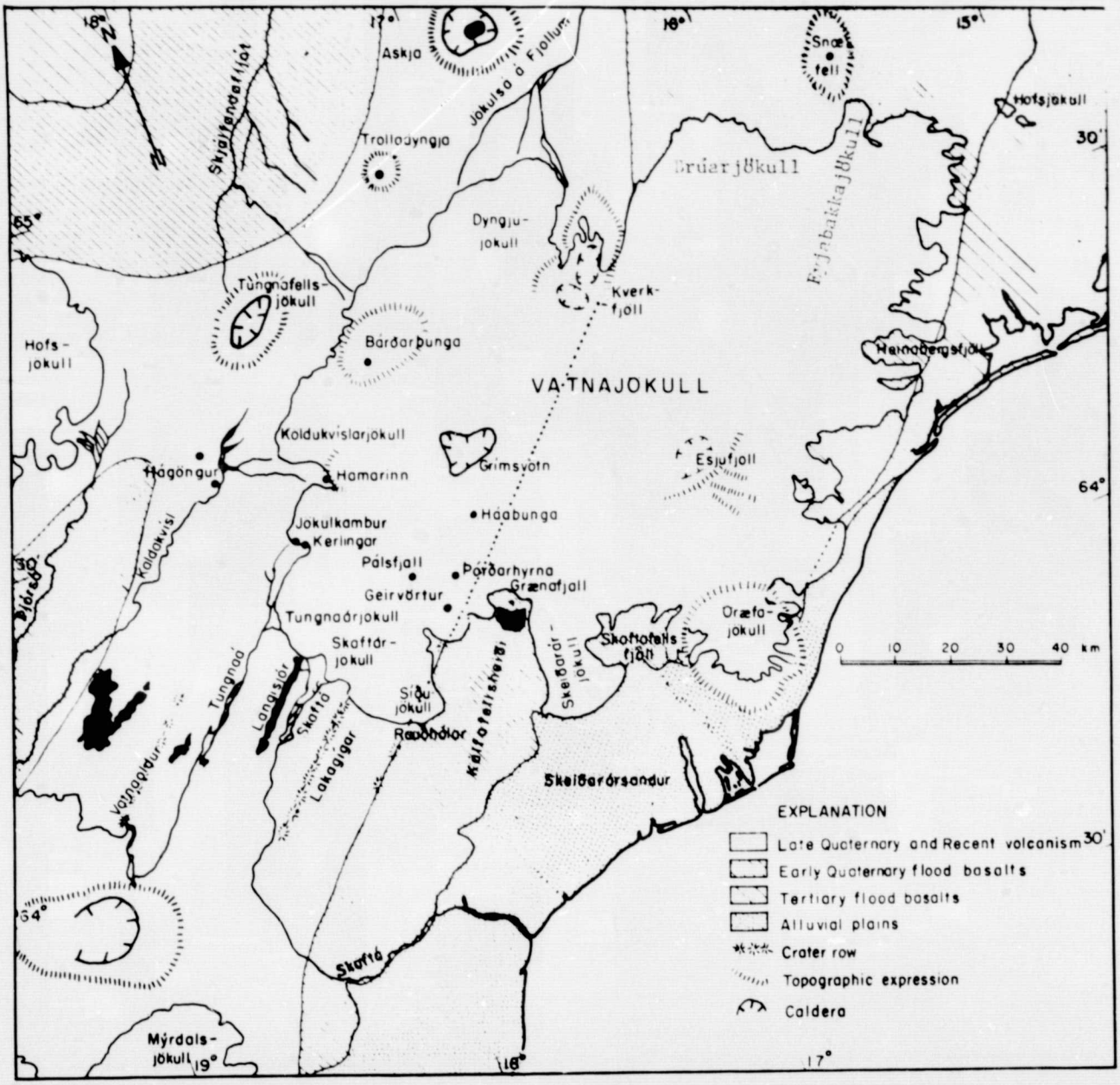

Figure 24. Geologic sketch map for Vatnajökull and surrounding area, Iceland. I covers most of the area shown on Figures 12, 21 and 22. [From Thorarinsson and others, (in press)].

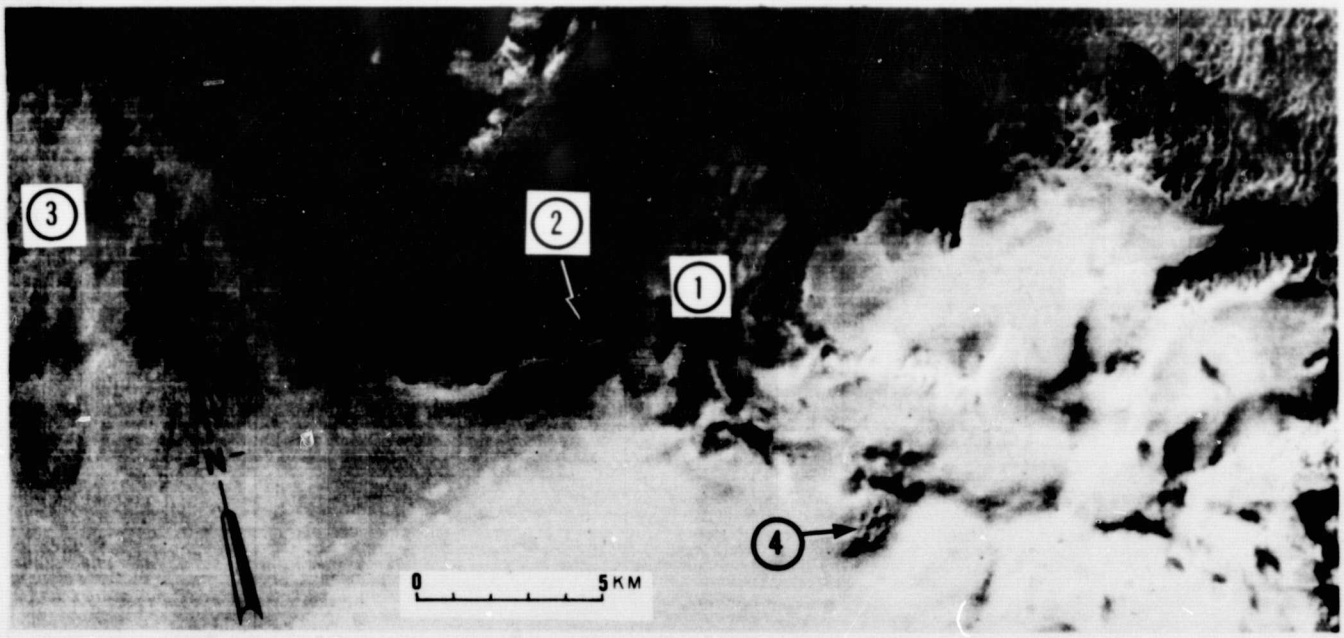

Figure 25. Positive enlargement (20X) of 3d generation, NDPF, 70 mm negative (original scale of 1:3,369,000) of ERTS image of Eyjabakkajökull, Iceland [Ingólfshöfði, D8, 14 Oct. 72, (1083-12023-5; partial, uncatalogued image)]. Original enlargement was 1:168,450. Eyjabakkajökull (1), an outlet glacier on the northeast part of Vatnajökull, was in the process of surging when it was imaged. A glacier-margin lake is visible at (2). Part of another surging glacier, Brúarjökull is visible to the left (3). Possible crevasse patterns resulting from the surge are visible at (4).

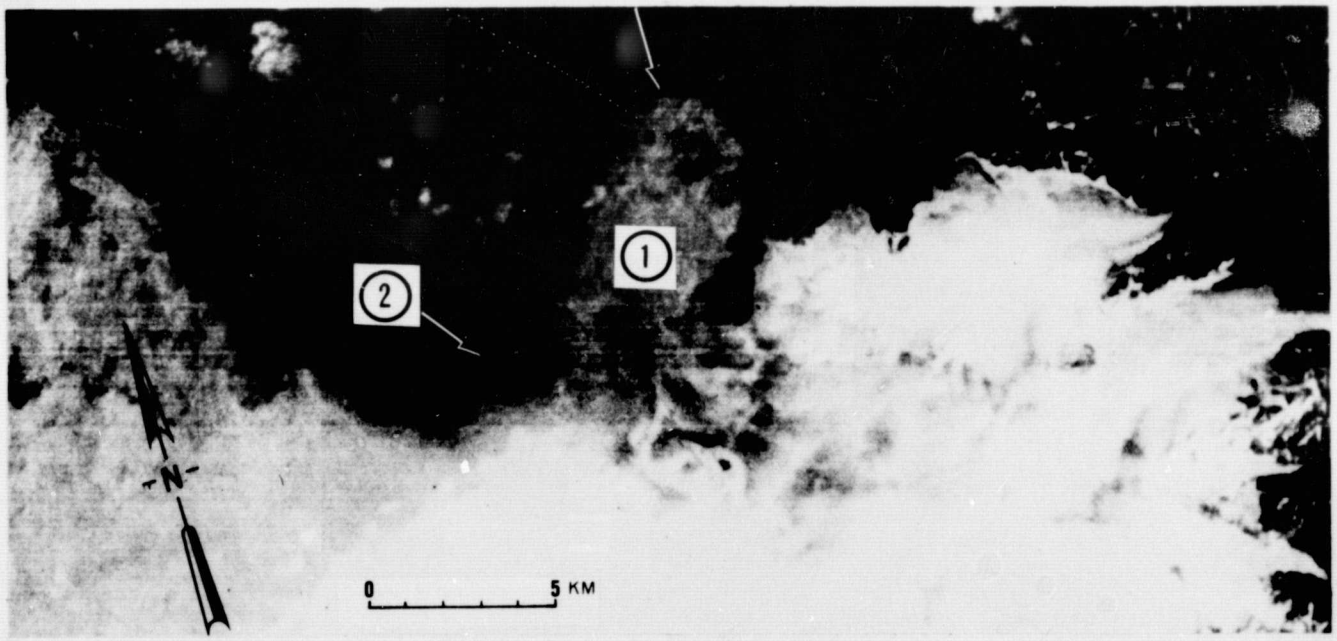

Figure 26. Positive enlargement (20X) of 3d generation, NDPF, 70 mm negative (original scale of 1:3,369,000) of ERTS image of Eyjabakkajökull, Iceland (Vatnajökull, D7, 22 Sep 73, 1426-12070-5). Original enlargement was 1:168,450. Eyjabakkajökull (1) had apparently completed its surge. Between 14 Oct. 72 and 22 Sept. 73, Eyjabakkajökull had surged approximately 1.8 km. Note the increase in surface area of the glacier-margin lake (2).

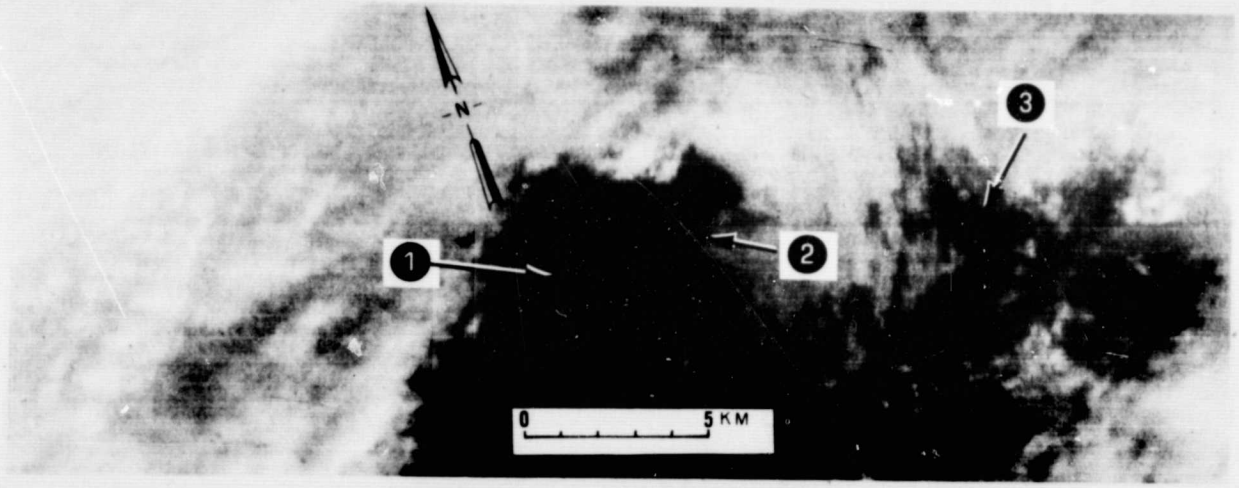

Figure 27. Positive enlargement (20X) of 3d generation, NDPF, 70 mm negative (original scale of 1:3,369,000) of ERTS image of Grænalón, Iceland [Ingólfshöfði, D8, 14 Oct. 72, (1083-12023-5; partial, uncatalogued image)]. Original enlargement of 1:168,450. First image of the ice-dammed lake Grænalón (1) taken by ERTS-1. Ice dam is visible at (2). A distinctive pattern of distorted medial moraines is visible at (3), although somewhat obscured by clouds.

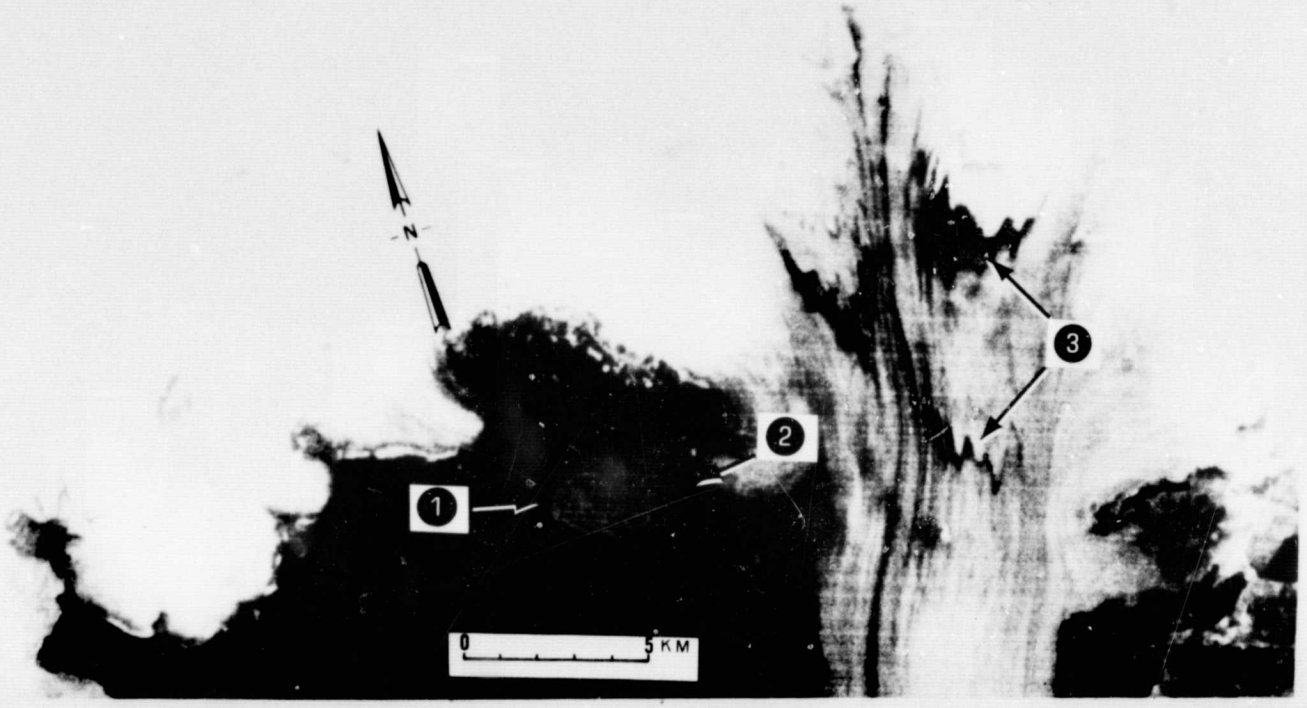

Figure 28. Positive enlargement (20X) of 3d generation, NDPF, 70 mm negative (original scale of 1:3,369,000) of ERTS image of Grænalón, Iceland (Vatnajökull, D7, 22 Sept. 73, 1426-12070-5). Original enlargement of 1:168,450. Image of the ice-dammed lake Grænalón (1) after the August 1973 jökulhlaup. Ice dam is visible at (2). Note the distinctive patterns of distorted medial moraines at (3). The interval between the two may represent the time between two successive jökulhlaups. If the motion of Skeiðarárjökull, as measured on Figures 27 and 28, is 600 m and this represents an average annual rate of motion, then the interval represents about 6 or 7 years. The increase in area of lake Grænalón can be monitored on Figure 27 (14 Oct. 72), Figure 12 (31 Jan. 73), and Figure 21 (30 Jul. 73). The latter shows the largest area prior to the jökulhlaup. Note that the area of Grænalón after the jökulhlaup (Figure 28) is still slightly larger than the area shown on Figure 27.

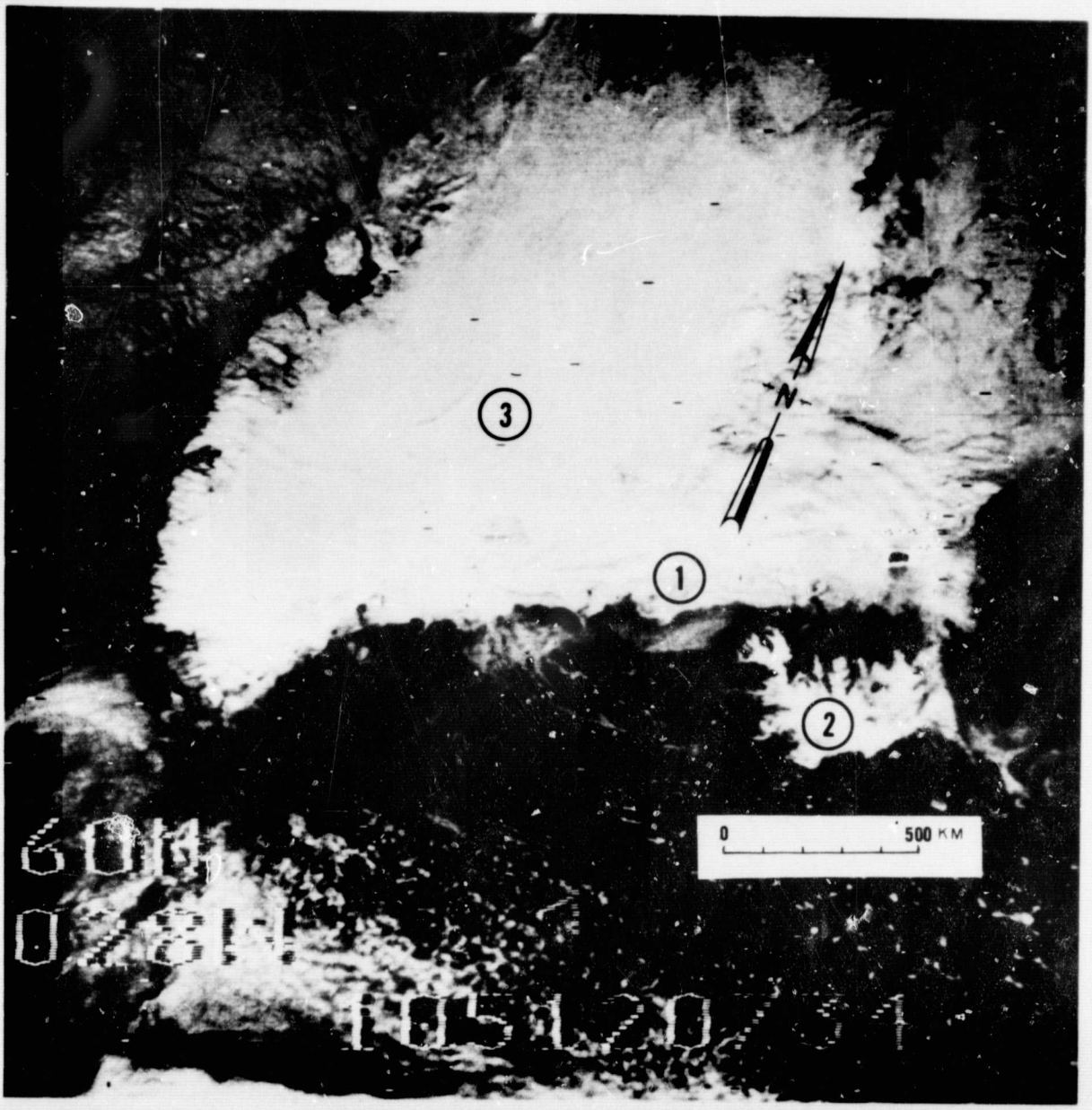

Figure 29. Nimbus III image of sea ice (1) in the Denmark Strait between Iceland (2) and Greenland (3). (Iceland, 15 Apr. 69, Nimbus III, IDCS, Orbit 16). Compare with Figure 18, a NOAA-2 image of sea ice in the Denmark Strait. Image courtesy of NASA, Goddard Space Flight Center, Greenbelt, Md. From figure in Anon., 1971, p. 63.

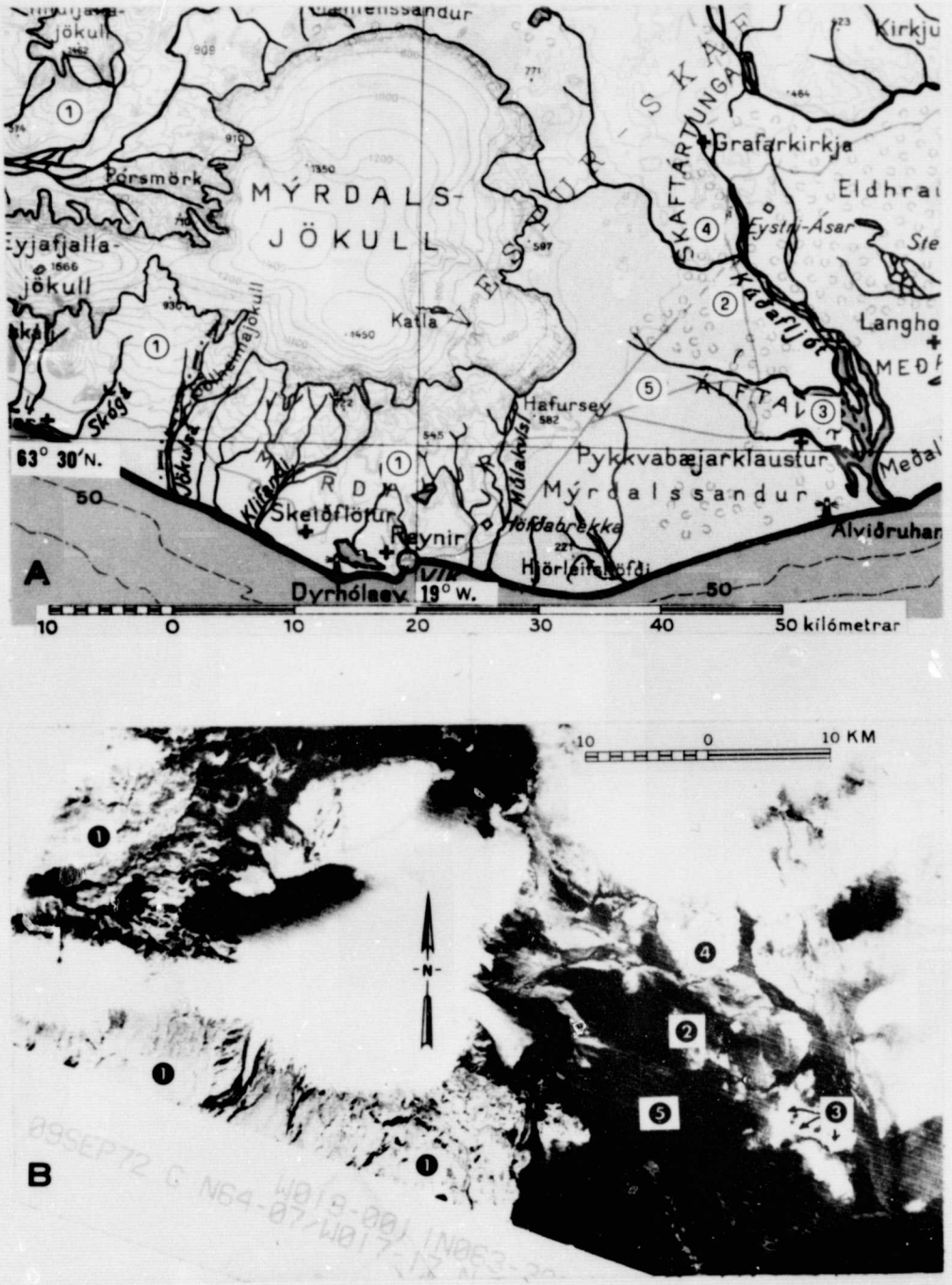

Figure 30. Comparison of 1:500,000-scale map (A) of Iceland (Ísland, Geodætisk Institut, Copenhagen, Denmark, 1945) with an ERTS-1 image (B) of the same area (Vatnajökull, D7, 9 Sept. 72, 1048-12080-7). Note the different outline of Mýrdalsjökull and some of its outlet glaciers. Four of the five different vegetation classes discernible on ERTS imagery of Iceland (not including barren lands -5) can be mapped on the false-color, MSS composite of this scene: natural grassland, 1; reclaimed land, 2; cultivated land, 3; and dwarf forests, 4; by their different hues of red and purple. Not shown on this image but visible on Figure 23, is an example of the vegetation class, lichen-covered basalts, which have a distinctive purplish hue on flase-color, MSS composites of Iceland.

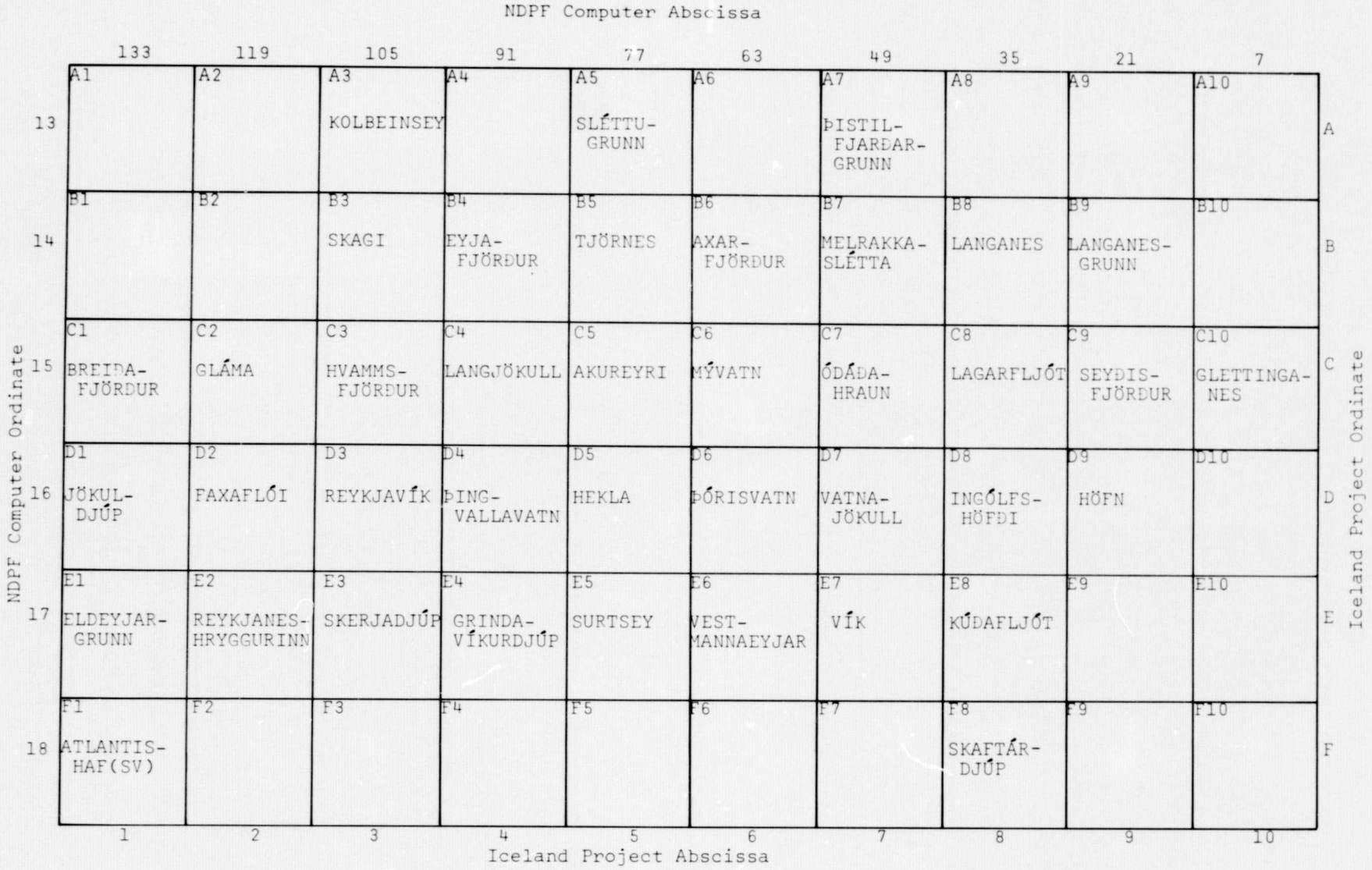

Figure 31. Geographic names and data acquisition matrix for ERTS-1 imagery of Iceland.

TABLE 3. SUMMARY OF STUDIES IN ICELAND WITH ERTS-1 IMAGERY

Discipline	Experiments	Research Objectives	Research Results
GEOLOGY	Geothermal	Delineation of geothermal areas by extent of snow-melt pattern	Delineation of part of geothermal area by snowmelt pattern. Delineation of geothermally altered ground in 3 geothermal areas.
GEOLOGY	Volcanic Eruptive	Delineation of areas of new basalt flows and tephra falls	Delineation of new basalt flows in 3 areas and tephra fallout pattern in 1 area. Image of effusive volcanic eruption.
GEOLOGY	Geologic Structure	Mapping, on a regional basis, of faults, fissures, lineaments, and other structural features in the neovolcanic zone	Mapping of many new structural geologic and volcanic features, particularly within icecaps, and on snow-covered terrain at low sun angle (<10°).
GEOLOGY	Volcanic Geomorphology	Mapping of the regional aspect of volcanic landforms	Regional distribution of different volcanic landforms mappable, particularly unique landforms.
GEOLOGY	Marine Geology and	Mapping of any changes in the coastline of Iceland and any submarine features visible	Planimetric revisions of maps (to 1:100,000 scale) of Surtsey (erosion) and Heimaey (volcanic eruption) feasible. Mapping of seasonal change of sediment plumes from glacial rivers.
HYDROLOGY	Ephemeral Snow and Ice	Mapping of changes in snow cover over time; mapping of surface water distribution, and mapping of ice freeze-ups and thaws on major lakes	Mapping of surface water distribution can be achieved. Some mapping (lack of seasonal imagery) of changes in snow cover and thaw of lake ice.
HYDROLOGY	Glaciological Features	Delineation of areas covered by glaciers; mapping of changes in ice-margin lakes; mapping of nunataks; and mapping of depositional glacial features	Delineation of 90% of the area covered by icecaps; mapping of changes in glacier-margin lakes; mapping of some nunataks and some depositional glacial features. Mapping of surging glacier (1.8km movement and flow of another glacier (600m/11 mos.).
HYDROLOGY	River Flooding	Mapping of spring runoff, floods along river valleys, and changes in distributaries from glaciers	Mapping of changes in distributaries from glaciers. Mapping of changes in lake and outwash plain caused by a jökulhlaup.

TABLE 3 - CONTINUED

Discipline	Experiments	Research Objectives	Research Results
OCEANOGRAPHY	Sea Ice	Mapping of changes in ice floe concentrations with time off northern and eastern coasts	No usable imagery.
AGRICULTURE/ FORESTRY	Grasslands and Forest	Delineation of grasslands and particularly change in vigor with time	Mapping of 5 classes of vegetation: grasslands, cultivated areas, reclaimed land, forested areas, lichen-covered lava flows, and barren areas on false-color composites.
CARTOGRAPHY	-	-	Compilation of an orthoimage mosaic of Iceland at 1:1,000,000 (false-color composite) and planned 1:500,000- and 1:250,000-scale orthoimage mosaic maps. Study of landforms with stereoscopic images. Measurement of 100m elevation difference. Planimetric revisions on existing maps.

UNITED STATES
DEPARTMENT OF THE INTERIOR
GEOLOGICAL SURVEY

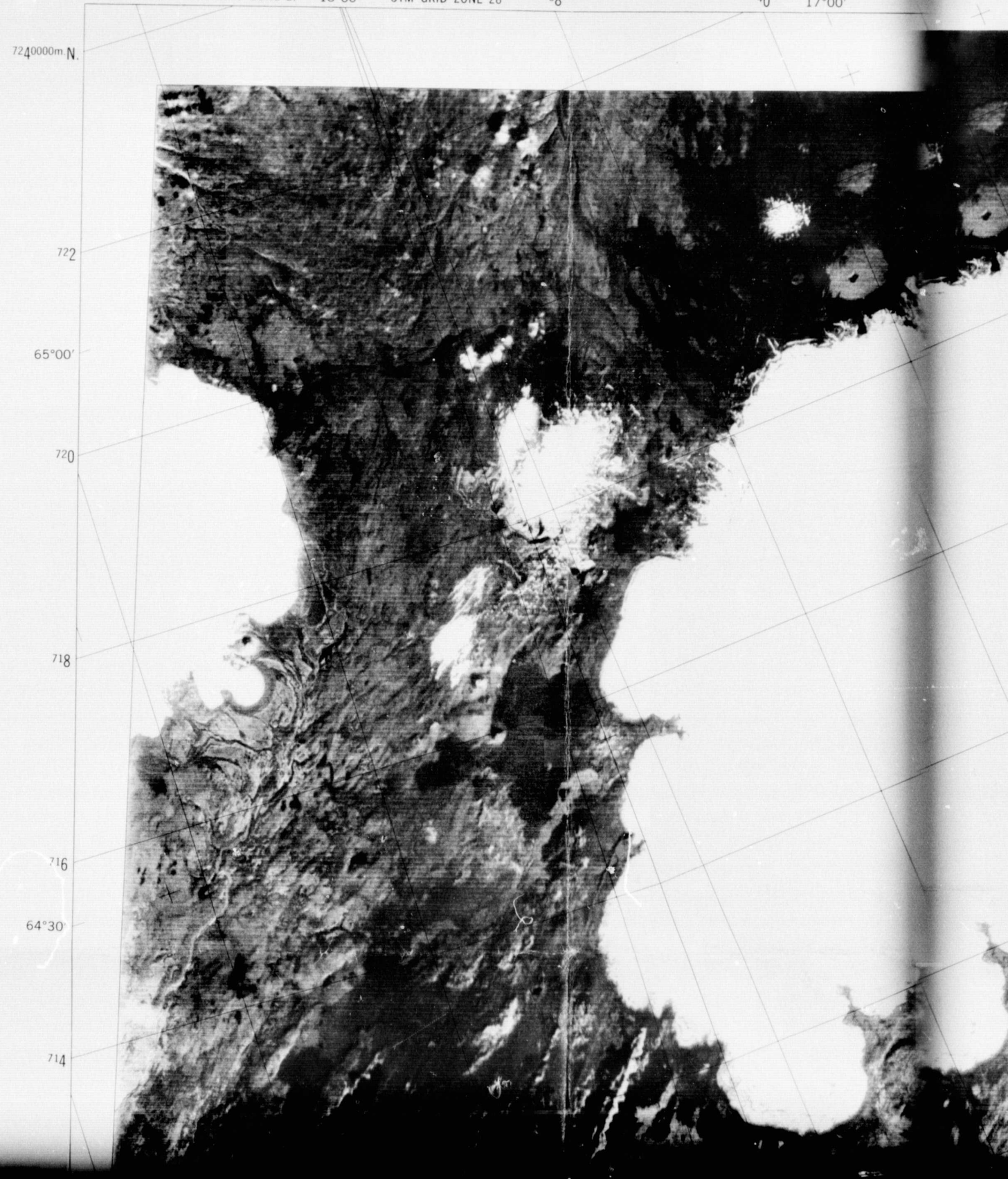

VATNAJÖKULL, ICELAND

FALL SCENE

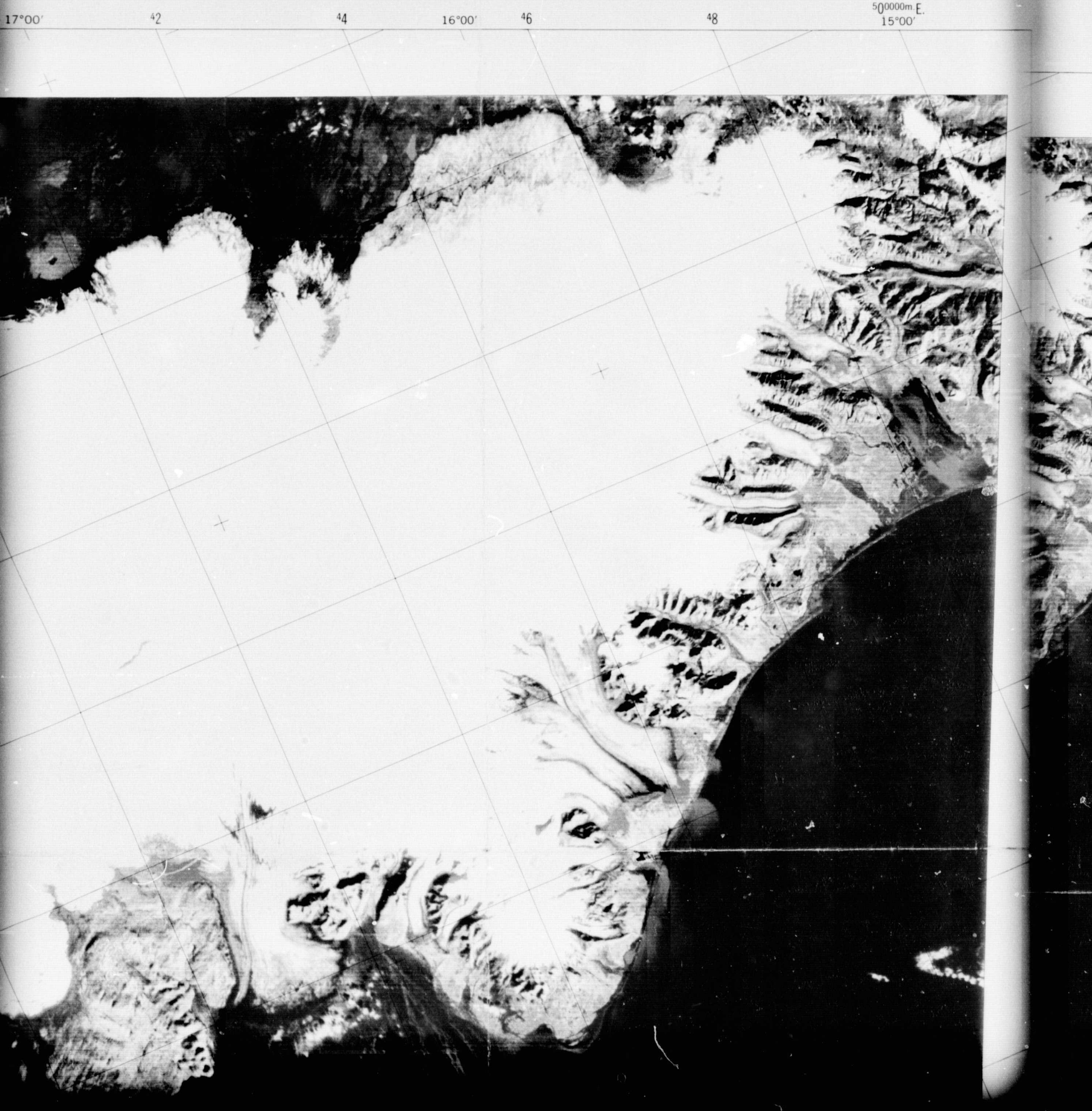

SATELLITE IMAGE MAP
NASA LANDSAT-1

1:500 000

N6359W01723

500000m E.
15°00′

716 0000m N.

64°30′

714

712

710

64°00′

708

706

LOCATION DIAGRAM

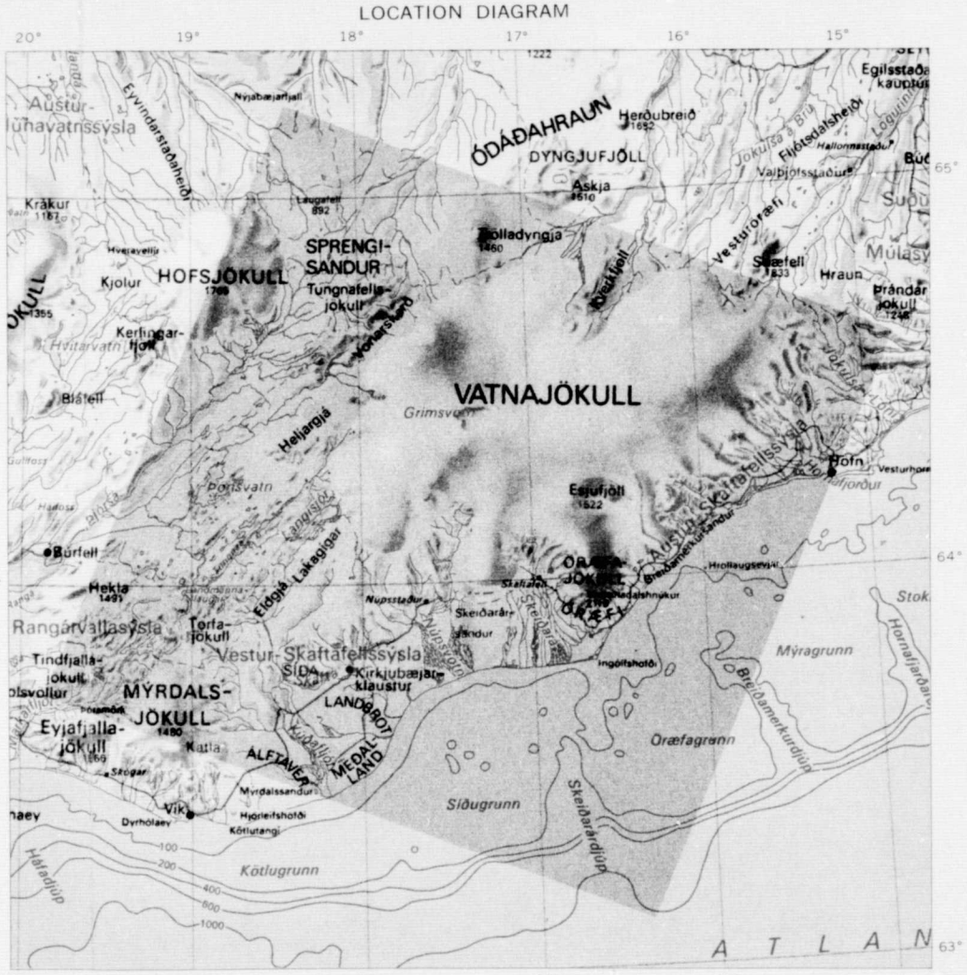

INDEX TO 1:250,000-SCALE
LANDMÆLINGAR ÍSLANDS TOPOGRAPHIC MAPS

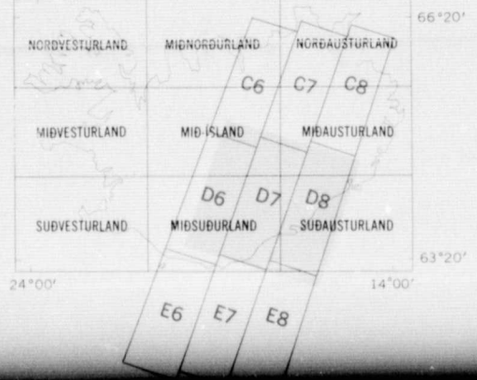

SATELLITE IMAGE INDEX

C6	Mývatn	N6520W01728
C7	Ódádahraun	N6520W01602
C8	Lagarfljót	N6520W01436
D6	Þórisvatn	N6359W01849
D7	Vatnajökull	N6359W01723
D8	Ingólfshöfði	N6359W01556
E6	Vestmannaeyjar	N6238W02002
E7	Vík	N6238W01837
E8	Kúðafljót	N6238W01710

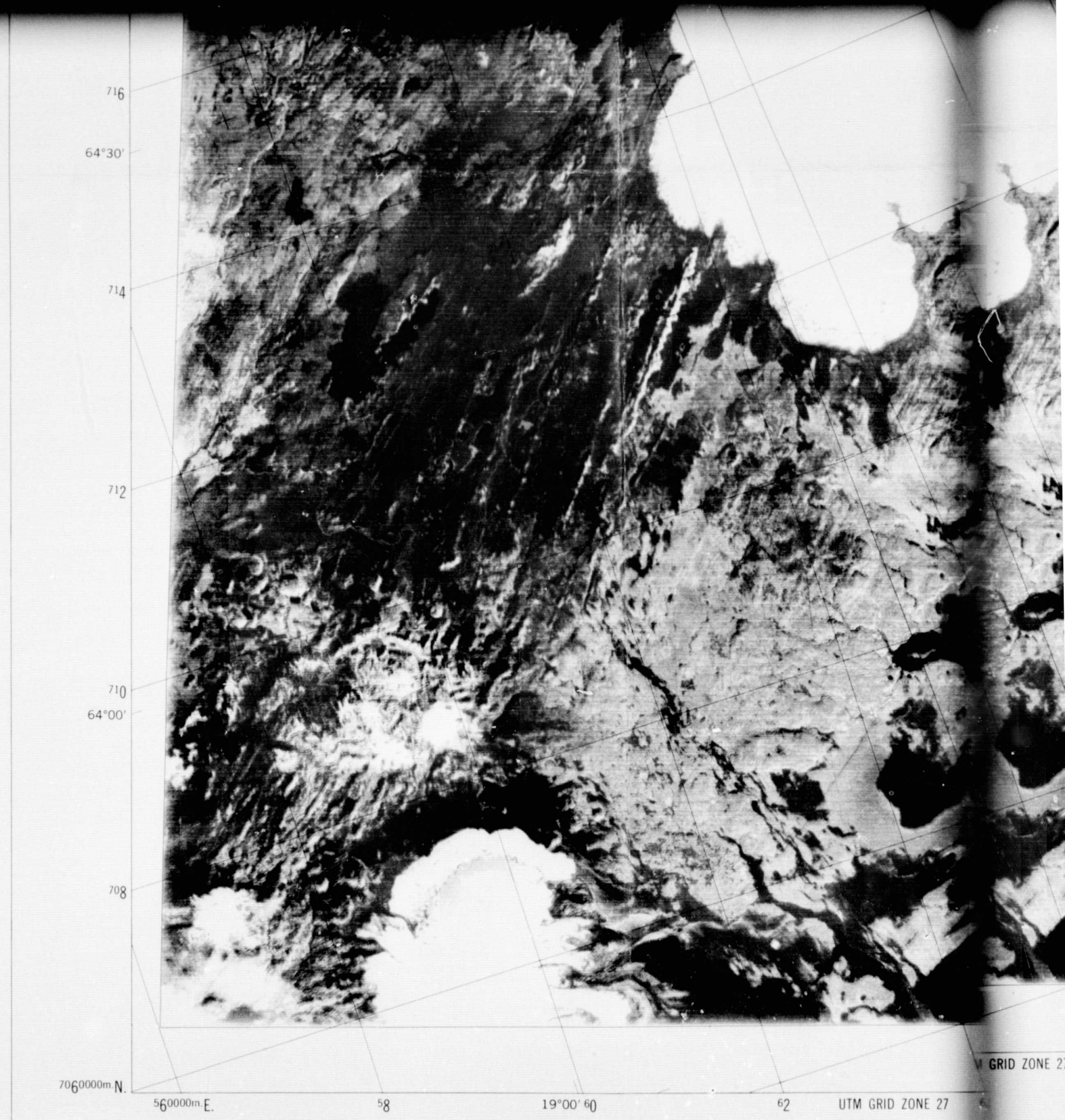

Prepared and published by the U. S. Geological Survey in cooperation with the Iceland Geodetic Survey (Landmælingar Íslands) and the Icelandic National Research Council (Rannsóknaráð Ríkisins)

Information on cost and availability of LANDSAT imagery may be obtained from U. S. Geological Survey, EROS Data Center, Sioux Falls, South Dakota 57198

FOLDOUT FRAME 4

GRID ZONE 27 64 18°00′ 36 UTM GRID ZONE 28 38 17°00′ 40 420000m E.

SCALE 1:500 000

20 10 0 KILOMETERS 20 40

20 000 10 000 0 METERS 20 000 40 000

20 10 0 STATUTE MILES 20

FOR SALE BY U. S. GEOLOGICAL SURVEY, RESTON, VIRGINIA 22092

FOLDOUT FRAME 5

INDEX TO 1:250,000-SCALE
LANDMÆLINGAR ÍSLANDS TOPOGRAPHIC MAPS

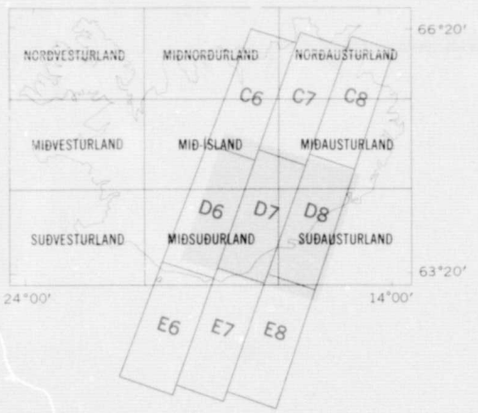

SATELLITE IMAGE INDEX

C6	Mývatn N6520W01728
C7	Ódáðahraun N6520W01602
C8	Lagarfljót N6520W01436
D6	Þórisvatn N6359W01849
D7	Vatnajökull N6359W01723
D8	Ingólfshöfði N6359W01556
E6	Vestmannaeyjar N6238W02002
E7	Vík N6238W01837
E8	Kúðafljót N6238W01710

Imagery recorded in discrete spectral bands with Multispectral Scanner (MSS) on NASA LANDSAT-1 (ERTS-1), orbit 5937, 12:07 p. m. I. l. t., September 22, 1973. NASA image E 1426-12070. Orbital altitude 920 km (570 mi). Area 33 000 km^2 (13 000 mi^2)

Generally in this false color imagery clouds, snow, and snow-covered glacial ice appear white, bare glacial ice is bluish, vegetation is shades of red, barren and urban areas are blue-gray, and clear and turbid water are dark blue and powder-blue, respectively

The water shades do not directly relate to depth. Repetitive imagery obtained by LANDSAT sensors will show different conditions of vegetation, hydrography, snow cover, and areas covered by glacial ice

Printed with yellow plate for band 4, magenta plate for band 5, and a cyan plate for band 7

20 000-meter Universal Transverse Mercator grid, zones 27 and 28

International Spheroid Horizontal Datum WGS 66

UTM GRID AND 1973 MAGNETIC NORTH
DECLINATION AT CENTER OF IMAGE

VATNAJÖKULL, ICELAND
FALL SCENE

N6359W01723

1973

INTERIOR—GEOLOGICAL SURVEY, RESTON, VIRGINIA—1976

EXPERIMENTAL PRINTING

UNITED STATES
DEPARTMENT OF THE INTERIOR
GEOLOGICAL SURVEY

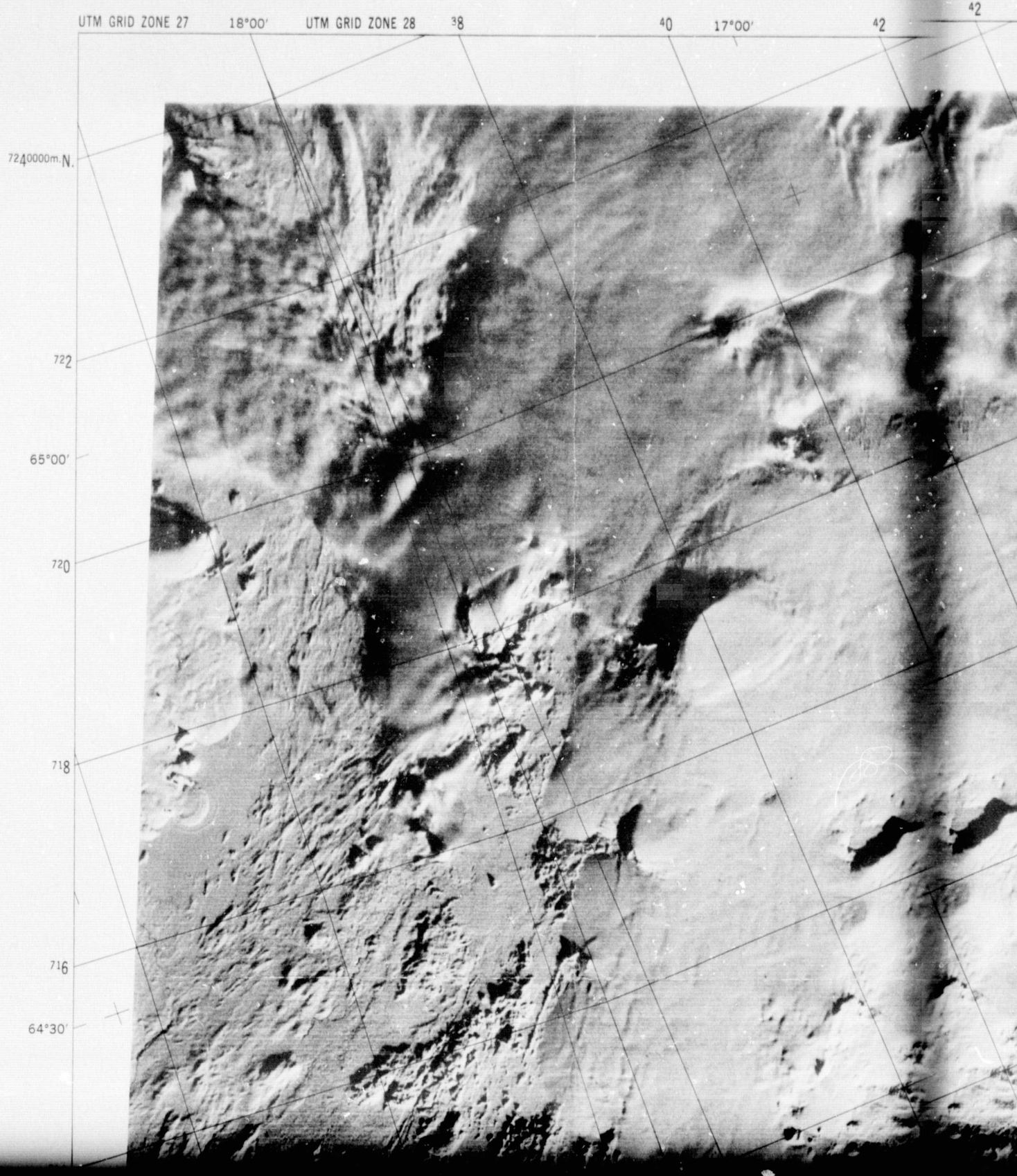

VATNAJÖKULL, ICELAND
WINTER SCENE

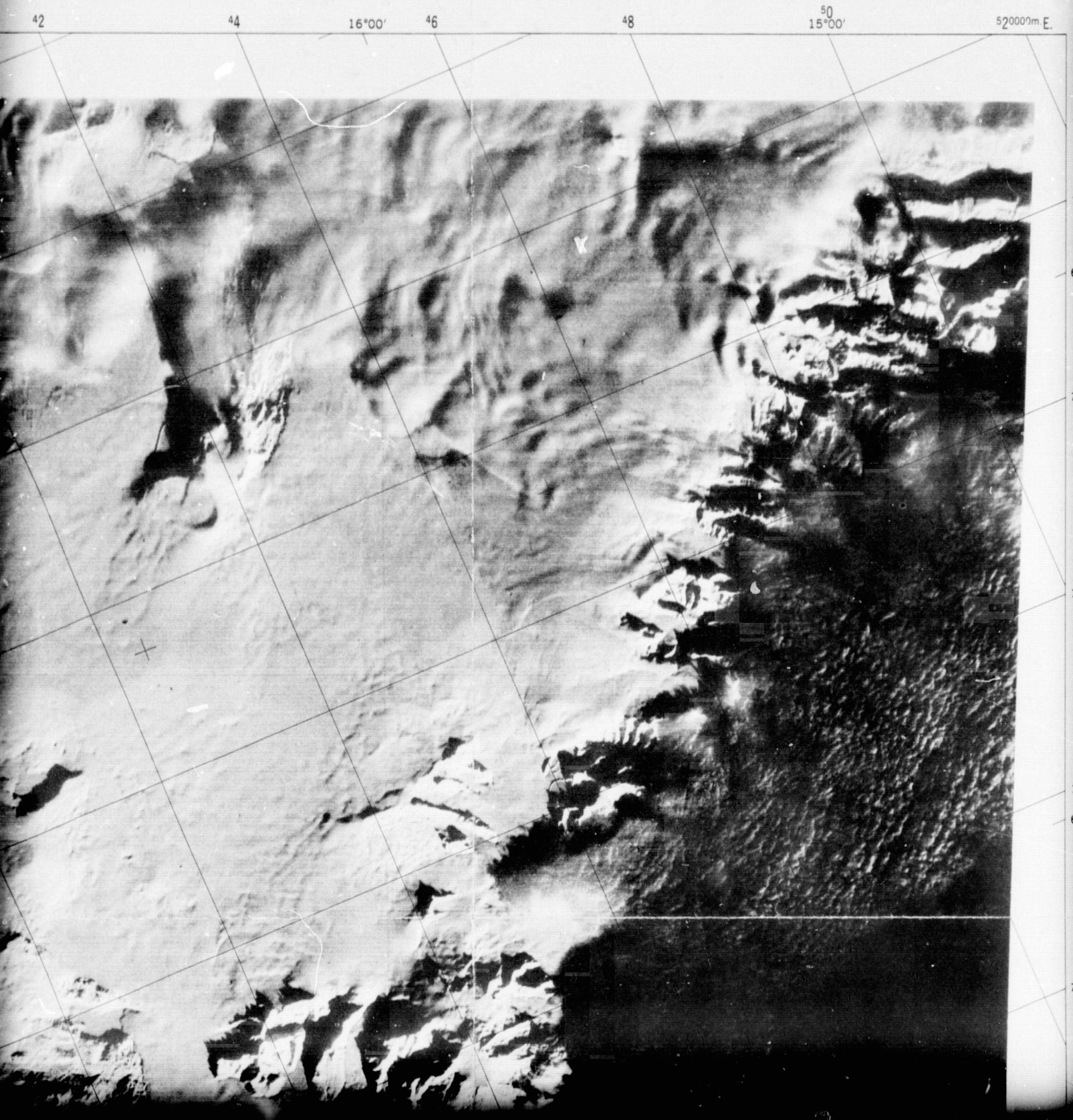

SATELLITE IMAGE MAP
NASA LANDSAT-1
1:500 000

N6359W01723

235–015

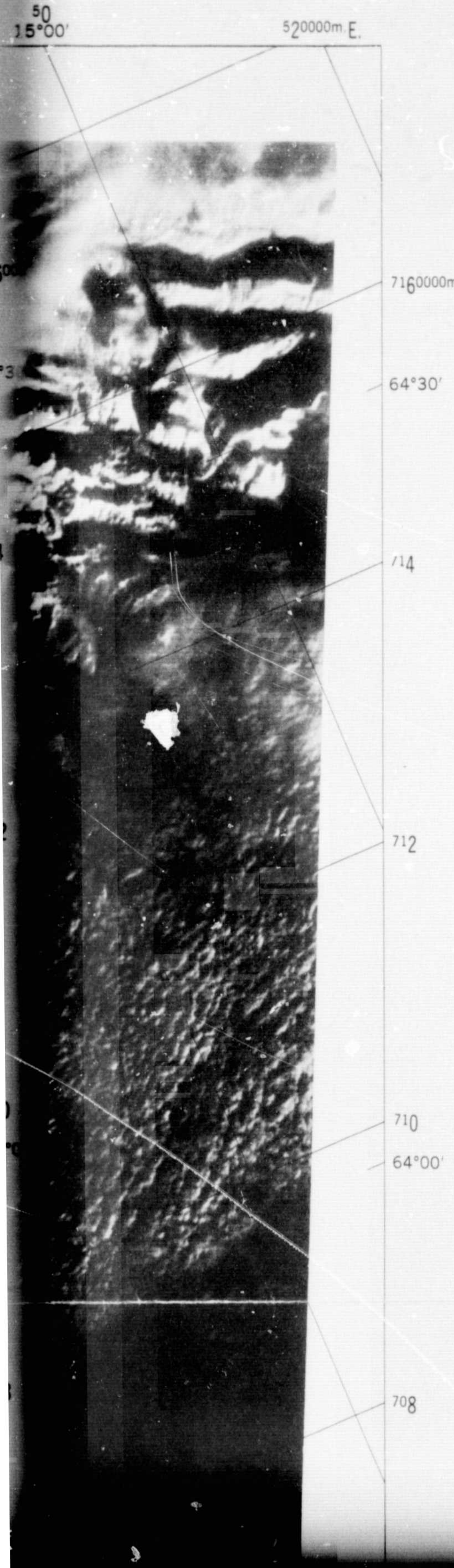

LOCATION DIAGRAM

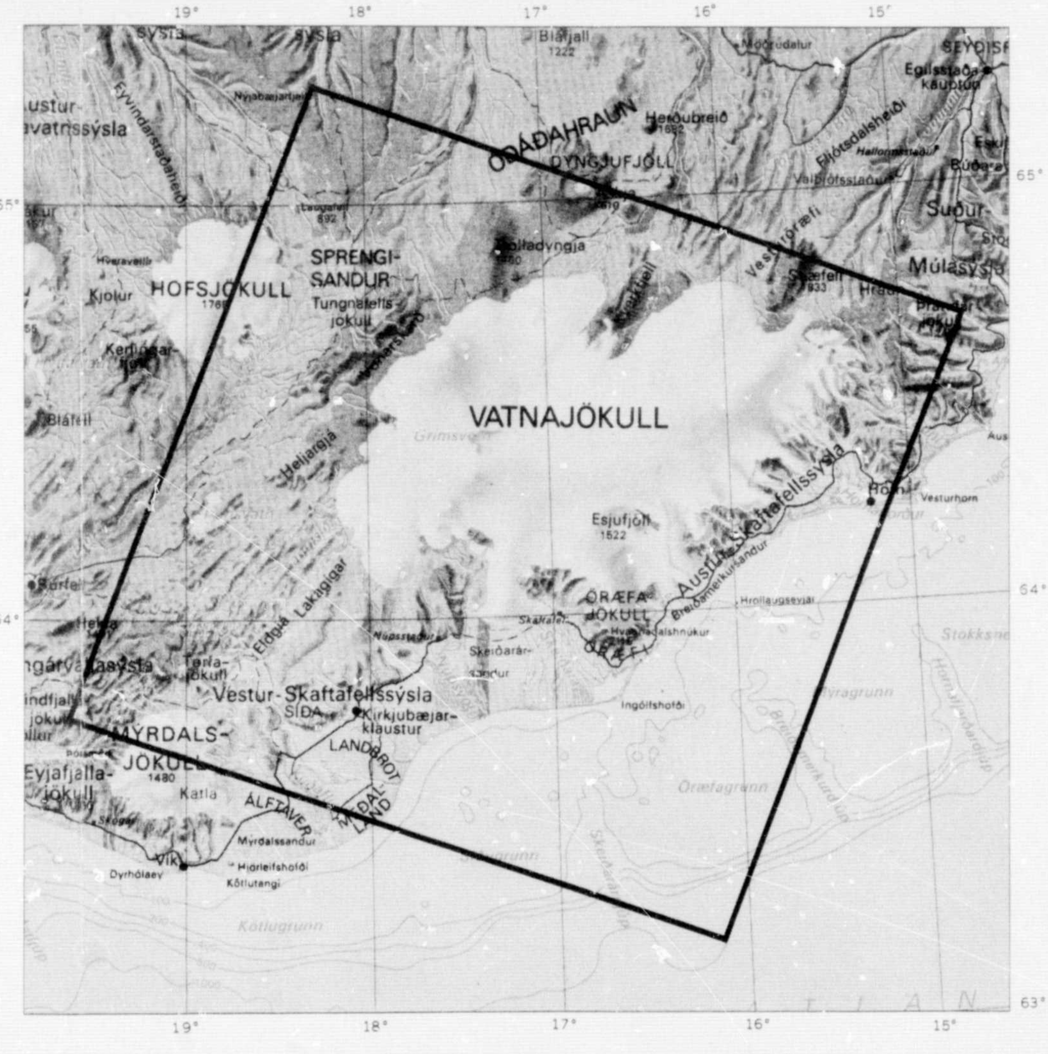

INDEX TO 1:250 000-SCALE
LANDMÆLINGAR ÍSLANDS TOPOGRAPHIC MAPS

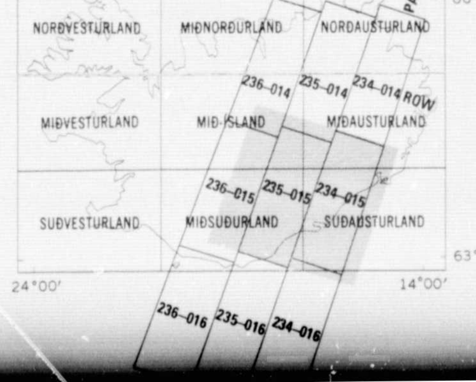

SATELLITE IMAGE INDEX

PATH–ROW	NOMINAL SCENE NAME AND CENTER
234–014	Lagarfljót N6520W01436
234–015	Ingólfshöfði N6359W01556
234–016	Kúðafljót N6238W01710
235–014	Ódáðahraun N6520W01602
235–015	Vatnajökull N6359W01723
235–016	Vík N6238W01837
236–014	Mývatn N6520W01728
236–015	Þórisvatn N6359W018[illegible]

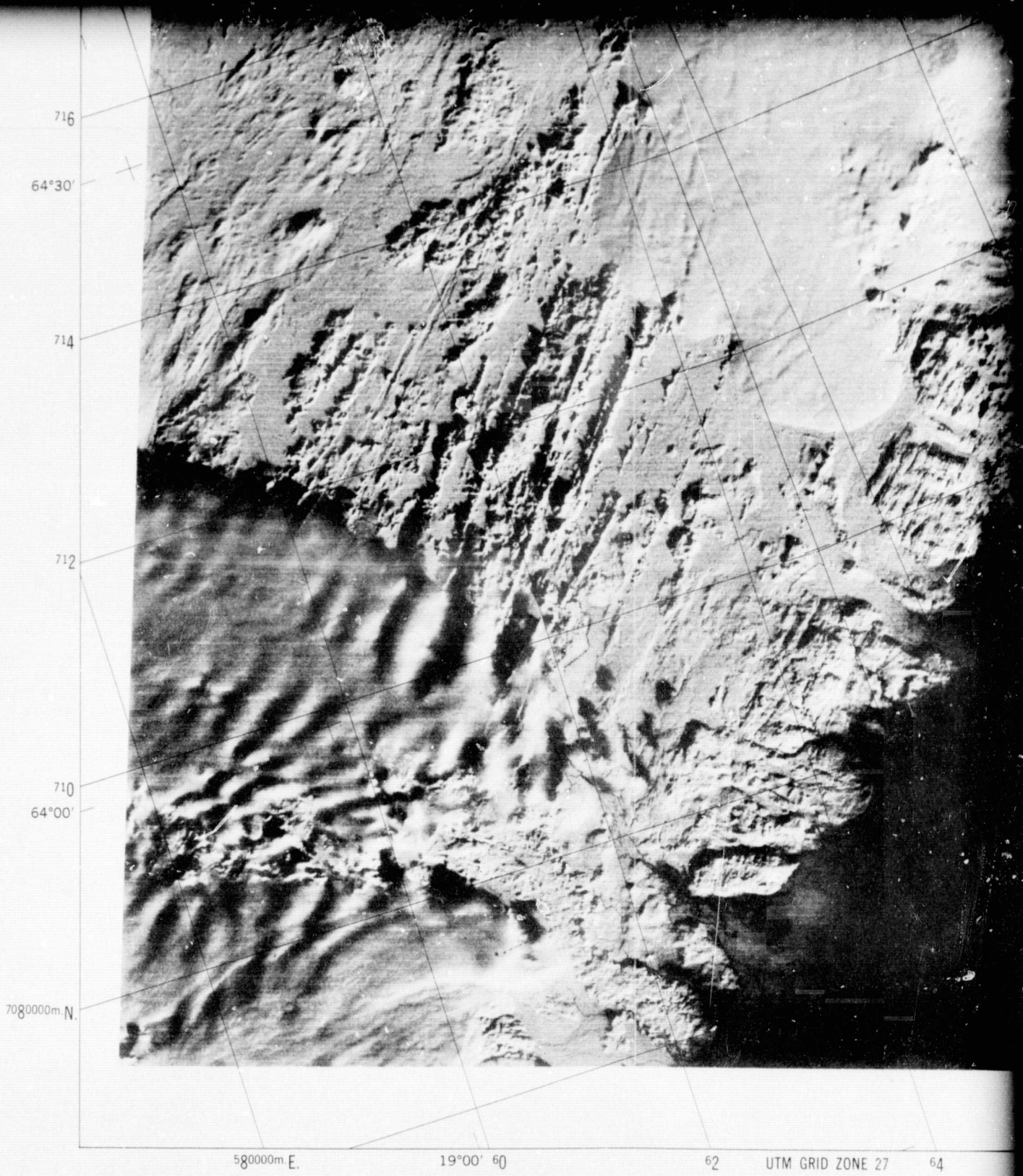

Prepared and published by the U. S. Geological Survey in cooperation with the Iceland Geodetic Survey (Landmælingar Íslands) and the Icelandic National Research Council (Rannsóknaráð Ríkisins)

Information on indexing, cost, and availability of Landsat imagery may be obtained from U. S. Geological Survey, EROS Data Center, Sioux Falls, South Dakota 57198

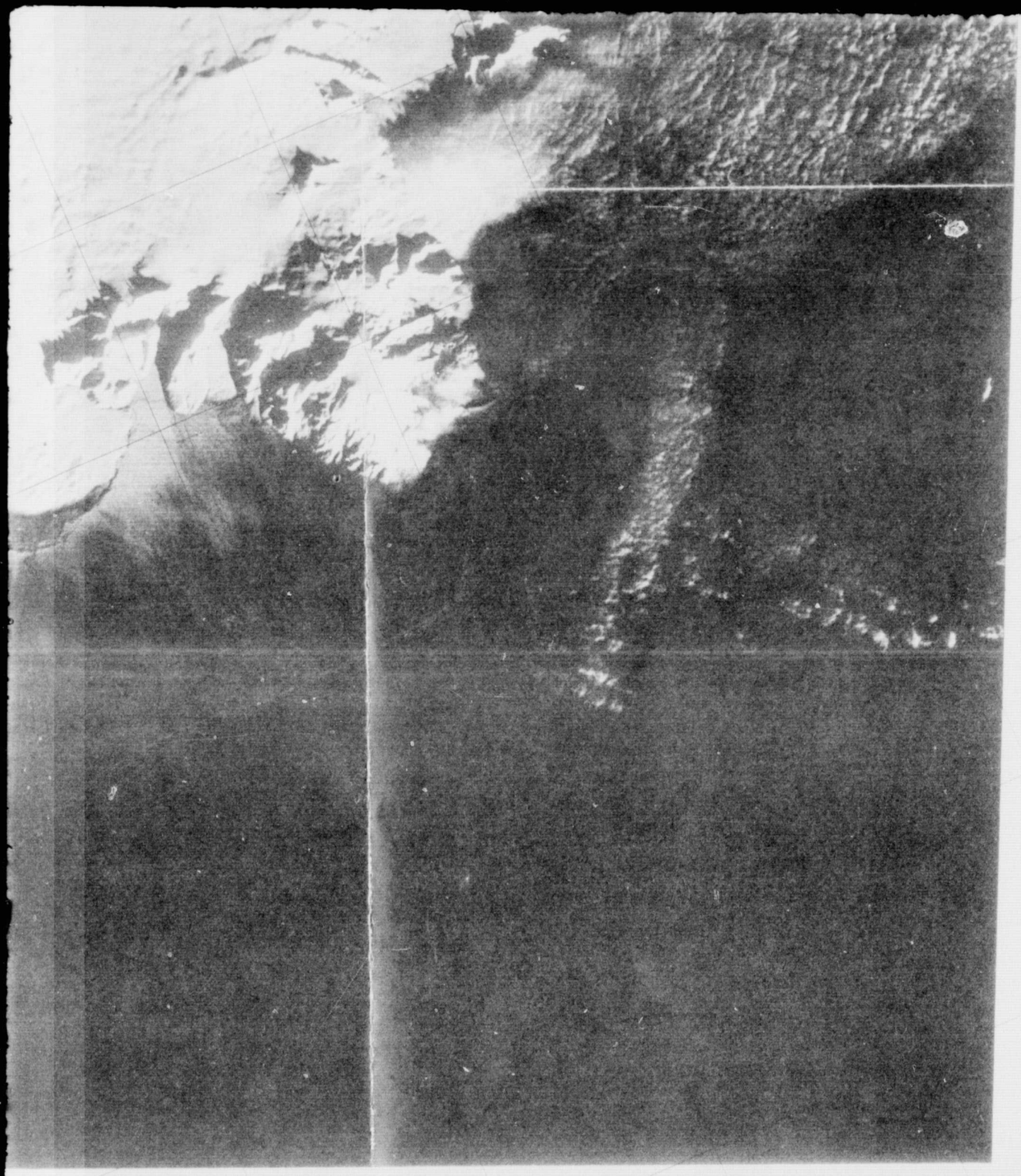

710
64°00'
708
706
63°30'
704
702
7000000m N.
36
UTM GRID ZONE 28
38
17°00'
40
42
44 0000m E.

SCALE 1:500 000

KILOMETERS 20 10 0 20 40

METERS 20 000 10 000 0 20 000 40 000

STATUTE MILES 10 0 20

FOR SALE BY U. S. GEOLOGICAL SURVEY, RESTON VIRGINIA 22092

LANDMÆ
NORÐVESTUR
MIÐVESTUR
SUÐVESTUR
24°00'
MN GN
21°18'
1°56
UTM GRID AND 1973 MA
DECLINATION AT CENTE

FOLDOUT FRAME 5

1 C-2

ORIGI
OF PO

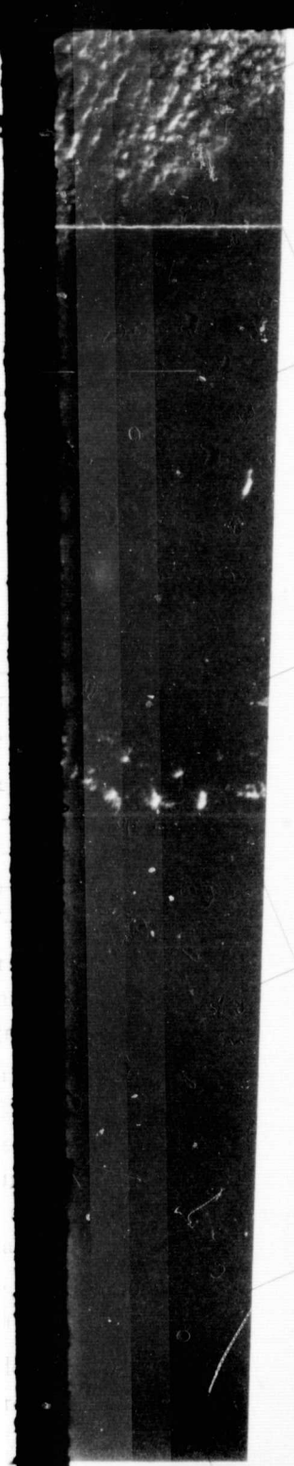

64°00′

708

706

63°30′

704

702

700 0000m N.

410000m E.

INDEX TO 1:250 000-SCALE
LANDMÆLINGAR ÍSLANDS TOPOGRAPHIC MAPS

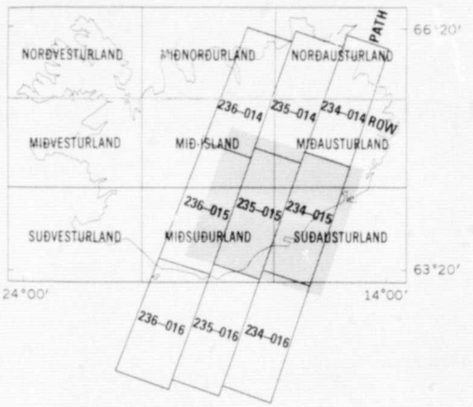

SATELLITE IMAGE INDEX

PATH–ROW	NOMINAL SCENE NAME AND CENTER
234–014	Lagarfljót N6520W01436
234–015	Ingólfshöfði N6359W01556
234–016	Kúðafljót N6238W01710
235–014	Ódáðahraun N6520W01602
235–015	Vatnajökull N6359W01723
235–016	Vík N6238W01837
236–014	Mývatn N6520W01728
236–015	Þórisvatn N6359W01849
236–016	Vestmannaeyjar N6238W02002

PATH-ROW information based on *Index to Landsat coverage, North America, WPS-2, ed. 1, Aug. 1972—July 1974*, published by the U. S. Geological Survey, 1975

Imagery recorded with Multispectral Scanner (MSS) on NASA Landsat–1 (ERTS–1), orbit 2674, 12:08 p.m. I.l.t., January 31, 1973. NASA image E 1192–12084, band 6. Orbital altitude 920 km (570 mi). Area 33 000 km^2 (13 000 mi^2)

Recorded simultaneously in discrete spectral bands as follows:
Band 4—0.5 to 0.6 micrometer
Band 5—0.6 to 0.7 micrometer
Band 6—0.7 to 0.8 micrometer (near-infrared)
Band 7—0.8 to 1.1 micrometers (near infrared)

Repetitive imagery obtained by Landsat sensors will show different conditions of snow and ice cover, vegetation, hydrography, and urban areas

Landsat images taken at low sun elevation angles (generally less than 30°) show increased definition and contrast of topographic features. In unusual circumstances, such as this snow-covered mid-winter scene (7° sun elevation angle), subtle topographic details are revealed on the glacier and enhancement of topography beyond the glacier is evident

Imagery controlled to map identified (AMS Series C762, scale 1:50 000) positions

Well-defined features are positioned in relation to a best-fit standard grid

20 000-meter Universal Transverse Mercator grid, zones 27 and 28

International Spheroid Horizontal Datum WGS 66

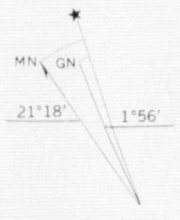

UTM GRID AND 1973 MAGNETIC NORTH
DECLINATION AT CENTER OF IMAGE

VATNAJÖKULL, ICELAND
WINTER SCENE

N6359W01723
235–015
1973

INTERIOR—GEOLOGICAL SURVEY, RESTON, VIRGINIA—1974
EXPERIMENTAL PRINTING

Appendix 1: Satellite Geological and Geophysical Remote Sensing of Iceland (SR 9651)

Scientific Disciplines and Subdisciplines Addressed During the Project*

1. Range Resources

   1C. Range Survey
   1G. Stress Detection

2. Land Use Survey and Mapping

   2B. Orthographic Mapping
   2D. Polar Regions Mapping

3. Mineral Resources, Geological Structure and Landform Surveys

   3C. Volcano Surveys
   3F. Geothermal Surveys
   3H. Water Erosion
   3I. Geomorphic and Landform
   3J. Lithologic Surveys
   3K. Structural Surveys
   3L. Disaster Assessment

4. Water Resources

   4D. Limnology
   4F. Flood Assessment and Prediction
   4G. Snow Surveys
   4H. Glacier Surveys

5. Marine Resources and Ocean Surveys

   **5A. Locating Biologically Rich Areas
   **5B. Surveys of Current and Ocean Dynamics
   5E. Sea Ice Monitoring
   5H. Coastal Zone Processes

8. Interpretation Techniques Development

   8E. Image Enhancement Techniques

10. Multidisciplinary Resources Surveys

   10A. Foreign Country (Iceland)

*Significant research results within a particular scientific subdiscipline are emphasized by underscoring.

**Post-contract research on dynamic marine phenomena off the southwest coast of Iceland on an MSS band 4 image (mesoscale eddies and concentrations of phytoplankton).

Appendix 2: Satellite Geological and Geophysical Remote Sensing of Iceland (SR 9651)

List of ERTS-1 Reports to NASA
(15 January 1973 - 1 December 1974)

Williams, R.S., Jr., 1973, Geological and geophysical remote sensing of Iceland: Type I Prog. Rpt., 15 Jan. 1973 - 30 Apr. 1973, 1 May 1973, 8 p.

Williams, R.S., Jr., 1973, Satellite geological and geophysical remote sensing of Iceland: Data Analysis Plan, 1 Jun. 1973, 12p.

Williams, R.S., Jr., 1973, Satellite geological and geophysical remote sensing of Iceland: Type I Prog. Rpt., 1 May 1973 - 30 June 1973, 1 Jul. 1973, 8p.

Williams, R.S., Jr., 1973, Satellite geological and geophysical remote sensing of Iceland: Special Rpt. No. 1, "Námafjall Geothermal Area, Iceland: Preliminary Analysis of ERTS-1 Image #1229-12142," 1 Aug. 1973, 5p.

Williams, R.S., Jr., 1973, Satellite geological and geophysical remote sensing of Iceland: Type II Prog. Rpt., 15 Jan. 1973 - 31 Aug. 1973, 1 Sept. 1973, 29p.

Williams, R.S., Jr., 1973, Satellite geological and geophysical remote sensing of Iceland: Type I Prog. Rpt., 1 Sept. 1973 - 31 Oct. 1973, 1 Nov. 1973, 8p.

Williams, R.S., Jr., 1973, Satellite geological and geophysical remote sensing of Iceland: Special Rpt. No. 2, Reprint, "Iceland: Preliminary Results of Geologic, Hydrologic, Oceanographic, and Agricultural Studies with ERTS-1 Imagery," 1 Dec. 1973, 20p.

Williams, R.S., Jr., 1973, Satellite geological and geophysical remote sensing of Iceland: Special Rpt. No. 3, Reprint, "Vatnajökull Area, Iceland: New Volcanic and Structural Features on ERTS-1 Imagery," 15 Dec. 1973, 3p.

Williams, R.S., Jr., 1974, Satellite geological and geophysical remote sensing of Iceland: Type I Prog. Rpt., 1 Nov. 1973 - 31 Dec. 1973, 1 Jan. 1974, 10p.

Williams, R.S., Jr., 1974, Satellite geological and geophysical remote sensing of Iceland: Type II Prog. Rpt., 1 Sept. 1973 - 28 Feb. 1974, 1 Mar. 1974, 49p.

Williams, R.S., Jr., 1974, Satellite geological and geophysical remote sensing of Iceland: Special Rpt. No. 4, Reprint, "Environmental Studies of Iceland with ERTS-1 Imagery," 1 Apr. 1974, 5p.

Williams, R.S., Jr., 1974, Satellite geological and geophysical remote sensing of Iceland: Type I Prog. Rpt., 1 Mar. 1974 - 30 Apr. 1974, 1 May 1974, 8p.

Williams, R.S., Jr., 1974, Satellite geological and geophysical remote sensing of Iceland: Special Rpt. No. 5, Preprint, "Volcanic Landforms of Iceland on ERTS Imagery: Their Relationship to Geologic Structure and Tectonic Setting," 15 Jul. 1974, 5p.

Williams, R.S., Jr., 1974, Satellite geological and geophysical remote sensing of Iceland: Type III Prog. Rpt., 15 Jan 1973 - 15 Aug. 1974, 1 Jan. 1978, p.

Post-Contract Period ERTS-1 Reports to NASA

Williams, R.S., Jr., 1974, Satellite geological and geophysical remote sensing of Iceland: Special Rpt. No. 6, Preprint, "Glaciological Studies in Iceland with ERTS-1 Imagery," 15 Sept. 1974, 3 p..

Williams, R.S., Jr., 1974, Satellite geological and geophysical remote sensing of Iceland: Special Rpt. No. 7, Reprint, "ERTS-1 Image of Vatnajökull Area: General Comments," 1 Nov. 1974, 8p.

Williams, R.S., Jr., 1974, Satellite geological and geophysical remote sensing of Iceland: Special Rpt. No. 8, Reprint, "ERTS-1 Image of Vatnajökull: Analysis of Glaciological, Structural and Volcanic Features," 15 Nov. 1974, 13p.

Williams, R.S., Jr., 1974, Satellite geological and geophysical remote sensing of Iceland: Special Rpt. No. 9, Reprint, "Environmental Studies of Iceland with ERTS-1 Imagery," 1 Dec. 1974, 52p.

Appendix 3: Satellite Geological and Geophysical Remote Sensing of Iceland (SR 9651)

List of Landsat Publications (1972-1977)

Richard S. Williams, Jr.
U.S. Geological Survey
Reston, Virginia 22092

U.S. Geological Survey, 1976, Vatnajökull, Iceland (Fall Scene): Landsat Image Format Series, N6359W01723, Experimental Printing, 1:500,000-scale, U.S. Geological Survey, Reston, Va.

U.S. Geological Survey, 1977, Vatnajökull, Iceland (Winter Scene): Landsat Image Format Series, N6359W01723, Experimental Printing, 1:500,000-scale, U.S. Geological Survey, Reston, Va.

Williams, R.S., Jr., 1972, Satellite geological and geophysical remote sensing of Iceland [abs.]: in Proc. Eighth Int. Symp. on Remote Sensing of Environment, Univ. of Mich., Ann Arbor, Mich., p. 1465-1466.

Williams, R.S., Jr., 1973, Coastal and submarine features on MSS imagery of southeastern Massachusetts: Comparison with conventional maps: in Proceedings of Symposium on Significant Results Obtained from ERTS-1, NASA, Goddard Space Flight Center, Greenbelt, Md., p. 1413-1422.

Williams, R.S., Jr., 1976, Dynamic environmental phenomena in southwestern Iceland: in U.S. Geol. Surv. Prof. Paper 929, p. 109-112.

Williams, R.S., Jr., 1976, Vatnajökull icecap, Iceland: in U.S. Geol. Surv. Prof. Paper 929, p. 188-193.

Williams, R.S., Jr., 1976, Cape Cod and Cape Cod National Seashore, Massachusetts: in U.S. Geol. Surv. Prof. Paper 929, p. 307-309.

Williams, R.S., Jr., 1976, Monitoring of natural and land resources of Iceland: in Abstracts, Assoc. of Amer. Geographers, Middle Atlantic Div., Annual Meeting, Mary Washington College, Fredericksburg, Va., p. 23.

Williams, R.S., Jr., and Thorarinsson, Sigurður, 1974, ERTS-1 image of Vatnajökull area: General Comments: Jökull, v. 23, (1973), p. 1-6.

Williams, R.S., Jr., and Carter, W.D., Editors, 1976, ERTS-1, A New Window on Our Planet: U.S. Geological Survey Professional Paper 929, 362p.

Williams, R.S., Jr.; Böðvarsson, Ágúst; Friðriksson, Sturla; Pálmason, Guðmundur; Rist, Sigurjón; Sigtryggsson, Hlynur; Thorarinsson, Sigurður; and Thórsteinsson, Ingvi, 1973, Satellite geological and geophysical remote sensing of Iceland - preliminary results from analysis of MSS imagery; in Proceedings of Symposium on Significant Results obtained from ERTS-1, NASA, Goddard Space Flight Center, Greenbelt, Md., p. 317-327.

Williams, R.S., Jr., Thorarinsson, Sigurður, and Sæmundsson, Kristján, 1973, Vatnajökull area, Iceland: New volcanic and structural features on ERTS-1 imagery [abs.]: in Geol. Soc. Amer. Abstracts with Programs, 1973 Ann. Mtngs., Dallas, Texas, p. 864-865.

Williams, R.S., Jr., Böðvarsson, Ágúst; Friðriksson, Sturla; Pálmason, Guðmundur; Rist, Sigurjón; Sigtryggsson, Hlynur; Sæmundsson, Kristján; Thorarinsson, Sigurður; and Thorsteinsson, Ingvi, 1973, Iceland: Preliminary results of geologic, hydrologic, oceanographic and agricultural studies with ERTS-1 imagery: in Proceedings of Symposium on Management and Utilization of Remote Sensing Data, American Society of Photogrammetry, Sioux Falls, South Dakota, p. 17-35.

Thorarinsson, Sigurður; Sæmundsson, Kristjan; and Williams, R.S., Jr.; 1974, ERTS-1 image of Vatnajökull; Analysis of glaciological, structural, and volcanic features: Jökull, v. 23 (1973), p. 7-17.

Williams, R.S., Jr.; Böðvarsson, Ágúst; Friðriksson, Sturla; Palmason, Guðmundur; Rist, Sigurjón; Sigtryggson, Hlynur; Sæmundsson, Kristján; Thorarinsson, Sigurður; and Thorsteinsson, Ingvi, 1974, Environmental studies of Iceland with ERTS-1 imagery: in Proc. Ninth Symposium on Remote Sensing of Environment, Univ. of Mich., Ann Arbor, Mich., v. 1; p. 31-81.

Williams, R.S., Jr.; Böðvarsson, Ágúst; Rist, Sigurjón; Sæmundsson, Kristján; and Thorarinsson, Sugurður, 1975, Glaciological studies in Iceland with ERTS-1 imagery [abs.]: Jour. of Glaciology, v. 15, no. 73, p. 465-466.

Williams, R.S., Jr., Mecklenburg, T.N., Abrams, M.J., and Gudmundsson, Bragi, 1977, Conventional vs. computer-enhanced Landsat image maps of Vatnajökull, Iceland: in Abstracts with Programs, 1977 Ann. Mtgs., Geol. Soc. Amer., Boulder, Colo., v. 9, no. 7, p. 1228-1229.